Charles University

Faculty of Medicine in Pilsen

Normal and Pathological Physiology

Brain oscillations and temporal structure of spatial memory pattern retrieval

Mozkové oscilace a časová struktura aktivace prostorové paměti

Dissertation

Supervisor: MUDr. Karel Ježek, PhD
Co-supervisor: Doc. MUDr. František Vožeh CSc.

Pilsen 2022

MUDr. František Zitrický

Acknowledgements

I would like to thank to my supervisor Dr. Karel Ježek for his guidance and support during my time as his student. I thank to my lab mates for opportunities to participate in many interesting projects and for stimulating and friendly environment for work and study. I thank to Dr. Karel Blahna for his support and many interesting discussions about science. Some of the most memorable moments were spent with my scientific colleague and friend Nikhil Ahuja.

I thank to my parents for all their support throughout the time of my study. My thanks go to my wife Nazila, who has always been by my side and who motivates me to thrive in all circumstances of life.

Declaration

I declare that I wrote this dissertation by myself and all the relevant resources are properly cited. At the same time, I declare that this thesis was not used to obtain another or the same degree.

I agree with permanent deposition of an electronic version of my thesis in the database of interuniversity project Thesis.cz for a permanent control of similarities of theses.

In Pilsen, 26.6. 2022

MUDr. František Zitrický

Souhrn

Hipokampus je mozková struktura která se podstatným způsobem podílí na mechanizmech epizodické paměti, prostorové navigace a na dalších komplexních kognitivních funkcích. Specifická autoasociativní architektura hipokampové sítě CA3 umožňuje kombinovat konvergující senzorické vstupy při vytváření komplexních mentálních reprezentací. U hlodavců se pyramidové neurony v hipokampu chovají jako „poziční neurony“, přičemž aktivita jednotlivých neuronů je vázaná na specifickou pozici subjektu v prostoru. Kolektivní aktivita pozičních neuronů představuje neurální reprezentaci prostoru, která je považována za fyziologický substrát prostorové paměti.

Cílem této práce bylo detailně popsat dynamiku hipokampové sítě během aktivace prostorové reprezentace. Analyzovali jsme proto aktivitu pozičních neuronů v hipokampové oblasti CA3 zaznamenanou během „teleportačního“ experimentu, při kterém jsou potkani vystavení náhlým změnám identity prostorového kontextu. Předchozí studie ukázala, že příslušné změny stavu sítě jsou doprovázené periodou instability, během níž dochází ke kompetitivním reaktivacím vzorců aktivity pro předchozí a současné prostředí.

Zjistili jsme, že změny stavu sítě jsou doprovázená výrazným zvýšením celkové populační aktivity pyramidových neuronů. Populační hyperaktivita byla nejvyšší krátce po změně identity prostředí a úroveň aktivity se vrátila k výchozím hodnotám během několika sekund. Detailní analýza poukázala na zvýšenou aktivitu pozičních neuronů během stavů spojených s reprezentací nového prostředí.

Dále jsme analyzovali kvalitu prostorové reprezentace krátce po změně identity prostředí. Zjistili jsme nárůst poziční chyby, dekódované z populační aktivity reprezentujici současné prostředí. Reprezentace pozice během aktivace mapy pro předchozí prostředí se nelišila od kontrolních podmínek, i přes absenci specifických vizualních stimulů.

Analýza separace prostorových reprezentací během stavových přechodů krátce po změně prostředí poukázala na výrazný nárůst koaktivace do té doby vzájemně segregovaných vzorců aktivity. K současné aktivaci neuronů specifických pro aktuální a předchozí prostředí docházelo během jednotlivých cyklů theta oscilací (ca. 125 ms), i na mnohem krátší časové škále (<10 ms). Současná aktivace odlišných vzorců může potencovat vznik asociací mezi původně separovanými paměťovými stavy.

Procesování prostorové paměti v hipokampových sítích vykazuje výraznou rytmickou organizaci. Analýza hipokampové oscilační aktivity během změny prostorového kontextu poukázala na nárůst amplitudy v theta a gama pásmu. Robustní theta oscilace zajišťují efektivní periodickou inhibici síťové aktivity, následovanou promptní aktivací příslušného paměťového stavu. Zesílená gama aktivita může podporovat koordinované procesování informace napříč anatomickými strukturami hipokampové formace.

Výsledky naší práce poskytují vhled do dynamiky aktivace paměťových stavů v hipokampu a přispívají k pochopení obecných mechanismů vybavení epizodické paměti.

Summary

The hippocampus is a brain structure essentially involved in episodic memory, spatial navigation and other complex cognitive functions. The distinct network architecture of hippocampal CA3 allows to combine converging sensory inputs in creation of complex neural representations. The hippocampus further interacts with the entorhinal cortex to organize knowledge into relational representations, also known as 'cognitive maps'.

In rodents, the hippocampal pyramidal neurons behave as place cells, where a neuron is active whenever the subject occupies specific location in the environment. The collective activity of the place cells represents a neural map that is reinstated during repeated exploration of the same space. The place cell maps are thus recognized as neural substrate of spatial memory.

In this work, we aimed at better understanding of hippocampal CA3 network dynamics during period of reinstatement of the appropriate place cell representation. We thus analysed CA3 place cell activity recorded during 'teleportation' experiment, where the rats are exposed to abrupt changes in spatial context identity. As shown previously, the network state transitions involve short competitive period, where network state quickly switches between the representations of the previous and the present environment.

We show that the network state transitions are accompanied by marked increase in total place cell activity. The network hyperexcitability displayed a peak shortly after the cue switch and averaged activity levels returned to baseline within several seconds. Further analysis revealed increased place activity during network states with decoded map for the new environment.

Next, we evaluated quality of place cell spatial code shortly after the change of environment identity. We detected increase in decoded position error associated with representation of the present context. Notably, place cell ensembles coding for the previous context continued to provide robust positional information, as the respective decoded position error values were comparable to the control conditions.

Furthermore, we detected a considerable mixing of the alternative place cell maps during the network state transition period. The coactivity of concurrent representations occurred during individual theta cycles as well as within short time intervals (<10 ms). The coactivation at such short timescale is relevant for organization of activity into functional cell assemblies and might facilitate synaptic plasticity. This might induce associations between originally segregated network states.

Additionally, we assessed hippocampal network oscillatory activity associated with spatial map recollection. We observed increase in theta and gamma rhythmicity following switch of context identity. We suggest that strong theta oscillations mediate effective network inhibition, allowing the relevant input to promptly update the network state. The enhanced gamma oscillations might support formation of cell assemblies and coordinate flow of information within the hippocampal formation.

Table of Contents

Abbreviations

CA .... Cornu Ammonis

DG....dentate gyrus

ESI...environment-specificity index

f .... frequency

Fig .... figure

LEC....lateral entorhinal cortex

LED .... Light Emitting Diode

LFP ....local field potential

LTP ....long-term potentiation

MEC....medial entorhinal cortex

n ....number

NMDA....N-methyl D-aspartate

s.d. ....standard deviation

SEM ....standard error of mean

SWR ....sharp wave-ripple

TC ....theta cycle

1 Introduction

1.1 Outline of hippocampal architecture

The hippocampus is a structure of the brain limbic system that is considered to be an essential component of neural circuitry for declarative memory. In addition, the hippocampus is extensively involved in multitude of other cognitive functions, as well as in emotional processing.
The hippocampus is localized within medial temporal lobe, positioned between thalamus and neocortex. In rats, it has a form of C-shaped cortical structure, localized in the caudal part of the brain (Fig. 1a).
The hippocampus is classified as a part of archicortex, referring to its relatively older evolutionary origin. This is associated with a distinct architectonical layout with a fewer cellular laminae in comparison to evoulutionary younger neocortex.
The foundations of hippocampal anatomy have been illuminated by classic histological studies performed by neuroanatomy pioneers such as Santiago Ramon y Cajal and Rafael Lorente de No, who also founded the basis for existing terminology.

The hippocampus consists of dentate gyrus (fascia dentata) and Cornu Amonis region (hippocampus proper), which has been traditionally diveded into CA1-CA4 subfields. The vast body of existing studies has establieshed distinct structural and functional properties of CA1 and CA3 hippocampal subfields. The relatively small CA2 region had been considered to be a mere transitory region, however, recent studies revealed its unique properties and central role in some of hippocampal functions (Middleton and McHugh, 2020). The CA4 is now considered to be a part of the dentate gyrus

The hippocampus is connected with entorhinal cortex and subicular complex and together these structures are referred to as hippocampal formation (Amaral, 1999). The entorhinal cortex represents a gate, through which highly preprocessed information from temporal, parietal and prefrontal cortex enters the hippocampal circuitry (Fig. 1c). The hippocampus thus stands at highly advanced position of information processing in the brain, enabling to combine information streams, including inputs from all sensory modalities, to create high order representations.
The hippocampal computations, especially in its ventral part, include processing of input from structures dedicated to emotional valence of stimuli, such as amygdala and orbitofrontal cortex. Furthermore, the hippocampal network is also significantly influenced by modulatory inputs arising from subcortical structures.

The main connectivity motif in the hippocampal formation is the classicaly described ‘trisynaptic loop‘ (Fig. 1b), where neurons in layer II of entorhinal cortex project via perfornat path to granule cells of the dentate gyrus, which give rise to mossy fibers projecting to the CA3 pyramidal neurons. The CA3 cells in turn project to CA1 population in form of Schaffer collaterals (Andersen et al., 1971). There is also a parallel route of information flow represented by direct entorhinal (layer III)-CA1 connections (Steward and Scoville 1976, Witter and Amaral, 1991, Amaral 1993).
The information from CA1 is conveyed to subiculum, which projects to the entorhinal cortex, thereby closing information processing loop in the hippocampal formation. The results of the computation are subsequently backprojected to the neocortex (Fig. 1c).

Another iconic element of the hippocampal connectivity is the abundance of the recurrent collaterals. Extensive recurrent connections are hallmark of CA3, as well as CA2 subregions. Single CA3 pyramidal cell recieves, in approximate numbers, mossy fiber afferents from 50 granule cells, perforant path connections from 4000 entorhinal cortex cells, but vast majority of afferents corresnpond to axon collaterals from other 12 000 CA3 pyramidal neurons (Rolls, 2007). It has been estimated, that 250 000 pyramidal cells in rat's hippocampmus can give rise to 60 -100 km of recurrent collateral length in total (Wittner et al., 2007; Buzsaki, 2015). This dense autoassociative connectivity is proposed to be essential for hippocampus' role in creating complex mental representations such as those associated with episodic memory.

The dentate gyrus, consisting of molecular layer, granule cell layer and the hilus contains two types of excitatory cells. The granule cells in the granule cell layer are the source of the main pathway connecting the dentate with CA3, while the mossy cells located in the hilus target the granule cells and inhibitory interneurons.

The excitatory cells in the hippocampus proper are the pyramidal cells, with cell bodies constituing a single sheet with characteristically richly arborized dendritic trees extending across the layers. The hippocampus proper can be viewed as a primarily trilaminar structure, in accord with structural principle of archicortex, however, subdivisions to further layers are traditionally described. Thus, it can be subdivided into (going from ventricular surface): alveus containing axons of pyramidal cells, stratum oriens containing basal dendrites of the pyramidal cells, the pyramidal cell layer, stratum radiatum and stratum lacunosum-moleculare, which contains apical dendrites of the pyramidal cells (O'Keefe and Nadel, 1978). The stratum lacunosum-moleculare contains perforant path synapses onto distal parts of pyramidal cells' dendrites, while the stratum radiatum is the termination site of the Schaffer collaterals.

In addition to the excitatory neurons, the hippocmpal circuitry includes several types of inteneurons. The inhibitory interneurons are less abundant than the excitatory cells, but represent an essential component of the neruonal networks. Introducing inhibitory element into the circuitry not only counteracts excessive excitation, but also endows the network with non-linear features and self-organizing properties (Buzsaki, 2006).

The hippocampal interneurons display great variety, differing in morphology, network connectivty pattern and neurochemical characteristics (Freund and Buzsaki, 1996).

For example, parvalbumin-positive basket cells and axo-axonic cells target the pyramidal somas and axonal initial segments, respectively, performing perisomatic inhibition. In contrast, somatostatin positive oriens-locunosum neurons target distant segments of pyramidal dendtrites, regulating dendritic excitability. Furthermore, there is a family of interneurons specialized in inhibiting other interneurons (Gulyas et al., 1996).

The specific connecitvity gives basis for the involvement of the interneurons in network computation. Accordingly, perisomatic inhibition by the basket cells orchestrates pyramidal cells firing and output

The connectivity of oriens-lacounosum moleculare neurons allows them to regulate dendtritic excitability, as well as modulate interplay between streams of information flow within hippocampal formation (Leão et al, 2012).

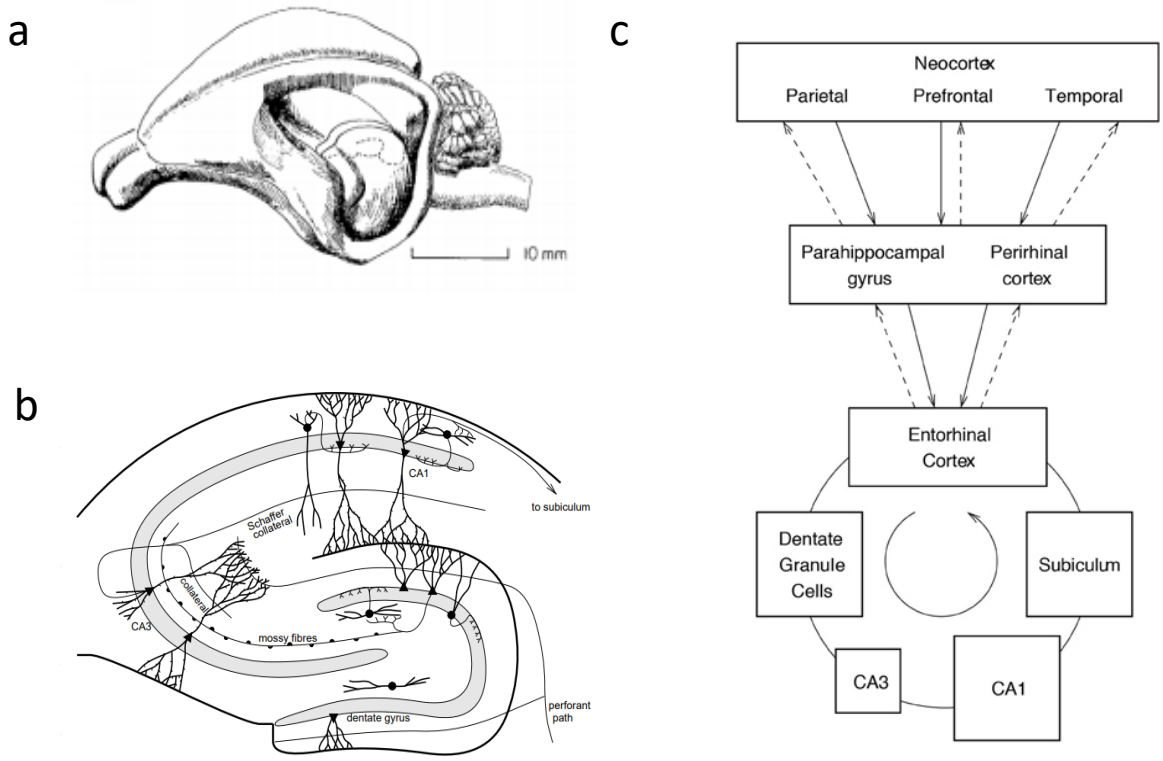

Figure 1 (a) Anatomical position of hippocampus in the brain of rat. Adapted from Andersen et al. (1971). (b) A scheme of hippocampal subfields and their connectivity. Adapted from Schultz et al. (1999) (c) The connectivity of hippocampal formation and associated structures. The arrows represent flow of information (solid: forward connections; dashed: backprojections). Reproduced from Rolls (2007).

1.2 Hippocampus and memory

The hippocampus, a part of classically described Papez's circuit, has been traditionally linked to emotional processing.
The essential role of the hippocampus in memory was put forward by a study of patients who developed memory deficits as a consequence of medial temporal lobe resection (Scoville and Milner, 1957). In the most famous case, a patient H. M. underwent extensive resection of major proportion of hippocampal formation bilaterally in an attempt to control his drug-resistant epileptic seizures. After the surgery, the patient developed strikingly apparent anterograde amnesia: he was not able to recall events of his hospital life, he was not able to recognize the hospital staff and read the same magazines without finding their content familiar. He also displayed signs of retrograde amnesia for episodic and semantic content, but his early memories seemed rather intact.
It was further observed that H. M. was still able to learn procedural skills such as drawing an outline of five-pointed star, while he was able to see his hand only in a mirror reflection (Milner, 1962). This suggested existence of multiple memory systems in the brain. Similar form of memory loss was later reported in other patients with hippocampal lesions (Zola-Morgan et al., 1986). This established that hippocampus is essential for declarative (explicit) memory, which includes episodic memory together with memory for factual information (semantic memory). On the other hand, the implicit memory, such as procedural skill acquisition, involves predominantly other brain regions (Squirre and Zola-Morgan, 1988).

Memory deficits are also observed in animal studies, where subjects, such as rodents and primates are affected by lesion of the hippocampus or some of its connections (Zola-Morgan et al., 1992; Morris et al., 1990; review Rolls, 2007). This includes memory for associations between events and respective spatial context and temporal relations (Eichenbaum, 2017).
The rats with damaged hippocampus can learn simple pair associations between stimuli, but only rats with functional hippocampus can learn flexible associations that are transitive and symmetric (Bunsey and Eichenbaum, 1996). Similarly, the rats with hippocampal lesions are able to learn single route in Morris Water Maze, but they can't solve the task for an arbitrary starting position (Eichenbaum et al., 1990). The hippocampus thus seems to be necessary for creating relational representation of acquired knowledge.
The flexible associations are also crucial for binding multiple aspects of experience within coherent episodic memory and it is believed that hippocampus enables such associations by virtue of its specific autoassociative network connectivity.

The amnesic patients with bilateral hippocampal damage also show considerable impairment in imaging new rich fictitious experience, supporting the idea that hippocampus is essential not only for remembering, but also for creating complex associations with respective spatial context (Hassabis et al., 2007). This constructive function might explain observed activation of hippocampal formation in processes such as prospective thinking, 'mind wandering' associated with default network entrainment and navigation (Hassabis and Maguire, 2007).

1.2.1 Functions of dentate gyrus

The dentate gyrus is positioned as an intermediate stage of information processing between the entorhinal cortex and CA3. The entorhinal neurons project onto several times larger population of dentate granule cells (Schmidt et al., 2012), giving rise to sparse granule cell entrainment. The emergence of the sparse code is facilitated by inhibition-mediated competitive dynamics (Rolls, 2007). It has been proposed that this 'expansion recoding' enables similar entorhinal inputs to be decorrelated into more distinct dentate codes in a process called 'pattern separation'.

This would serve an important function, as the hippocampus needs to discriminate even between the experiences that share many common features and store them as distinct episodic memories.

The projections of the granule cells, the mossy fibers, create large synapses near the cell bodies of the CA3 cells (Amaral and Dent, 1981), which display high efficiency, where bursting of a single granule cell can trigger firing of its CA3 target (Henze et al., 2002).

This contrasts with much weaker synaptic connections between the perforant path and CA3 dendrites. However, the CA3 activation elicited by mossy fibers allows for associative plasticity of perforant path-CA3 synapses (McMahon and Barrionuevo, 2002) as well as plasticity at recurrent collaterals synapses between the active CA3 cells. The computational analysis revealed that mossy fiber input might be particularly important for inducing distinct CA3 network patterns by overcoming the randomizing effect of the recurrent collaterals, which would dominate if the new pattern was relayed solely by relatively weak perforant path input (Rolls and Treves, 1992).

While the mossy fiber input can effectively induce storage of sparse, orthogonal patterns in CA3 autoassociative network, it is supposed that the facilitated connections allow the perforant path to successfully drive the retrieval process.

The role of dentate gyrus in pattern separation is supported by observation that only very small fraction of the granule cells are active during exploration of single environment (GoodSmith et al., 2017, Senzai and Buzsaki 2017). Moreover, the dentate gyrus generates different codes for similar environment, whereas CA3 maintains the same representation (Leutgeb et al., 2007; Neunuebel and Knierim, 2014). This is consistent with the model where pattern separation in dentate gyrus is complemented with pattern completion in the CA3.

The theoretical considerations propose that dentate gyrus is especially important during memory encoding. This is supported by experimental studies (reviewed in Heinmueller and Bartos, 2020), however, in some instances, such as during contextual fear condition, learning can occur without involvement of dentate gyrus (Kitamura et al., 2015).

In addition, the dentate seems to be involved in some forms of memory retrieval, in particular where recall is needed during behavior planning (Heinmueller and Bartos, 2020). For example, synchronous activation of dentate neurons occurs before shock-zone avoidance in active allothetic place avoidance task (van Dijk and Fenton, 2018).

Another intriguing feature of the mammalian dentate gyrus is presence of adult neurogenesis, with young, adult-born granule cells displaying specific profiles of excitability, connectivity and synaptic plasticity. The experimental findings suggest that young, adult-born granule are particularly important in mechanisms of pattern separation, such as contextual discrimination (Nakashiba et al., 2012; Clelland et al, 2010; Heinmueller and Bartos, 2020).

1.2.2 The autoassociator network in CA3

The events of everyday life that need to be stored in the episodic memory might in principle consist of arbitrary combination of experience. Furthermore, we are expected to recall whole episode from any associated reminding cue. This means that neuronal network suitable for episodic memory computations needs to be able to store arbitrary combinations of stimuli and should be able to recall whole pattern from a partial cue.
It has been suggested, that such computations can be performed by the highly interconnected network of CA3 neurons. The CA3 network is recognized as the most prominent system of recurrent excitatory collaterals in the brain (Wittner et al., 2007, Buzsaki et al., 2015), with axonal branches of a single pyramidal cell spanning up to two thirds of septo-temporal extent of the hippocampus. The recurrent collaterals are also responsible for majority of excitatory synaptic connections within the region, suggesting strong influence over CA3 activity dynamics (Rolls, 2007). This high level of autoassociativity of CA3, in addition to its position as a convergence node of sensory inputs, makes it particularly apt candidate for mediating flexible associative representations, such as those in episodic memory.
The role of the recurrent collaterals was already recognized by David Marr, referring to it as 'collateral effect' (Marr, 1971). Backed by anatomical considerations, computational model of CA3 as an autoassociative memory network was developed (Morris and McNaughton, 1987; Rolls, 1987, Rolls and Treves 1992; Rolls, 1996). The main principles of the theory are CA3 network's ability to store arbitrary combination of inputs by modifiable synapses in autoassociative network, which enables memory formation in single-trial manner. Subsequently, even a partial cue can trigger retrieval of whole pattern by activation spreading along recurrent collaterals, in a process called 'pattern completion'.
Moreover, the mutual excitation of neurons sustains the activity pattern until it is disrupted by inhibition or sufficiently strong input relocates the activity bump to another position within the state space.

The experimental evidence supports role of CA3 in pattern completion. The mice with deficit in CA3 plasticity by selective NMDA gene knock-out, display degraded performance in water maze when only a subset of original cues was present (Nakazawa et al., 2002).
The hallmarks of autoassociative pattern completion, also called attractor dynamics, are also revealed by the electrophysiological recordings of hippocampal neuronal activity (Lee et al. ,2004, Colgin et al., 2010), which enables to study its fine temporal kinetics in real time (Jezek et al. 2011).
The attractor theory further predicts CA3 codes to be sparse, which should maximize capacity and minimize interference between the stored patterns (Rolls, 2007). This is in line with experimental observations (Leutgeb et al, 2004, Alme et al, 2014).

1.2.3 Functions of CA1

Several computational advantages have been attributed to existence of additional stage of hippocampal 7information processing, represented by CA1 (Rolls, 2007).
CA1 neurons receive dual input, combining information from dentate-CA3 stage computation with direct entorhinal input (Amaral, 1993). The CA1 responses can reflect sensory similarities across different experiences, complementing robust orthogonalization in dentate-CA3 network. Moreover, experimental evidence suggests that CA1 network can dynamically switch between modes reflecting processing of input

from the entorhinal cortex (information about the current state of the external world) and CA3 (internally driven memory retrieval), respectively (Colgin et al., 2009; Schomburg et al. 2014; Wang et al., 2020).
The dual entrainment of CA1 neurons can further support memory processing by associative plasticity at CA3-CA1 synapses, which ensures that pattern completion in CA3 is reflected in corresponding activity pattern in CA1 (McClelland et al., 1995; Rolls 2007).
The CA1 representations are less sparse in comparison with CA3 representations (Leutgeb et al., 2004), which means that information content can be distributed among higher number of active neurons. This transformation creates representation that is more robust to information loss at subsequent stages of processing (Rolls, 2007).
Further, converging input from CA3 gives rise to conjunctive representation of multiple components of episodic memory content by individual CA1 cells, which might enable more efficient reactivation of neocortical representations during retrieval (Rolls 1990, Kesner and Rolls, 2015).
The CA1 is the hippocampal subfield that most directly influences activity in downstream populations. This was reflected in a study where subtle changes of environment were associated with substantial remapping of the dentate gyrus activity, but only CA1 remapping was associated with change in behavioral performance (Allegra et al., 2020).

1.2.4 Functions of CA2

The CA2 region is a small, but highly interconnected hippocampal subfield. It has been overlooked for a long time, but its unique connectivity and recent studies suggest important involvement in hippocampal information processing (Middleton and McHugh, 2020). It is bidirectionally connected with the CA3 and layer II of the entorhinal cortex, in addition to feedforward projections to CA1. Based on this connectivity profile, it has been hypothesized that CA2 regulates switching between encoding (entorhinal cortex to CA1 flow) and retrieval mode (CA3 to CA1 flow) (Middleton and McHugh, 2020).
The efferents from the dorsal CA2 extend to ventral hippocampus, suggesting that CA2 might be instrumental in integrating functions of dorsal and ventral part of the hippocampus. The circuitry involving dorsal CA2 and its projections to ventral hippocampus is important for social memory processing (Middleton and McHugh,2020; Hitti and Siegelbaum, 2014; Meira et al., 2018; Okuyama et al., 2016).
The CA2 has been also shown to be involved in coordinating activity pattern replay during memory consolidation (He et al., 2021), with particular importance for consolidation of social memory (Oliva et al, 2020).

1.2.5 Memory retrieval and backprojections to neocortex

Memory recollection is postulated to involve widespread reinstatement of the original activity patterns, corresponding to content of the encoded memory (Damasio, 1989). The hippocampus is suggested to enable retrieval by triggering such a coherent reactivation of the respective neural representations, particularly in the neocortex.
The CA1 and subicular efferents project to layer V of the entorhinal cortex, which is source of backprojections to necocortex (Lavenex and Amaral, 2000), allowing entrainment of originally active neurons. The specificity of neocortical activity entrainment by feedback input can be achieved by

mechanisms of synaptic plasticity. According to the theory (Rolls, 2007), the modifiable synapses allow for associative potentiation of connections between the active neocortical cells and their respective entorhinal afferents. This would ensure that only the neocortical neurons participating in the original pattern would be recruited during retrieval. The retrieval cascade thus would exploit hippocampal associative capabilities to selectively bring together activity patterns in distributed cortical area, reflecting pieces of memorized experience.

1.2.6 Memory engrams in hippocampus and neocortex

The graded retrograde amnesia in hippocampal lesion patiensts, where early memories are less affected, led to hypothesis that hippocampus is essential for processing recent memories, and that memory becomes hippocampus-independent with time. However, retrograde amnesia after hippocampal damage can still extend for several years (Scoville and Milner, 1957; Squire 1986).
The observatiations potinted to gradual reorganization of involved memory networks in a process called memory consolidation (Squire and Zola-Morgan, 1988).
It has been proposed that memory trace is gradually ‘transfered‘ for extrahippocampal storage, likely in neocortex. Thus, necorticortical representations reinstatment would underlie recall of both early and remote memories, but role of hippocampus in the process would become dispensable with time.

Nevertheless, neuroimaging studies show hippocampal activation even during recall of remote episodic memory (Fink et al., 1996). Furthermore, impaired retrieval of even very remote episodic memories, in contrast to general semantics, was reported in the patients with hippocampal lesions (Cermak and O’Connor, 1983). Based on these observations, Nadel and Moscovitch (1997) introduced the multiple trace theory, as an update of the standard model of memory consolidation. According to the theory, the hippocampus remains involved in detailed recall of episodic memory, while representation of the semantic ‘gist‘ becomes hippocampus-independent. The semantic essence is extracted from multiple memory traces created in hippocampus for every experience. Thus, hippocampal damage should affect quality of recall of old episodic, but not semantic memories.
This view also resonates with classic theory of David Marr, who considered hippocampus as a storage of ’simple memory‘ - "recording information as it occurs, without trying to produce best possible classification of the input on the spot“ (Marr, 1971). The classification would be gradually performed by neocortex, which would recognize and learn important features of the stored memory trace.
The concept of ’offline‘ memory cosolidation involving hippocampo-neoocortical communication has been supported by a substantial experimental evidence (Rotschild et al. 2018, Kitamura et al., 2017).
However, the nature of declarative memory temporal dependence on the hippocampus remains a subject of ongoing active research (Sutherland et al., 2020; Gilmore et al., 2021).

The specific role in the memory processing is atributed to the medial prefrontal cortex, which receives direct projections from ventral hippocampus and carries information about context-related aspects of the memorized experience. It is proposed that the medial prefrontal cortex coordiates memory retrieval by ensuring recall of pattern that is relevant for particular context (Eichenbaum, 2017). The prefrontal cortex is also involved in schema-based learning, which exploits common features across the tasks to enhance the task acquisition (Spalding et al., 2015).

The medial prefrontal cortex seems to be particularly imprtant for processing of remote memories. Based on this, some authors argue that medial prefrontal cortex might in part substitue the role of hippocamus for more remote memories (Tonegawa et al., 2018). Employing recently developed methods for tracing and manipulation of memory engram cells, it was revealed that learning induces rapid formation of memory engrams in both hippocampus and medial prefrontal cortex (Kitamura et al., 2017). However, the prefrontal engram cells undergo gradual functional and structural maturation, which is dependent on the interaction with the hippocampus. Despite the revealed insights, the precise role of the prefrontal cortex in memory is yet to be elucidated (Tonegawa et al., 2018, Eichenbaum, 2017)

1.2.7 Cellular substrate of memory engram

Learning has to be associated with adaptive changes in the structure of neural tissue that lead to subsequent change in neuronal activity dynamics and eventually to change in the behavior. Such modifications, occurring either on presynaptic or postsynaptic sites, are expected to be directly or indirectly reflected in change in functional synaptic connectivity and they can be thus formalized as change in synaptic weights (Churchland and Sejnowski, 1992). Donald Hebb in his influential book *Organization of Behavior* (Hebb, 1949) proposed a principle that would govern learning-associated synaptic modifications: coactivation of mutually connected cells facilitates strength of the underlying synapses. A consequence of increased synaptic strength is increased response of postsynaptic neurons to respective presynaptic activity.
This enables related neuronal representations to be represented by functionally coupled neurons and creation of more complex representations (Churchland and Sejnowski, 1992).

Bliss and Lomo (1973) performed a study on anesthetized rabbits that revealed a potential physiological substrate of memory-related synaptic plasticity. They observed that high-frequency stimulation of the perforant input to dentate gyrus led to enhanced postsynaptic response to subsequent low-frequency pulse, compared to the baseline conditions. This response enhancement persisted in intact preparation for up to several weeks (Bliss & Gardner-Medwin, 1973) and was later named long-term potentiation (LTP).

What are the molecular mechanisms of the LTP? The central role is attributed to NMDA glutamate receptors, which are ion channels allowing cellular influx of calcium. The special feature of NMDA receptors is that they get activated when both 1.) glutamate binds to the receptor's site and 2.) membrane is depolarized above a specific threshold. This conjunctive ligand binding and voltage sensitivity enables NMDA receptor to detect coincidence of two events, allowing it to act as 'Hebbian molecule'. Sufficiently strong input stimulation facilitates synapses within input-specific site in homosynaptic LTP, as observed by Bliss and Lomo. In addition, the synapses can be facilitated when the respective input is relatively weak, but sufficient depolarization is provided by coincident activation of other strong input converging on the same downstream target. This form of plasticity plays an essential role in hippocampal memory system.

Activation of NMDA receptors triggers influx of calcium ions, activating intracellular signalling cascades, which in later phases involve transcription changes at genes level. Early phase of LTP includes facilitated activation of AMPA receptors and insertion of new ones, while later stage, responsible for long-lasting LTP

is dependent on protein-synthesis and leads to morphological changes such as increase in dendritic spines (LTP mechanisms reviewed in Citri and Malenka, 2008).

While described features fit well with the idea of LTP as a substrate of memory storage mechanism, providing direct experimental evidence for this hypothesis has been difficult.
Pharmacological interventions that interfere with LTP induction and LTP maintenance impair spatial memory (Morris et al., 1990; Pastalkova et al., 2006). However, since the effects of these interventions are not necessarily limited to LTP mechanisms, they cannot be considered as definitive proof of LTP-memory link. Only recent technological advances have enabled employment of more selective approach. In one such a study, pairing optogenetic stimulation of auditory input to amygdala with a foot shock delivery led to fear conditioning and input-specific changes in amygdala indicative of LTP. The memory was then inactivated by reversing the LTP by long-term depression at respective synapses but subsequent optogenetic potentiation of the auditory input rescued memory (Nabavi et al., 2014).

The novel techniques of memory engram cells labelling and subsequent manipulation by optogenetic tools have enabled unpreceded possibilities to probe the nature of memory trace. It was shown that optogenetic reactivation of the labelled engram cells induces memory recall, confirming theoretical predictions (Liu et al., 2012). The techniques were even used to create a false memory: when the dentate cells active during contextual conditioning were later reactivated in another context, it led to artificial association between the context and aversive stimulus (Liu et al., 2014).
Further, it was directly demonstrated that learning induces enduring physical changes on the engram cells in the form of increase in dendritic spines. The application of anisomycin supressed the increase in the dendritic spines and prevented memory recall. However, it was still possible to induce recall by optogenetic activation of labelled dentate engram cells (Ryan et al., 2015). This suggests that memory can still persist in a form of silent engram, probably defined by functional connectivity, but cannot be effectively accessed by natural cue for appropriate recall (Tonegawa et al., 2015).

1.3 The cognitive map in the hippocampal formation

The question of the nature of space and its relation to mind has intrigued many thinkers throughout the history. The epistemological approaches to spatial cognition range from empiricism, where mental representation of space is crafted solely based on sensory experience, to rationalism, emphasizing role of reason in spatial knowledge acquisition (Boccara, 2014). A different position was held by Immanuel Kant, who argued for the notion of space as a priori existing feature of perceptual experience (Kant, 1781).

The mental representation of space was also studied by behavioral psychologists. Tolman (1946) observed, that when familiar route to reward was blocked, the rats tended to select the newly introduced corridor that extended towards the place of reward. This ability suggests that rather than relying on simple stimulus-response strategy during navigation, the rats were able to create representation of space or cognitive map.

What information can be utilized by brain to create spatial representations? In general, there are two main principles that can support navigation (Buzsaki and Moser, 2013). In map-based, allocentric navigation, the position of subject is defined in relation to landmarks and spatial relationships between them. On the other hand, egocentric navigation is based on computing distances and directions involved during travel from starting reference position. This computation, also known as path integration, requires information about motion speed, elapsed time and direction of movement.

Both allocentric and egocentric navigation can be effectively combined to infer position of the subject in the spatial environment (Buzsaki and Moser, 2013). When there is deficit of reliable landmarks, for example in darkness, self-motion-based path-integration might become predominant mode of navigation. However, the path integration tends to accumulate errors and benefits from frequent cue-based update of the actual position.

The key milestone in search for neural basis of spatial navigation was discovery of place cells by O'Keefe and Dostrovsky in 1971. They employed the technique of extracellular recordings to record activity from hippocampus in freely moving rats and observed that individual cells fire consistently when a rat was occupying a particular position of the environment. The analysis of place cell activity led to formulation of the theory of hippocampus as a cognitive map by O'Keefe and Nadel (1978).

Later, other neuronal components of brain navigation system were described. Among them, particularly significant was the observation of strikingly regular spatial firing of grid cells in the medial entorhinal cortex by research team of May-Britt and Edvard Moser (Fyhn et al., 2004; Hafting et. al, 2005). The place cells and the grid cells provide unique opportunity to observe single neuron correlates of highly complex cognitive processes in the brain. This major breakthrough led to Nobel Prize in Physiology or Medicine for 2014, which was awarded to John O'Keefe, May-Britt Moser and Edvard Moser, "for their discoveries of cells that constitute a positioning system in the brain."

Following discoveries in rodents, individual constitutents of 'brain's GPS' were also observed in hippocampal formation of humans, typically neurosurgical patients with electrodes positioned in medial temporal lobe and engaging in virtual navigation tasks (Ekstrom et al., 2003; Jacobs et al., 2013). This reveals considerable universality of principles employed by brain to develop mental representations of physical space. The extraordinary transparency of spatial code makes it very suitable tool not only for

studying correlates of navigation and spatial memory, but also for elucidating more general principles of neural computation underlying higher cognitive functions.

1.3.1 The cellular components of brain navigational system

Place cells

During spatial exploration, individual pyramidal cells of the hippocampus are typically active at specific locations of environment. The cells with such spatial modulation are called place cells and spatial locations of their increased activity are the respective place fields. Each active place cell thus represents specific position in the environment and collectively the place cells are thought to form substrate of mental representation of space, also known as a cognitive map (O'Keefe and Nadel, 1978). The established place cell map is reactivated upon re-exposure to the familiar spatial environment (Muller et al., 1987), suggesting a link to spatial memory. The hippocampus is able to create and store multiple maps for different spatial environments. The vast capacity of hippocampus in generating distinct spatial representations was demonstrated in an experiment where rats were able to create uncorrelated CA3 place cell maps for 11 different but similar environments they were exposed to (Alme et al., 2014).

The change of sensory cues such as visual landmarks leads to change in place cell activity, in the process called remapping. For example, rotation of a visual cue can induce corresponding rotation of place field position (Muller and Kubie, 1987). However, place cell firing is also controlled by idiothetic self-motion cues, which can support place field when extrasensory cues are limited, such as after turning off lights (Quirk et al., 1990). In a recent study (Jayakumar et al., 2019) with an augmented reality, the rats run on a circular track, while the projected visual landmarks moved with different velocity relative to movement of a rat. During such a conflict between visual cues and path integration, firing of the place cells was under robust control of the visual cues, in accord with the view where the sensory landmarks exert correcting influence over path integrator. The hippocampus thus integrates inputs from upstream entorhinal areas, combining both extrasensory and idiothetic information to create place cell map of the environment.

The extent of place field remapping across different environments reflects their mutual similarity. A situation with similar enclosures at the same location within global (room) reference frame gives rise to rate remapping, where the place fields maintain their positions but firing rates within the place fields are different across environments. Such a rate modulation might represent code for different experience occurring within given spatial context (Colgin et al., 2008). If the environments are substantially different, the place cells manifest global remapping, completely changing place field positions. This form of remapping is reinforced when the enclosures are placed each at a different location in space (Colgin et al., 2010). The global remapping of place cells might involve selective activity of a cell in only one of the environments. In a contrast to gradual nature of the rate remapping, the global remapping tends to occur in abrupt all-or-none manner (Colgin et al., 2008; Colgin et al. 2010).

The place cells' properties are dependent on anatomical localization within the hippocampus. The size of firing fields of place cells systematically increases from dorsal to ventral pole of hippocampus (Kjelstrup et al., 2008).

Some differences in place cell coding properties exist between CA1 and CA3 subfields. A lower proportion of CA3 place cells have a place field in a given environment, compared to CA1 place cells (Leutgeb et al., 2004). Furthermore, the place cell maps for similar environments tend to have lower overlap in CA3, which shows strong tendency towards orthogonalization.
Interestingly, pyramidal cells in the CA2 subfield were shown to code for position of a rat during epochs of immobility (Kay et al, 2016).

Despite having well-defined place field, discharge of a place cell is very variable during individual passes through the respective firing field (Fenton and Muller,1998). This phenomenon of activity 'overdispersion' suggests that hippocampal network might switch between different 'substates' or 'maplets' existing within the complex structure of the cognitive map. The excessive variance in place cell discharge might be also related to switching between modes of current sensory input processing and internally driven simulation-like non-local activity (Dvorak et al., 2021). Furthermore, the hippocampal ensembles can dynamically alternate between distinct representations, such as when switching between different reference frames is required for navigation (Kelemen and Fenton, 2010).

The properties of place cells make them seemingly ideal candidate for neuronal substrate of navigation and spatial memory. Still, the involvement of place cells in navigation has been mainly implied based on observation of correlation between their activity and spatial position. Direct evidence for a role of place cells in spatial memory and navigation comes from recent studies, employing manipulation of place cell activity with optogenetics. One of them took advantage of dissociation between place cells' activity and subject's location during sleep (de Lavilleon et al., 2015). Therein, triggering reward stimulation in mice brain whenever a particular place cell was active during sleep induced goal-directed preference towards the respective place field in subsequent active behaviour. In another study, optogenetic activation of place cells coding for reward position induced behaviour associated with consuming reward, while spatially inappropriate activation of other place cells disrupted navigation to rewarded locations (Robinson et al., 2020).

The place cell maps represent more than mere space; they are influenced by cognitive and affective variables associated with the spatial context. For example, induction of contextual fear conditioning was observed to be accompanied by place cells' remapping (Moita et al., 2004). This is consistent with a more general notion of the cognitive map, which includes mapping of variables beyond spatial domain, or even creating map-like representations of purely non-spatial relationships (Aaronov et al, 2017).

Spatial code in the dentate gyrus

The excitatory cells in the dentate gyrus also display place cell-like activity, which differs across the mossy cell and the granule cell populations. While the mossy cells have tendency to fire at multiple locations in the explored environment, the active granule cells tend to have a single place field (Senzai and Buzsaki, 2017, GoodSmith et al., 2017). The single place fields emerge from more disperse activation with accumulated experience (Kim et al., 2020), as predicted by theories of dentate as a competitive network (Rolls, 2007). However, due to their very sparse activation, firing of only small fraction of granule cell population is typically detected during exploration.

Grid cells

What computations underlie generation of the hippocampal place cell code? As disrupting connections between hippocampal subfields spared place cell spatial firing (Brun et al., 2002), May-Britt and Edvard Moser searched for spatial signal in the medial entorhinal cortex, a structure one synapse upstream of the hippocampus. They observed that the cells in this area carry spatial signal, however, unlike place cells firing at a specific location, the spatially modulated cells in the medial entorhinal cortex have multiple firing fields forming a regular hexagonal lattice, tessellating surface of the explored environment. The neurons with such spatial coding properties were named grid cells (Fyhn et al., 2004, Hafting et al., 2005).

Configuration of firing fields of each grid cell has a characteristic grid spacing, which corresponds to distance between the firing fields, grid orientation, which defines relative grid rotation to a reference axis and grid phase, which corresponds to grid translation in space (Moser et al., 2018). The activity of a grid cell in substantially different environments is associated with realignment of the grid pattern in relation to reference coordinates, while the grid spacing remains constant (Fyhn et al., 2007).

The grid cells are organized into a small number of discrete modules, where cells within a module have the same spacing and grid orientation but differ in grid phase (Stensola et al., 2012). Moreover, the cells within the same module show coherent shift in their grid offset across environments (Fyhn et al., 2007; Stensola et al., 2012). The size of grid fields and spacing increases in discrete steps from dorsomedial to ventrolateral part of medial entorhinal cortex, in analogy to increase of place fields along dorsoventral axis of hippocampus.

A mathematical analysis revealed that modular organization of hexagonally firing cells enables effective representation of two-dimensional space while minimizing number of neurons required (Wei et al., 2015). The principle of economy further predicts the ratio between grid scales in adjacent modules to be √e, which is in accord with experimental observation.

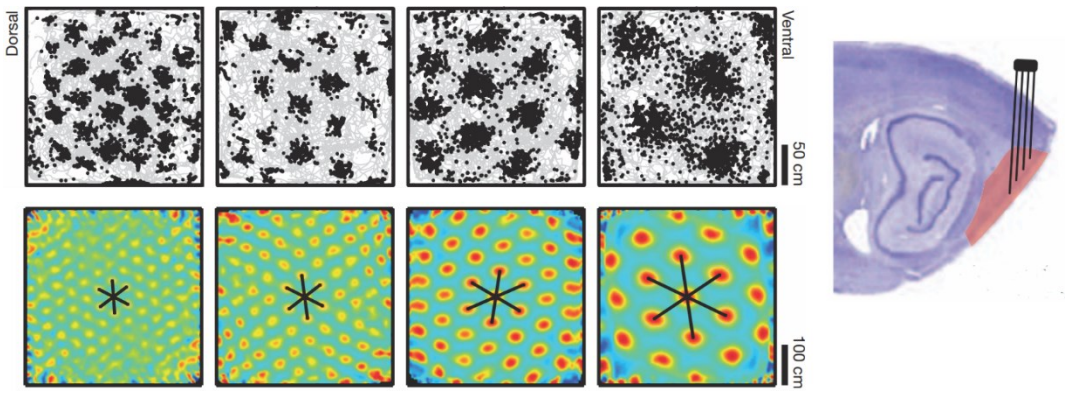

Figure 2 Spatial activity of four example grid cells. Up: Spiking activity superimposed on trajectory of a rat. The firing fields of a grid cell form a regular grid tessellating the environment. Bottom: Spatial cross-correlograms of the firing rate maps, highlighting periodicity of firing pattern and increase in grid spacing from dorsal to ventral medial entorhinal cortex (from left to right). Right: Illustrative depiction of the respective recording sites. Adapted, with a permission, from Stensola et al. 2012.

The smoothness of grid maps and a notion that grid cells maintain their firing fields after removal of silent cues suggested that grid firing might be under primary control of self-motion cues, and thus be driven by path integration. Indeed, mice with selective grid cell dysfunction are impaired in performing path-integration (Gil et al., 2018). The head-direction cells and speed cells might provide grid cells with essential signal needed for path-integrating computations, while environmental sensory cues might play a role in determination of context-specific grid parameters and correcting errors produced by path integrator (Moser et al., 2008).

It is supposed that grid cells provide path integration signal to support hippocampal place fields. Within the concept, individual place cells receive input from particular subset of grid cells with respective grid parameters, leading to spatially defined place cell activity. The realignment of grids across environments goes hand in hand with global remapping in place cell population (Fyhn et al., 2007). However, place fields are only partially disrupted by ablation of medial entorhinal cortex (Hales et al., 2014), while grid firing is lost during hippocampal inactivation (Bonnevie et al., 2013). This points to bidirectional hippocampal-medial entorhinal functional loop, where activity of place cells and grid cells influence each other, while, in addition, spatial modulation of place cells can be supported to a great extent by the parallel stream of information from lateral entorhinal cortex.

The regular hexagonal firing of grid cells led to conjecture that grid cell activity provides spatial metric, a form of 'geographic coordinates' in allocentric map. However, recent studies suggest that regular hexagonal modulation might be not invariable property of grid cell activity. When rats explore enclosures with less regular boundaries, such as trapezoids, the perfect hexagonal symmetry becomes broken (Krupic et al., 2015). Moreover, grid fields tend to accumulate around the reward locations, distorting regularity of grid map (Boccara et al., 2019, Butler et al., 2019). Thus, it seems that disrupted statistical symmetry of the task structure is reflected in distortion of grid symmetry. This suggests involvement of grid cell activity beyond simple metric of space.

Border cells

A proportion of cells in medial entorhinal cortex was shown to have firing fields along environmental borders in particular orientation that is specific for given cell (Solstad et al., 2008). Neurons with similar coding properties were also found in subiculum and parasubiculum (Lever et al., 2009; Solstad et al., 2008). Based on connectivity pattern within hippocampal formation, the subiculum was suggested as the source of border-specific entorhinal signal (Lever et al., 2009). The border cells display similar firing along inserted barriers which are parallel to preferred border orientation and maintain border cell firing across different environments (Solstad et al., 2008). The border-related firing can be utilized for navigation in that it might provide information about environmental boundaries and barriers for route planning and might also help to stabilize path integration.
The existence of cells tuned to distance and direction relative to environmental borders was proposed by simple boundary vector cell model of place cells, where spatial modulation of place cells emerges from thresholded summation of several boundary vector cells (Hartley et al., 2000).

Head direction cells

Representation of direction of travel is expected to play an essential role in network computations supporting spatial navigation. The head direction cells, which provide directional signal were first described in postsubilculum (Ranck, 1984) and later in several other linked structures, including brainstem, mamillary bodies. anterior dorsal thalamic nucleus, entorhinal cortex, retrosplenial cortex and others (Peyrache et al., 2015; review Taube, 2007). The head direction cells display tuning to subject's head orientation (planar azimuth), with each cell firing with maximal frequency for a specific angle of head direction. The directional information is assumed to be utilized by the grid cells for path integration; this can be achieved by the direct projection from the postsubiculum to the medial entorhinal cortex (van Groen and Wyss, 1990).

The vestibular system providing information about head rotation seems well-suited source of input to control head direction signal. This is confirmed by observation that lesions of vestibular system lead to loss of head direction tuning (Stackman and Taube, 1997). In addition, rotation of prominent visual cue leads to corresponding rotation of preferred angle (Taube et al, 1990). The observation of unaltered tuning after switching off lights (Taube et al, 1990) and experiments with allothetic-idiothetic cue mismatch (Stackman and Zugaro, 2005) further indicate that both allothetic and idiothetic cues influence head direction tuning (Taube, 2007).

While sensory inputs effectively control head direction firing during typical behavioral conditions, activity of the head direction cells population also displays robust internal organization. When network activity is decoupled from the sensory drive, such as during sleep, firing of head direction cells resembles continuous drift along a virtual ring (Peyrache et al., 2015). This is consistent with ring-attractor network model, where external input and intrinsic network interactions cooperate to move activity packet along one-dimensional circular manifold.

Object-vector cells

Positional representation referenced to objects would be particularly useful for landmark-based navigation. Neurons with this form of modulation were observed in recordings from superficial layers of medial entorhinal cortex of mice (Høydal et al., 2019). The firing rate of these cells depends both on direction and distance from object placed in the environment, with firing field robust to the object displacement within testing enclosure and generalizing across different objects. The activity is independent of heading direction within the field, indicating object-vector coding within allocentric framework.

Speed cells

A dedicated population of cells carrying speed signal was found in the medial entorhinal cortex (Kropff et al., 2015). The cells display linear relationship with running speed, which is context-invariant. They might thus represent theoretically predicted cellular correlate of speed signal that is utilized for path-integration and supports spatial activity of grid cells.

1.3.2 Medial vs lateral entorhinal cortex in representation of space

The hippocampal place cells are controlled by inputs from both medial and lateral entorhinal cortex, respectively, which are supposed to provide the place cell population with different information. The classical model suggested that the medial entorhinal cortex is source of spatial signal, while the lateral entorhinal cortex would provide less spatially tuned sensory information (Hargreaves et al., 2005). Within the dichotomy, the lateral and the medial entorhinal cortex are also viewed as extension of 'what' and 'where' streams of sensory information flow described at earlier stages of sensory processing.
The neurons within lateral entorhinal cortex display coding for egocentric relation to objects (Wang et al., 2018), as well as more complex traces of experience (Tsao et al., 2013), including flow of time (Tsao et al., 2018).
In contrast, the cells in the medial entorhinal cortex code for spatial relationships within allocentric framework; collectively they can represent relational aspects and create the respective map.
The medial entorhinal cortex thus might provide allocentrically defined spatial context of experience, while the lateral entorhinal cortex reflects the respective egocentrically perceived sensory content (Knierim et al., 2014).

1.3.3 From physical to abstract space

While the cells within the hippocampal formation display robust spatial coding properties, involvement of the same networks in in cognitive processes beyond spatial navigation argues for hippocampal coding not restricted to the domain of physical space. Are there hippocampal codes for more abstract cognitive spaces? The question has been investigated in several recent studies.
In one study, the rats were trained to use a joystick to continually change frequency of presented sound stimulus towards a rewarded frequency zone (Aaronov and Tank, 2017). Many of the cells in the hippocampus and the medial entorhinal cortex displayed tuning for a specific range of frequency, having discrete firing fields in a continuous frequency space. The cells in the medial entorhinal cortex tended to have multiple firing fields, resembling the grid cells. This is in support for the idea that hippocampal-entorhinal network can employ coding mechanisms used for spatial navigation to map non-spatial concepts.

Another experiment showed that the cells in the entorhinal cortex of monkeys display grid cell-like firing to map position of gaze in visual scene (Killian et al., 2012).
In a particularly noteworthy study (Constantinescu et al., 2016), the human participants observed morphed birds with changing length of their legs and neck, in order to achieve a target configuration. During such a navigation in abstract "bird space", the fMRI signal from the medial entorhinal cortex and other areas displayed precise six-fold modulation, which is observed during spatial navigation and is considered to be a proxy for grid cells firing. The network mechanisms implemented for representation of physical space can be thus utilized for mapping representations even in abstract conceptual space.
Altogether, the results of the studies indicate that navigation-related hippocampal mechanisms may represent more general computational principle for mapping relational knowledge.

The entorhinal grid cells and object vector cells display similar activity patterns across different environments and objects, respectively. The activity of the cells in the medial entorhinal cortex might thus generalize across different tasks with same statistical structure (Behrens et al., 2018). Accordingly, the hippocampal-entorhinal system might be designed to represent relational knowledge in more general sense and statistical structure of the task analogous to navigation in space subsequently leads to emergence of analogous coding properties at a single-neuron level.
It is also possible that the hippocampal-entorhinal circuitry mechanisms that were originally developed for spatial navigation, later evolved to represent more general cognitive spaces (Bellmund et al., 2018).

1.3.4 Representation of time in lateral entorhinal cortex

The creation of episodic memories requires integration of memory content within respective spatial and temporal context (’what‘, ’where‘ and ’when‘). How time is represented in the hippocampal formation has been an intriguing question. In the hippocampus, specific sequences of neuronal activity were observed during delay period of working memory task (Pastalkova et al., 2008, MacDonald et al., 2011). The phenomenon of these ’time cells‘ or ’episode cells‘ reveals neuronal representation of time during short periods of learned behavior. However, effective coding of time suitable for episodic memories requires it to arise spontaneously without training and to be able to reflect different timescales of various experiences.
Tsao et al. (2018) observed that many cells in the lateral entorhinal cortex display ramping activity, either increasing or decreasing firing across specific time intervals, such as duration of single trial of foraging in square enclosure or duration of whole recording session of repeated foraging trials. The significant modulation of activity by time at a single cell level was reflected in accurate decoding of temporal epochs ranging from individual trials down to 1 second long intervals. In a subset of experiments with more stereotyped structure of behavior, where rats run on 8-shape maze, the decoding accuracy for an individual trial decreased, while representation of time within a particular trial increased. This indicates that rather than working in a rigid clock-like mode, the temporal code is flexible and possibly emerging inherently from integrating the change of experience. The lateral entorhinal cortex thus possesses temporal signal that emerges spontaneously to represent time, making it well-suited to constitute adaptively flexible time code for episodic memory processing.

1.4 Rhythms of the hippocampal network

1.4.1 Rhythms of the brain

Neuronal oscillations, arising from periodic changes in excitability of neurons, are phenomenon spanning multiple levels of brain organization, from single cell level to distributed neuronal networks.
The synchronous transmembrane currents across neuronal population can give rise to extracellularly detectable rhythmic changes of local field potential. This is reinforced when anatomical organization allows for effective summation of contributions by individual neurons, such as in the hippocampus.
The important role in rhythm generation is attributed to inhibitory interneurons, which orchestrate precise timing of excitation and inhibition in neuronal networks (Zitricky and Jezek, 2017).
The neuronal oscillations' repertoire is rich and in mammalian forebrain covers frequency range from 0,05 Hz to 500 Hz (Buzsaki & Draguhn, 2004). The oscillatory patterns oftentimes represent signature of specific network states in respective brain regions.

Are the oscillations present in neuronal populations just mere epiphenomenon of network activity or represent an essential feature enabling effective network computation?
In a seminal study, Gray et al. (1989) observed synchronous oscillatory responses across spatially separated, feature-specific columns in visual cortex, underlying coherent representation of stimulus properties. This led to hypothesis that synchronous oscillations might provide a solution to so-called 'binding problem', which reflects a need for spatially distributed processing of different stimulus aspects to be coherently unified within a single percept.
Based on this and further studies, neuronal synchrony at various timescales has been conjectured to be basis of reciprocal interaction between neuronal populations.
The oscillations can coordinate neuronal interaction via multiple complementary mechanisms.
Synchronous excitation of neurons can enhance activation of their downstream targets. The effectiveness of the interaction is further potentiated by oscillatory coupling between the upstream and the downstream populations. The excitatory fluctuations of membrane potential increase neurons' responsiveness to incoming input, providing a window of opportunity for entrainment of spiking activity.
The communication through coherence hypothesis (Fries, 2005) postulates that coherent oscillations between distinct neuronal populations are important for effective transfer of information.
Moreover, network oscillations can coordinate mechanisms of synaptic plasticity by synchronizing activity within the critical time window (Buzsaki and Wang, 2012). In addition, the synaptic strength can be either reinforced or weakened, depending on precise timing of input arrival in relations to phase of ongoing oscillations (Hasselmo et al., 2002).
The temporal structure provided by oscillations also enables active neurons to represent information by precise timing of spikes relative to background oscillation (O'Keefe and Recce, 1993; Kayser et al., 2009). This combination of phase code with firing rate considerably expands coding capacity of spike train (Kayser et al., 2009).

1.4.2 Hippocampal oscillations

Analysis of local field potential recordings from rodent hippocampus led to recognition of network modes with characteristic oscillatory signatures (O'Keefe and Nadel, 1978; Colgin 2016). The active behavior, associated with locomotion and exploration, requiring active processing of sensory information, is accompanied by slow sinusoidal theta oscillations. Theta rhythmicity also governs hippocampal network during REM stage of sleep. The epochs of quiet sitting, drinking, eating and grooming and epochs of NREM sleep are associated with slower pattern called large irregular activity. This state is also associated with occurrence of tens of milliseconds lasting "spikes", referred to as sharp wave-ripples.
The rhythmic activity in the hippocampus has been shown to be essentially involved in memory processing. The theta/non-theta states duality inspired two-stage model of memory trace formation (Buzsaki, 1989), where theta is associated with online flow of information from neocortex, creating initial memory trace, which is further consolidated during plasticity-inducing population bursts associated with sharp wave-ripples during non-theta epochs.

1.4.2.1 Theta oscillations

Theta rhythm in rats corresponds to 5-12 Hz oscillation. It is dominant hippocampal oscillatory pattern during locomotion and attending to sensory stimuli, as well as during REM sleep. Theta waves in rat are not completely symmetrical, but resemble sawtooth pattern, with steeper ascending component.
Theta oscillations are not synchronous across whole hippocampus, but represent travelling waves spreading along septotemporal axis (Lubenov and Siapas, 2009).
Theta amplitude and waveform significantly vary across hippocampal recording sites. In contrast, frequency of theta oscillations tends to be highly stable across whole hippocampus (Kropff et al., 2021).
Power of theta increases with speed of locomotion (Whishaw and Vanderwolf, 1973), while frequency is linearly modulated by positive acceleration (Kropff et al., 2021).

Theta generation

The classical model of theta generation has been based on the observation that disruption of the medial septum abolishes theta oscillations in hippocampal network (Winson et al., 1978, Mizumori et al., 1990). The medial septum, containing GABAergic and cholinergic neurons targeting hippocampal formation, was proposed to serve as a pacemaker of hippocampal theta rhythm. The septal GABAergic cells target perisomatic interneurons and their discharge at theta frequency generates rhythmic disinhibition of the pyramidal cells (Toth et al., 1997). Theta oscillations at pyramidal level are further co-regulated by cholinergic entrainment of inhibitory interneurons, presumably modulating theta amplitude (Lee et al., 1994; Teles-Grilo Ruivo and Mellor, 2013).
In addition to afferents from the septum, there are other complementary generators of hippocampal theta rhythmicity (Buzsaki, 2002). At the level of distal dendrites of the pyramidal cells, excitatory postsynaptic potentials at theta frequency are evoked by input from the entorhinal cortex. This is associated with emergence of a prominent theta dipole in the stratum lacunosum-moleculare.

As a result of phase shift between the theta generators, hyperpolarization of the pyramidal cell bodies is coincident with dendritic depolarization (Kamondi et al., 1998). This gives rise to the characteristic phase reversal observed in hippocampal theta depth profile (Buzsaki, 2002).

However, spontaneous emergence of theta oscillations has been observed in isolated hippocampus in vitro (Goutagny et al., 2009). Similarly, theta oscillations were also observed in a computational simulation of hippocampal network without rhythmic input (Bezaire et al., 2016). Thus, tendency to oscillate at theta frequency seems to be inherent to intrinsic properties of hippocampal network, involving several types of interneurons with specific microcircuitry organization.

Functions of theta oscillations

Importance of hippocampal theta for memory processing has been indicated by observations of amnesia resulting from experimentally disrupted theta rhythmicity.
In an early study, Winson (1978) showed that loss of theta after electrolytic lesion of the medial septum was associated with inability of rats to navigate towards previously learned reward locations. Memory deficits after septal disruption were confirmed by further studies (Mizumori et al, 1990; Leutgeb and Mizumori, 1999).
Subsequent research revealed that theta oscillations can support hippocampal computations by multiple complementary mechanisms.

Theta oscillations represent periodic excitation and inhibition of hippocampal network, with periods of higher excitability being associated with higher probability of pyramidal cell activity. In this way, theta mediates “chunking” of hippocampal computation into discrete packets, providing network with flexibility to express the relevant activity pattern according the momentary computational demands.

Timing of the place cell discharge in relation to theta phase displays specific pattern in form of theta phase precession, enabling phase coding to be employed in representing information (O’Keefe and Recce, 1993). Moreover, at population level, neuronal activity is sequentially organized into internally coordinated ‘theta sequences’, which are important for memory processing. In a delayed T-maze task, inactivation of the medial septum and resulting theta disruption led to loss of fine-scale sequences of activity, which was associated with memory deficit (Wang et al., 2015). Similarly, memory impairments follow disruption of theta-coordinated activity by application of cannabinoids (Robbe and Buzsaki, 2009).

Theta oscillations have been also proposed to mediate temporal segregation of memory encoding and retrieval, two main modes of ‘online’ memory processing (Hasselmo et al., 2002). According to the model, the encoding stage occurring at peak of pyramidal theta is associated with strong entorhinal input depolarizing the dendrites of CA1 pyramidal neurons. At the same time, input from CA3 is weak, but enhanced LTP enables heterosynaptic associations. During theta trough, strong CA3 input drives retrieval of stored pattern.

Theta oscillations can support synchrony between hippocampus and functionally related regions.
Theta rhythms are detected in various extrahippocampal structures, including neocortex, striatum and amygdala (Seidenbecher et al., 2003; Tort et al., 2008).

A prominent example of a structure displaying theta coupling with hippocampus is the prefrontal cortex. Hippocampal-prefrontal interactions are involved in many cognitive functions, such as working memory, decision-making and memory recall.
During working memory task, neurons in the medial prefrontal cortex increase their phase locking to hippocampal theta (Wilson a Jones, 2005). Notably, the phenomenon is weakened in the genetic model of schizophrenia (Sigurdsson et al., 2010).
The prefrontal cortex is also important for behavioral flexibility and increase in theta coherence between hippocampus and the medial prefrontal cortex was observed upon learning of new rule in Y-maze task (Benchenane et al., 2010).
In summary, these findings provide evidence for the notion that hippocampal-prefrontal interactions are acccompanied by theta coupling between the regions.

Further, theta-mediated coordination of activity might be important for sensory information processing. In a study, where rats were trained to use their whiskers to discriminate between surface textures, the discriminatory period of the task was associated with phase locking of both whisker movements and activity of primary somatosensory cortex neurons to hippocampal theta (Grion et al, 2016). Robust phase locking of sensory sampling to theta might be particularly important in the view of model, where theta phase-specific computations underlie current sensory information processing vs future state prediction (Wang et al., 2020).

Theta phase precession and its mechanisms

During traversal of a place field, the place cell firing occurs at progressively earlier phase of ongoing theta oscillations. The phenomenon was first described by O'Keefe and Recce (1993) and is known as theta phase precession. They showed that theta phase of spiking activity correlated more strongly with position of the rat in the place field than with elapsed time since the place field entry. Originally observed on a linear track, theta phase precession was also detected during traversals of place fields in two-dimensional arenas (Huxter et al.,2008). The spike-phase relationship thus provides additional possibility to represent information in addition to rate code.
A proposed biophysical model of phase precession assumes interaction between ramping dendritic excitation and somatic inhibition (Kamondi et al., 1998). As a rat enters a place field, the driving entorhinal input triggers progressively increasing excitation at the dendrites of the respective place cell, which in turn overcomes somatic inhibition at a progressively earlier phase of the theta cycle.
Furthermore, temporal interplay between inputs from upstream regions can contribute to spike time tuning of hippocampal place cells. The discharge of CA1 place cells is controlled by entorhinal input at the peak of theta, while CA3 input predominates in phases closer to trough of theta cycle. The gradual change in relative strength of the inputs in control of a place cell firing modulates spike-theta phase relationship (Fernandez-Ruiz et al., 2017).
The entorhinal grid cells display theta phase precession that is independent of hippocampal feedback input (Hafting et al., 2008). The ablation of the medial entorhinal cortex leads to loss of phase precession of hippocampal place cells (Schlesiger et al., 2015). In contrast, blockade of CA3 output does not eliminate phase precession of CA1 place cells (Middleton and McHugh, 2016).

Spike timing consistent with theta precession can also arise from coordinated interactions between asymmetrically connected cell assemblies, as proposed by network connectivity models (Romani and Tsodyks, 2015).
Altogether, theta phase organization of place cell activity likely emerges through interaction of various factors, including temporal pattern of external inputs strengths, single cell-level biophysical properties and coordination between cell assemblies.

Theta sequences

During movement on a linear track, spikes of active place cells are organized into sequential order reflecting order of the place fields on the track (Skaggs et al., 1996). As a consequence, these 'theta sequences' represent time-compressed version of sequential place cells' activation occurring at behavioural timescale (Fig. 3). Accordingly, single theta cycle binds together activity of neurons with place fields centres at past, current and future positions, representing a segment of animals' trajectory.
While theta sequences are consistent with theta phase precession, they cannot be fully accounted for by phase precession of individual place cells (Foster and Wilson, 2007).
Theta sequences are absent during first run on a novel track, while individual place cells still display phase precession (Feng et al., 2015). The emergence of theta sequences with experience suggests that their generation might depend on synaptic plasticity mechanisms occurring during learning. The synaptic plasticity modifies connectivity strength between neurons, which can influence internal coordination of cell assembly activation.
Then during repeated traversal of familiar space, the activation of place cells can be influenced by internally coordinated activity, where activity of a cell assembly activates another cell assembly based on synaptic connectivity influenced by the previous experience (Dragoi and Buzsaki, 2006).
A similar mechanism of internally-coordinated cell assemblies' activation is proposed to underlie sequences of episode cells, occurring during delay period of working memory task (Pastalkova et al., 2008). Theta oscillations thus might be essential in mediating internally driven cell assembly activation. In this line, suppression of theta leads to disruption of theta sequences and diminished episode cells activity (Wang et al., 2015).
Internal coordination of activity gives rise to prospective coding and other forms of generative activity. At a decision point of T-maze task, theta sequences sometimes reflect possible trajectories of the animal (Johnson and Redish, 2007). A similar 'look-ahead' pattern can be involved in representing intended actions: in a task where a rat could run along several segments of a track to stop at one of feeders along the way, the length of the 'look-ahead' sequences was related to length of intended trajectory (Wikenheiser and Redish, 2015).
It remains to be elucidated, to what extent the neuronal coordination underlying theta sequences reflects intrinsic dynamics within hippocampal network as opposed to coordination inherited from upstream structures, such as the entorhinal cortex.
Recent work has modified the original model of theta sequences, which postulated forward-depicting sequences spanning from past to future locations. It was revealed that prospective forward sequences alternate with retrospective reverse sequences within individual theta cycles, with the retrospective component occurring near theta peak and the prospective component near theta trough, respectively (Wang et al., 2020).

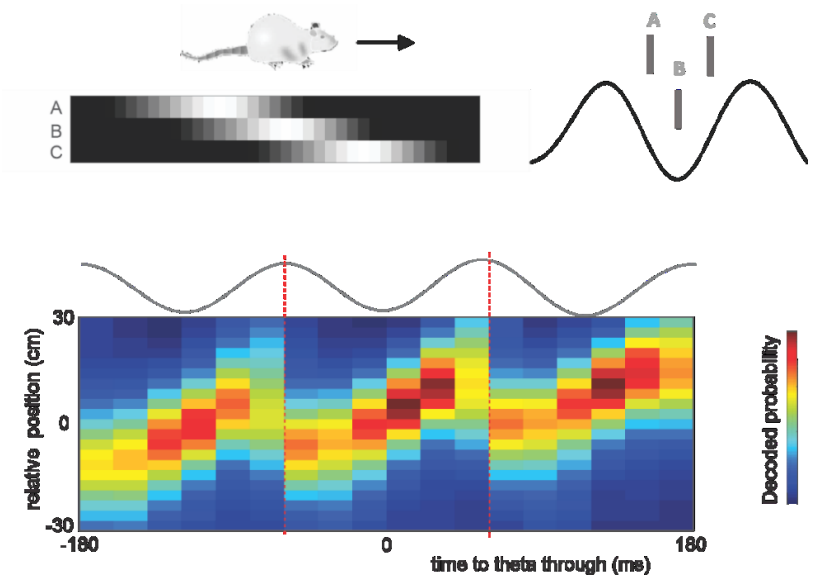

Figure 3 Place cell activity within a theta cycle reflects order of the place fields in a space, giving rise to time-compressed representation of a segment of the trajectory. Bottom: Bayesian decoding of theta sequences related to the current position of a rat, averaged across a session. Data: Zitricky et al., unpublished.

1.4.2.2 Gamma oscillations

Gamma oscillations correspond to fast rhythms within 25-150 Hz range. In the hippocampus, gamma rhythmicity typically emerges in association with theta states, where gamma oscillations co-occur with higher amplitude theta oscillations. The further division of hippocampal gamma into distinct components includes slow gamma (25-50 Hz}, mid-frequency gamma (60-100 Hz) and fast gamma (>100 Hz) rhythms. Functional distinction between the gamma subtypes is suggested by observations of their different modulation by phase of theta, different dependence on speed of locomotion and association with different stages of memory tasks (Colgin, 2015).
Recent unsupervised approaches (Lopes-dos-Santos et al., 2018, Zhang et al., 2019) identified two different subcomponents within mid-frequency gamma range, however better understanding of its functional relevance requires further investigation.

Gamma generation

The theoretical models of gamma generation emphasize the effectiveness of the perisomatic inhibition in network synchronization (Buzsaki & Wang, 2012). Within the framework of 'I-I model', the gamma oscillations arise in interconnected network of interneurons driven by tonic or stochastic input. In the 'E-I model', gamma rhythmicity is produced by reciprocal interplay between pools of excitatory and inhibitory neurons (Buzsaki & Wang, 2012).

The experimental evidence supports the notion that slow gamma in CA1 is entrained by input from CA3, while mid-frequency gamma is driven by input from the entorhinal cortex (Schomburg et al. 2014, Yamamoto et al., 2014). In accordance, maximal slow gamma power is detected in stratum radium and maximal mid-frequency gamma power is present in stratum lacunosum-moleculare (Schomburg et al., 2014).
The spectral component corresponding to fast gamma band in CA1 is maximal at the level of stratum pyramidale and is related to spiking activity of pyramidal cells (Schomburg et al., 2014, Dvorak and Fenton, 2014). Its generation is, however, not fully understood, and can reflect both inhibitory post-synaptic potentials of pyramidal cells and contamination by spiking activity.

Functions of gamma oscillations

The network oscillations in gamma frequency band are widely detected across different brain regions, pointing to their potentially universal role in neural computation. The synchronous neuronal activity within a temporal window of gamma cycle facilitates effective integration of the network output by the respective downstream reader population. Such a binding of activity by gamma corresponds to formation of functional cell assemblies (Buzsaki and Wang, 2012). This is further supported by a notion that duration of gamma cycle corresponds to the critical time window of spike-timing-dependent plasticity. Accordingly, hippocampal gamma oscillations orchestrate cell assembly dynamics associated with hippocampal network activity.
Specifically, it has been observed that slow gamma oscillations underlie CA3-CA1 coupling, while mid-frequency gamma synchrony accompanies medial entorhinal cortical-CA1 communication (Colgin et al., 2009, Schomburg et al., 2014).
Experimental evidence provides link between hippocampal gamma rhythm and memory operations. For example, hippocampal gamma power displays increase on the central arm of T-maze alternation task, when the animal needs to make memory-guided decision (Montgomery and Buzsaki, 2007).
Furthermore, different frequencies of gamma oscillations have been implied in different functional modes of hippocampal network (Colgin, 2015). During run on a linear track, slow gamma states are associated with place cells signaling upcoming locations, while place cell activity during mid-frequency gamma states tends to represent current or recent positions (Bieri et al., 2014; Zheng et al., 2016).
Different stages of spatial memory task are also associated with predominance of different frequencies of hippocampal gamma oscillations. The encoding stage is associated with dominance of mid-frequency gamma, while retrieval enhances expression of slow gamma (Lopes-dos-Santos et al., 2018). Similarly, it was observed that avoidance of shock-zone in allothetic place avoidance task is associated with periods of dominance of slow gamma, during which place cells represent the shock zone (Dvorak et al., 2018).
These findings are consistent with a view, where during mid-frequency gamma states, the sensory input conveyed from the entorhinal cortex is instrumental in encoding of the new information. On the other

hand, slow gamma underlying CA1-CA3 coupling promotes recollection, including reactivation of non-local representations.

1.4.2.3 Sharp wave-ripples

The sharp waves-ripples (SWRs) are large negative deflections of local field potential in CA1 stratum radiatum, typically accompanied by fast oscillatory 'ripple' pattern (110-200 Hz) in the CA1 pyramidal layer. Another, more variably present spectral component of SWR is a peak in slow gamma spectrum (20-40 Hz). The observed increase in slow gamma power was originally linked to enhanced CA3-CA1 synchrony (Carr et al., 2012), however a recent finding showed that it might reflect spectral signature of concatenated SWR events (Oliva et al., 2018).

SWRs are associated with highly synchronous spiking activity of hippocampal neurons, where high fraction of neuronal population dramatically increases firing rate (5-6 fold for CA1 pyramidal neurons) and synchrony during a population event. The spike content of SWR-associated bursts is, however, specifically organized and related to spiking patterns during active behaviour

Sharp wave-ripple generation

Removing various hippocampal afferents, such as those from neocortex and septum tends to increase rather than decrease occurrence of sharp wave-ripples (review Buzsaki, 2015). In addition, sharp wave-ripples emerge in isolated hippocampus in vitro, suggesting that SWRs can arise locally in the hippocampus (Maier et al., 2003). However, the SWR events occurring in vivo are influenced by flow of information from upstream cortical areas (Rotschild et al., 2016). Moreover, during awake rest periods, generation of SWR crucially involves input from the medial entorhinal cortex to CA1 (Yamamoto et al., 2017).

Depth-voltage profile associated with SWR is consistent with activation of Schaffer collaterals, indicating involvement of CA3 to CA1 transmission during SWR events (Buzsaki et al., 1983; Buzsaki, 2015). It has been proposed that during SWR initiation synchronous burst is ignited and amplified within CA2-CA3 recurrent collateral system (Oliva et al., 2016) and excitation is propagated by Schaffer collaterals to entrain concurrent CA1 population burst. The excitatory burst of pyramidal cells drives spiking of inhibitory basket cells at ripple frequency (Schlingloff et al., 2014). While optogenetic blockade of CA3 input to CA1 disrupts SWR generation both during awake state and sleep epochs, inhibition of layer III of medial entorhinal cortex projections to CA1 selectively impairs SWR generation associated with awake state. It has been furthermore observed, that awake SWRs in the hippocampus tend to be preceded by ripple events in the entorhinal cortex (Yamamoto et al., 2017).

SWR functions

Memory consolidation

SWR events have emerged as an essential biomarker for processes of memory consolidation. According to the existing model, learning during active theta states gives rise to labile memory trace that undergoes SWR-mediated consolidation into long-lasting trace. This is assumed to involve transfer of information to neocortex and further synaptic potentiation (Buzsaki et al., 1994).

Learning stage of a memory task facilitates SWR occurrence in subsequent sleep (Eschenko et al., 2008). Conversely, suppression of SWR events during sleep following learning in hippocampus-dependent memory tasks leads to memory performance deficit on par with those observed in hippocampally lesioned animals (Girardeau et al., 2009).

The SWR-mediated memory consolidation theory also postulates reactivation of awake neuronal activity patterns to occur within SWR episodes. First observation supporting reactivation of behavior-related neuronal activity in subsequent sleep was made by Pavlides and Winson (1989), who found that place cells coding for locations occupied by the rats in awake session displayed higher firing rate in following sleep compared to other place cells.

Further pieces of evidence came from studies showing SWR-related reactivation of behavior-related activity patterns at the level of cell pairs (Wilson and McNaughton, 1994) and sequences (Nadasdy et al., 1999; Lee and Wilson, 2002). Notably, the sleep replay of wake-detected sequences was observed to occur at shortened, several times “time-compressed” timescale during SWR episodes. These studies paved the way for further extensive research, that has clearly established phenomenon of SWR-associated time-compressed replay (Fig. 4).

To directly address importance of SWR-replay content for memory consolidation, Gridchyn et al. (2020) trained animals to find rewards at specific locations at two different environments. When reactivation of only one environment was disrupted in subsequent sleep, memory recall was impaired specifically in that environment.

Memory consolidation is proposed to involve dialogue between hippocampus and neocortex. What is the role of hippocampal SWRs in this dialogue? It was observed that replay in the hippocampus and neocortex occur in coordinated fashion (Ji and Wilson, 2007). In particular, the neocortical activity pattern preceding SWR biases hippocampal replay, which in turn predicts subsequent neocortical pattern (Rotschild et al, 2017). This might be viewed in a framework where neocortical activity influences replay in the hippocampus, which subsequently triggers widespread coordinated neocortical reactivation, supporting consolidation of coherent memory representation.

Awake replay

SWR-associated replay occurs also during awake epochs and it has been proposed to underlie multiple cognitive functions (Joo and Frank, 2018).

The sequences during awake SWRs are replayed both in ‘forward’ and ‘reverse’ fashion (Foster and Wilson, 2006; Diba and Buzsaki, 2007). The reverse replay frequently occurs at sites of reward, with its rate increasing with reward value (Ambrose et al., 2016). This might serve creation of value gradient assigned to representation of trajectory leading to reward location (Foster and Wilson, 2006).

The multiple experiments suggest involvement of awake replay in activity pattern stabilization and task learning (Roux et al., 2017; Dupret et al., 2010; Jadhav et al., 2012).
Moreover, the forward sequences are related to prospective preplay of intended trajectories (Pfeiffer and Foster, 2013), or reactivated paths to avoided zones (Wu et al., 2017).
SWR-associated patterns might also mediate constructive imagination-like activity going beyond simple retrieval: the place cell sequences sometimes depict trajectories that have never been undertaken by the animal (Pfeiffer and Foster, 2013), including trajectories through unexplored space (Olafsdottir et al., 2015).
Altogether, awake replay seems to be instrumental in retrieval, imagination, such as during evaluating possible actions, that is, during various forms of mental simulation on one hand and in memory trace consolidation on the other. However, the functions do not need to be mutually exclusive, and every awake ripple-associated retrieval might serve consolidation as well (Joo and Frank, 2018).

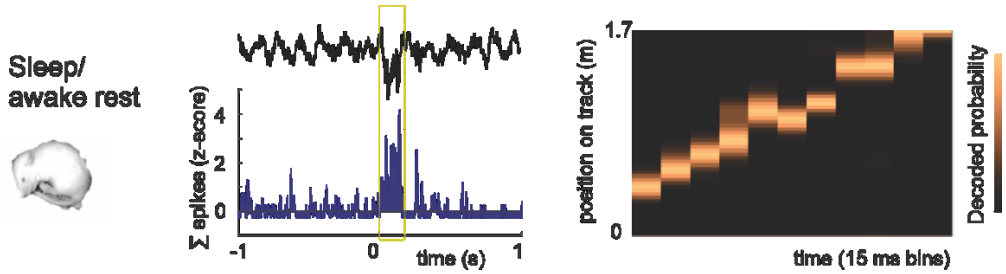

Figure 4 The sharp wave-ripple pattern in local field potential is coincident with an activity burst within hippocampal population. Right: Bayesian decoding of trajectory replay during a SWR (colormap for decoded posterior probability normalized for each temporal bin).

1.4.3 The rhythmic activity in human hippocampus

Theta oscillations are observed in monkey and human hippocampus, albeit they are expressed in brief bouts, which are considerably shorter than rodent theta states (Watrous et al., 2014). The original reports suggested that human theta corresponds to lower frequency band, but recent study found 8 Hz oscillations in posterior hippocampus of humans that was modulated by speed of locomotion (Goyal et al., 2020). The current data indicate involvement of hippocampal theta in human memory and spatial cognition (Herweg et al., 2020), supporting a view, where similar oscillatory mechanisms underlie these hippocampal functions in rodents and humans.
Memory processing in human hippocampus also involves rhythmicity in the gamma band (van Vugt et al., 2010). In line with rodent data, faster gamma oscillations increase during memory encoding, while slow gamma power increase accompanies memory retrieval (Griffiths et al, 2019).
Sharp wave-ripples are also detected in recordings from human hippocampus and they have been shown to support memory consolidation and recall (Norman et al., 2019) and to mediate memory-related sequences of cortical spiking activity (Vaz et al., 2020).

1.5 Attractor dynamics

A particularly fruitful approach in conceptual understanding and quantitative modelling of the nervous systems is looking at the neural network via scope of dynamical systems theory. A dynamical system represents set of variables that undergo evolution in time according specific rules; in the context of brain it is typically represented by activity of neurons developing in time in response to e.g. their mutual interactions.

Behaviour of dynamical system might display existence of specific states, towards which all nearby states tend to evolve, called attractor states. The area of state space within which dynamics flow towards the attractor state represents the basin of the respective attractor and its size corresponds to attractor stability.

The flow of activity can be also viewed within a conceptual framework of energy landscape, where activity tends to move from states of higher energy towards the states associated with lower energy. The energy minima represent stable activity patterns and thus correspond to the attractor states (Fig. 5). The non-increasing energy functions describing behaviour of a system with attractor dynamics are mathematically formalized as Lyapunov (energy) functions.

Attractor states might exist in form of discrete points in a state space (discrete attractors) or as continuous attractors, consisting of isoenergetic continuum of states throughout which system can smoothly transition.

Attractor dynamics approach has been successful in understanding network activity in hippocampal formation and beyond. It has been fruitfully applied in modelling processes such as memory and navigation in hippocampal formation, oculomotor integration, working memory in prefrontal cortex, motor preparation and others (review Khona and Fiete, 2021).

Abnormalities in attractor dynamics have been linked to pathological network states associated with neuropsychiatric disorders. Schizophrenia has been proposed to be associated with shallow attractor basins leading to considerable instability of network state. On the other head, depression and mania might arise from pathologically hyperstable attractors in non-reward and reward regions of the brain, respectively (Rolls, 2021).

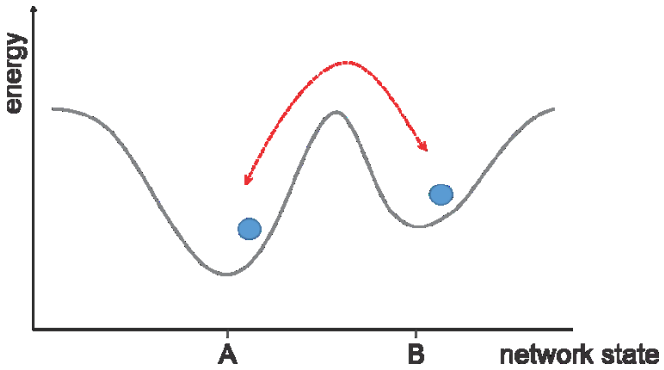

Figure 5 The network state (here represented by a blue ball) travels across an energy landscape with a tendency to settle down in the valleys (energy minima), corresponding to attractor states. (Figure courtesy of Dr. A. Navvabi, inspired by Rolls et al. (2008)).

1.5.1 The Hopfield model

In his classic paper, JJ Hopfield (1982) applied mathematical framework known in statistical physics as Ising model to describe neural network behaviour consistent with memory operations.
The main idea of the Hopfield model is that learning modifies synaptic strengths between the neurons and during the recall, the network state update rule will ensure that it eventually converges onto stored prototype activity pattern.

The neurons in the Hopfield model are binary units which can exist in two states: V=1 if neuron is firing and V=0 otherwise. There is also a symmetric connection between each pair of neurons - the network thus formally corresponds to fully connected, undirected graph.
The active neurons provide excitatory input to the other neurons, which depends on the strength of their mutual connection. This can be mathematically expressed as:

$$\boldsymbol{H(t) = \sum_j w_{ij} V_j}$$

where H(t) is excitatory input to neuron i in time t, w_{ij} is synaptic strength between neurons i and j and V_j is activity of neuron j in time t.
The neurons asynchronously readjust their state to active/inactive, depending on whether total excitatory input is higher or lower than given threshold.
The pattern is stored in form of synaptic weights, which can be set to

$$\boldsymbol{w_{ij} = cP_iP_j}$$

where c is a constant and P_i and P_j are activity of neurons i and j in stored pattern. This rule captures Hebbian rule - neurons that fire together, wire together.

It can be shown that function defined as

$$\boldsymbol{E = -\sum_i \sum_j V_i V_j}$$

is decreasing with each update of the network state until minimum is reached, which means that it represents network's energy function. The neurons will update their activity states and eventually will settle down onto stable activity pattern. It can be shown that activity configuration corresponding to the stored pattern is the minimum of the energy function (the proof is based on implementing the formula for synaptic weight within the energy function formula).

The Hopfield network can thus successfully recall the stored pattern. The analysis can be extended to the case of multiple stored patterns, where each pattern represents one local minimum in energy landscape. The network state will move downhill the energy valley towards the closest local minimum.

Despite many biologically unrealistic simplifications such as binary neurons or full network connectivity with symmetric connections, Hopfield model has many alluring features. The abilities to store and subsequently retrieve memories by effective pattern completion are hallmarks of episodic-like memory computations.

The idea of autoassociative 'content-addressability' superimposed on structuro-functional properties of hippocampal system gave rise to theory of hippocampus as autoassociative network (McNaughton and Morris, 1987; Rolls, 1987; Treves and Rolls 1992). The theory has been extended to biologically more realistic networks with graded response units and diluted connectivity (Treves and Rolls, 1991). The CA3 region of the hippocampus with dense recurrent collateral architecture seems well-fitted for performing autoassociative computations. During learning, the activity pattern in CA3 is induced by strong input from the dentate gyrus and the pattern is stored in the form of synaptic strengths in Hebbian manner, as in the case of the Hopfield network. The recall in the hippocampus can be initiated even by a partial cue provided by the entorhinal input, since autoassociative dynamics is able to retrieve the whole pattern. This essential feature of pattern completion recapitulates Hopfield network dynamics.
Interestingly, Hopfield network's 'error-correcting' ability displays also some extent of robustness in regard to noise in information stored in synaptic weights (MacKay, 2003). Within the biological context this would mean that memory can still be successfully retrieved despite some level of synaptic loss, for example due to damage or physiological synaptic turnover.

1.5.2 Continuous attractors

The continuous attractor is represented by continuous set of points in state space, such as a line, a ring, a plane and other manifolds. The stable pattern can be associated with inherent flow of activity packet along the attractor manifold, as in the case of periodic orbit, or might consist of continuum of quasi-stable fixed points, where arbitrarily small perturbation can relocate the systems' state position within the manifold. The latter is typically the case in the context of neurobiological modelling. However, the true continuous attractor represents rather theoretical limit, which would be approached by neural network realization with infinite units. The models with finite size networks rather describe quasi-continuous attractor landscape, fabricated from densely packed point-like discrete attractors (Stella, 2014).

The continuous attractor models are especially useful for tracking neural representations of smoothly changing stimuli, so that smooth change of input can lead to smooth readjustment of network state without need of crossing considerable energetic barrier.

One dimensional continuous attractors have been widely employed for modelling neuronal system representing head direction (Skaggs et al, 1995; Zhang, 1996). In the models, head direction cells are organized into a virtual ring, where position of a cell corresponds to the preferred directional tuning in allocentric framework. The recurrent network architecture ensures mutual excitation of neighbouring cells with similar directional tuning. This recurrent connectivity pattern enables visual and angular velocity

input to smoothly move activity packet along the ring, effectively tracking changes in subject's heading direction. Moreover, the network can integrate angular velocity input and maintain the directional representation even in the absence of visual input, which is consistent with experimental findings (Taube et al, 1990).
The models are supported by observations of coordinated drift of head direction cells activity when the system is disconnected from external sensory drive, such as during optogenetic inhibition of angular velocity signal during darkness (Butler et al., 2017), or during sleep (Peyrache et al, 2015).

Interestingly, ring attractor dynamics have been also shown to underlie heading representation in Drospohilla brain (Kim et al., 2017). The so-called E-PG neurons, which track fly's heading direction are organized into physical ring with recurrent connectivity pattern allowing continuous movement of activity bump with fly's turning. Thus, in this case the physical layout of the neurons matches the topography of the conceptual ring. However, it is not clear if any such a correspondence exists in the case of mammalian head direction cells (Khona and Fiete, 2021).

Another candidate for neuronal implementation of continuous attractor dynamics are the grid cell, which as population provide smooth representation of space, likely by performing path integration. The continuous attractor network models typically treat the grid cells as units localized on vertices of a virtual 2-D lattice. The interaction between the units is ensured by recurrent connectivity, which might consist of radially symmetric excitatory efferent connections combined with directionally asymmetric inhibitory component, with directional profile specific for given cell (Fuhs and Touretzky,2006). Another approach considers solely the inhibitory interactions (Bourak and Fiete, 2009).

Similar to a situation where optimal packing of equally sized circles in a plane is a hexagonal lattice, the competitive interaction between the units settles down to attractor with hexagonally distributed packets of activity (on the virtual lattice). Each cell further receives directionally modulated velocity input, increasing in strength with preferred direction of movement for given cell, which is opposite to direction of inhibitory afferents. This arrangement moves activity bumps in direction of movement, resulting in experimentally observed hexagonal firing fields.

Experimental support for continuous attractor network models of grid cells comes from recent observations that coactivation patterns of grid cells reflecting spatial field overlap during wake active behaviour are preserved during sleep (Gardner et al., 2019; Trettel et al., 2019). Moreover, control of grid cells' activity by local recurrent interactions was indicated by experiments with optogenetic stimulation of medial entorhinal subpolulations (Zutshi et al., 2018). These observations suggest that grid cells' activity is strongly modulated by their recurrent connectivity, in accord with attractor network architecture. The question of precise involvement of excitatory vs inhibitory connections, however, remains unresolved.

The activity of place cells has been also suggested to emerge from continuous attractor dynamics (Tsodyks and Sejnowski, 1995; Samsonovich and McNaughton, 1997; Battaglia and Treves, 1998). In the models, the weights of recurrent collateral strengths are proportional to place fields' distances of respective cells. This is consistent with the principle of Hebbian learning, as the cells tend to be coactive in dependence of their place fields' overlap. In addition to the autoassociative connections, the cells' activity is modulated by position-related afferents, such as inputs conveying extrasensory and idiothetic information. The network activity stabilizes in a localized bump, which can move smoothly with respect to movement of subject in the space. The place cell map thus represents 2-D attractor manifold in state space and network can store multiple maps corresponding to different environments. The models seem to be particularly

plausible for implementation by CA3 place cells population, possessing extensive system of recurrent collaterals. The attractor-like activity patterns could be still detected in CA1, as they would be imposed by Schaffer collaterals from the upstream CA3 population.

1.5.3 Attractor dynamics in CA3 place cell populations

The attractor behaviour predicted by the theoretical model should be reflected in experimental observations of CA3 place cell population activity.
In one of the first studies that addressed the issue, Lee et al. (2004) recorded place cell ensemble activity from CA1 and CA3 regions while rats run on a circular track with a particular configuration of local and distal visual cues. After familiarization with the standard cue configuration, the cue miss-match was imposed by relative rotation of local and distal cues in opposite direction, for up to 180 degrees. The majority of CA3 place cells rotated their place field position in accord with local cues. This is consistent with robust pattern completion occurring in CA3 network. In contrast, no such a coherent response was observed in CA1 place cell population. This suggests that place cells in CA3 are dominated by memory-related attractor-like pattern completion, while activity of CA1 place cells is to a higher degree influenced by specifics of current experience, probably via parallel entorhinal input, which skips dentate gyrus-CA3 circuitry.

In another experiment, Wills et al. (2005) trained rats to explore circular and square enclosures to develop specific place cell representations for each of the two spatial contexts. The rats were then tested in a 'morph sequence', corresponding to octagonal boxes with varying adjacent side ratios, which represented gradual steps from square-like to circle-like shape. Rather than displaying gradual change of activity pattern, almost all of the cells abruptly remapped between the two original maps at the same point in the middle of the morph sequence. Such discrete transitions are hallmark of attractor dynamics, where in an intermediate shape the network state is "attracted" towards the closest established representations.
While the recordings in Wills et al. study were made from CA1, the authors argue that the observed behavior of CA1 place cells is manifestation of attractor dynamics emerging in CA3 autoassociative network, which in turn biases activity patterns in the downstream CA1 population

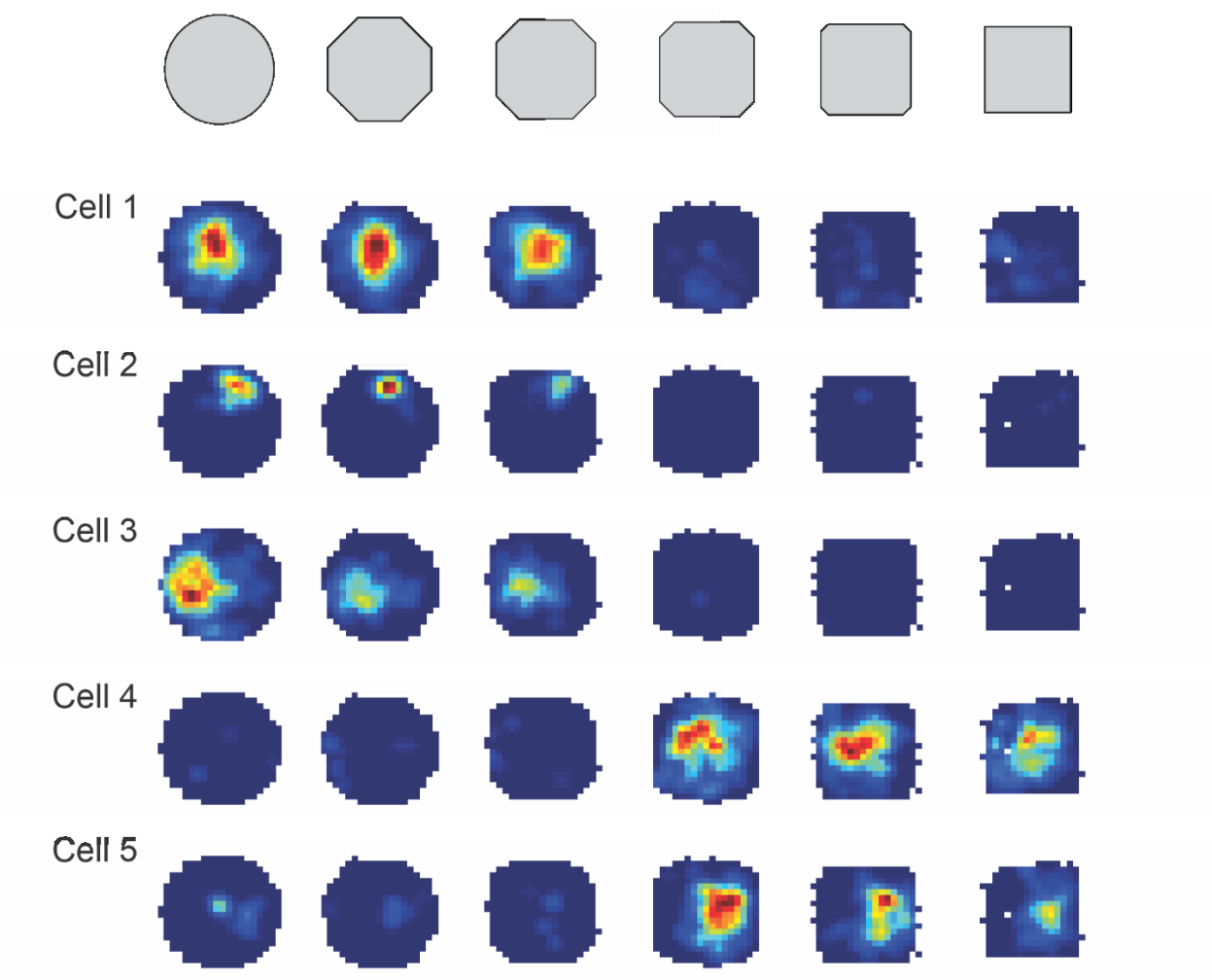

Figure 6 Example place cells with attractor-like responses during a morph sequence procedure. During a pretraining in circular and square enclosures, the place cells developed preference for activity in one environment. When a rat was exposed to sequence of enclosures with intermediate shapes (in scrambled order), the cells tended to abruptly switch between pre-established patterns in the hypothetical middle of a sequence. The colormap normalized for each cell with respect to peak rate value across sessions. (Zitricky, unpublished data).

1.5.4 Hippocampal-entorhinal loop and attractor dynamics

Since the global remapping is associated with grid cells' realignment (Fyhn et al., 2007), it is possible that abrupt transitions of place cell representations as observed in Wills et al. morphing paradigm are induced by entorhinal-hippocampal interactions, rather than originating in CA3 autoassociator itself. In another morhping experiment (Colgin et al., 2010), the rats were trained in circular and square enclosures that were either located at the same place or at different locations connected with a corridor. In the double location training group, where realignment of the grid cell path integrator across the environments was

assumed, the rats developed global remapping and subsequent morph test led to abrupt transition between the representations. In contrast, the rats which had undergone the single location training displayed rate remapping across contexts and gradual transition in the morph test. These results are in support for possibility of attractor-like transitions of hippocampal states induced by realignment of entorhinal path integrator.

Further, a computational model showed that plasticity of mutual hippocampal-entorhinal connections is sufficient for occurrence of sharp transitions observed in morph procedure, even in the absence of plasticity in the CA3 recurrent network (Renno-Costa & Tort, 2017). However, the hippocampal network with synaptic plasticity can produce sharp transitions without grid cells' input (Renno-Costa & Tort, 2017). Moreover, the associative pattern completion in place cells' representations is observed in pre-weanling rats before maturation of grid cell network (Muessig et al., 2016).

These results point to existence of complementary attractor networks in the hippocampal formation. When the spatial contexts are substantially different, global remapping with grid cells' realignment occurs, reflecting attractor states transitions in hippocampal-entorhinal loop. While the grid cell projections presumably provide robust control of place cell activation, their activity is also supposed to be influenced by self-organizing attractor dynamics within hippocampal network itself. Such an intrinsic coordination of hippocampal activity might be particularly significant during epochs with relatively weak entorhinal input, such as during specific phases of theta oscillations cycle (Jezek et al., 2011; Stella and Treves, 2011).

For a milder change of contextual cues, hippocampal-entorhinal loop maintains the original attractor state without grid cell realignment, while CA3 place cells display rate remapping. This may enable coding of specific episodes within the same general context (Renno-Costa & Tort, 2017). It is also consistent with the role of grid cells in generalization (Behrens et al., 2018).

1.6 Network state transitions in hippocampus

The adaptive behaviour in dynamically changing world requires brain to promptly retrieve relevant neural representations to guide future actions. The hippocampal circuitry displays capacity to create and store high number of distinct patterns, providing unique signature for each memorized episode. The mechanisms underlying effective recall of appropriate memory pattern remain poorly understood.

A particularly salient aspect of the hippocampal code is representation of space in the form of place cell maps (O'Keefe and Nadel, 1978). The retrieval cascade thus involves reinstatment of relevant spatial representation stored in hippocampal network. Upon entry to a familiar environment, the context-specific cues drive the entrainment of relevant place cell ensemble (Muller et al., 1987).

The hippocampal CA3 represents a network with high degree of autoassociativity, which is proposed to endow it with attractor dynamics. The interchange between activity patterns following change of context-defining sensory cues can be also conceptualized as a transition between two attractor states, coresponding to place cell maps of each of the environments.
According to the attractor network theory, CA3 recurrent collaterals are particularly instrumental in memory recall, where they enable ensemble self-excitation to reinstate stored activity pattern. This process of 'pattern completion' ensures that appropriate memory pattern will be retrieved even in presence of incomplete or noisy version of original input, as required with respect to dynamically changing nature of everyday experience.
In addition, the self-excitation in recurrent collaterals system sustains the activity configuration until it is disrupted by the sufficient change of the afferent input. This stabilization of memory state provides network dynamics with inertia to milder change of driving input. The network state transition thus involves interplay between this intrinsic self-sustaining dynamics and afferent flow of updated extrasensory information. This suggests that discrete attractor state transitions such as transitions between different place cell maps are highly competitive in nature. They can be also constrasted to smooth transition of activity packet within a single continuous attractor manifold.

1.6.1 Teleportation experiment

The short-lived nature of network state transitions makes effort to capture them experimentally challenging. The issue is elegantly resolved by 'teleportation' protocol, introduced by Jezek et al. (2011).
In the training stage of the protocol, the rats explore two diffent environments, connected with a corridor. This leads to association of each of the environments with distinct path-integrator coordinates, resulting in global remapping in CA3 place cell population across environments (Colgin et al., 2010).
The environments are square enclosures of the same size, but each of them equipped with different configuration of light cues. During the test phase, after rats have explored encosure with one of the sets light cues turned on, the lights are switched to the alternavie configuration, inducing an abrupt change in the context identity. The simultaneous recording of place cell activity allows to examine fine-scale dynamics of hippocampal network response to the environment change.

In the original study, it was observed that CA3 network can reactivate correct place cell representation within few hunders of miliseconds upon the switch of context identity. Howerer, rather than maintaining

the map of current environment, the network displayed instable period of switching back-and-forth between the maps of current and the alternative (previous) contexts. This flickering between the maps lasted for up to several seconds, until network settled to the correct state (Fig. 7).
The process was shown to be orginazed by theta oscillations, as within single theta cycle the network tended to express single of the competing representations. The discrete nature of map transitions is a hallmark of the attractor dynamics and the observation indicates a crucial role of hippocampal theta in their orchestration.

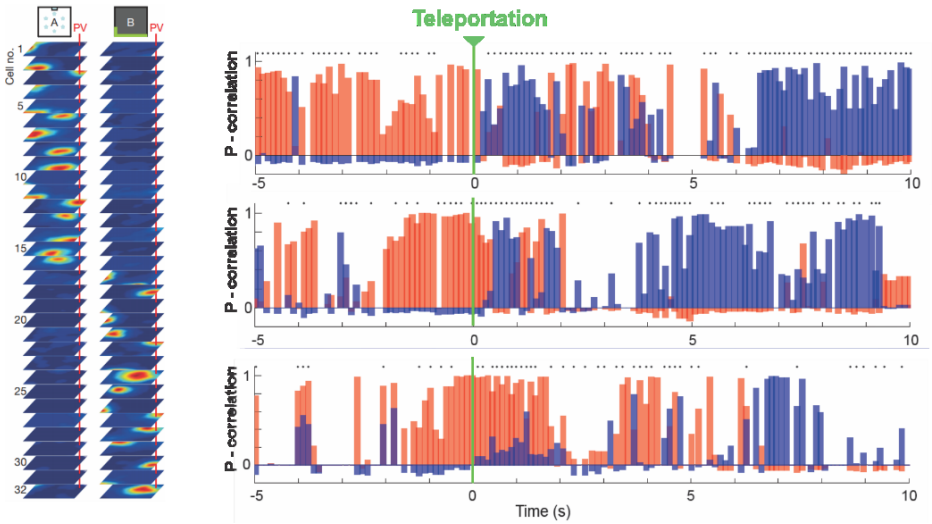

Figure 7 The CA3 network state dynamics during instantaneous shift of spatial context (teleportation). The network state was evaluated by correlating spiking activity within single theta cycle with pre-established template patterns (left) for respective position (right: red bars - correlation with template for original environment, blue bars - correlation with template for environment following teleportation). Modified from Jezek et al. (2011).

1.6.2 Computational models of teleportation

Model with conflicting information inputs

In a model introduced by Posani et al. (2018), the situation after teleportation involves conflict between the input conveying visual information which entrains representation of new environment and entorhinal path integrator input activating the place cell map of the previous context. The continuous attractor structure of modeled CA3 network with dynamics simulated for each theta cycle gives rise to transitions between the concurrent network states, recapitulating flickering observed in experimental data.
The path integrator receives feedback from the hippocampus and displays stochastic transitions between the states, depending on current hippocampal network state. Thus, activation of new spatial representation in the hippocampus by visual cue input increases probability of path integrator realignment to the congruent state. This leads to resolution of the conflict and termination of the flickering period.
The model predicts constant flickering frequency during the conflict period, which was confirmed by analysis of the experimental data. While flickering frequency during the conflict is constant, path integrator realignment times are exponentially distributed, which leads to gradual decrease in flickering when averaging across teleportation events, as reported by Jezek et al.
The idea of conflicting inputs was also implemented in a model by Stella and Treves (2011); however, their model did not explicitly involve the hippocampo-entorhinal feedback interaction.

Short-time plasticity-based model

The alternative model of flickering was introduced by Mark et al (2017), where flickering emerges as a result of network inertia enabled by short-term plasticity. The model assumes that after the cue switch, the synapses of the recurrent collaterals between place cells coding the previous environment remain facilitated for some period of time, which enables expression of the previous representation.
Biophysically, the short-term facilitation arises from calcium ion influx at the presynaptic site following spike generation, which leads to subsequent elevation of neurotransmitter release probability. The model is a continuous attractor network model, where autoassociative connections reflect distance between the locations coded by the place cells. In addition, each cell receives spatially modulated external input and theta modulated input. The spatially modulated external input has two components: one is environment specific while the other reflects environment features shared by both contexts. The competition between the ensembles is enforced by global inhibition.
The situation after the cue switch is modeled as an abrupt change of context-specific external input in correspondence with the change of the environment identity. Thus, in contrast to Posani et al. (2018) model, the flickering does not result from temporary conflict between sensory inputs recruiting concurrent ensembles. The previously active ensemble is rather entrained only by non-specific theta modulated input as well as context-invariant sensory input component, but the increased synaptic efficacy due to short term plasticity enables competition between the representations.
The model postulates that theta oscillations are essential for the previous map re-expression and predicts dependence of flickering frequency on theta amplitude. Moreover, flickering is expected to be related to

distance travelled by animal after the cue switch, as the place cells with enhanced synaptic efficacies have place fields clustered around the location occupied by the rat at the moment of teleportation.
In line with these predictions, analysis of Jezek et al. data revealed positive correlation of flickering frequency with amplitude of theta oscillations and decrease of flickering with distance travelled after the teleportation. These results provide experimental support for the model and suggest that considering short-term plasticity effects might be important for understanding emergence of flickering phenomena.

2 The goals of the thesis

1. We aimed to quantitatively evaluate hippocampal network activity during state transitions induced by switch of spatial context identity. Furthermore, we wanted to quantitatively evaluate network activity separately for network states expressing map for the present and the previous context, respectively.

Hypothesis: We hypothesized that spatial map reinstatement is associated with increased place cell activity, which might facilitate shift of the network state to the appropriate representation

2. We aimed to evaluate the quality of spatial coding by place cell population shortly after environment identity change.

Hypothesis: The competitive period of state transition is assumed to be associated with a conflict of input streams supporting the place cell activity, which could lead to degraded quality of spatial code. Moreover, the place cells' activity specific for new context might be less adherent to the current position during first moments of the map recollection.

3. We aimed to assess eventual mixing of the originally segregated network states during the competitive period of network state shift across the theta and shorter timescales.

Hypothesis: We hypothesized that conflicting inputs might induce considerable network state mixing despite existing attractor-like dynamics described previously.

4. We aimed to evaluate hippocampal oscillatory activity during change of spatial context and associated place cell map reinstatement.

Hypothesis: The awake processing of hippocampal information is robustly organized by oscillatory activity in theta and gamma frequency bands. We conjectured that network state transitions are associated with enhanced theta and gamma rhythmicity, which would support network state reset and information flow within hippocampal formation, respectively.

3 Hippocampal population dynamics during spatial memory state retrieval

The investigation of place cell activity during teleportation experiments provides unique opportunity to study spatial memory state transitions. This enables us to analyse nature of hippocampal spatial code during first moments of spatial map retrieval and associated instable period. Moreover, the competitive nature of state transitions might provide further insight into coordination of distinct attractor states across different timescales. In this chapter we aimed at describing CA3 population activity during spatial memory state retrieval in further detail. Since the hippocampal population activity is orchestrated by theta rhythm, we perform most of the analyses at the level of individual cycles of theta oscillations.

3.1 Methods

This work is based on analysis of data recorded during 'teleportation' experimental procedure described in Jezek et al. (2011). The description of the methodological procedures is partially reproduced from Zitricky and Jezek (2019).

3.1.1 Experimental procedures

Animals

The experiments involved six adult Long Evans male rats. After the surgery, the animals were kept in individual cages with ad libitum access to water and food. The recovery period spanned 10 days after the surgery. Afterwards, the subjects were mildly food deprived, while maintaining their body weight above 85 % of their original weight.

Electrode preparation and surgery

Single unit neuronal activity was recorded from hippocampal subfield CA3. The rats were implanted with a custom made 'hyperdrive' allowing an independent positioning of 14 tetrodes organized into a circular bundle. Tetrodes were twisted from 17 μm insulated platinum-iridium wire (90% and 10%, respectively, California Fine Wire Company). Electrode tips were platinum plated to adjust their impedance to 120 – 250 kOhm (at 1 kHz).

Anesthesia was introduced by placing the rat into a plexiglass chamber with seal top filled with isoflurane vapour. Then the animal was injected with an intraperitoneal injection of Equithesin (pentobarbital and chloral hydrate in a dose of 1.0 ml per 250 g body weight). After the head was shaved, the animal was

placed into the stereotaxic frame. Breathing, heart action and reflexes were monitored continuously. Hyperdrive was then implanted above the right dorsal hippocampus at coordinates AP 3.8 mm, DV 1.0 mm and ML 3.2 mm relative to bregma. Seven to nine stainless steel screws and dental acrylic were used to stabilize the implant on the skull. Two of the screws placed in the frontal bone served as the hyperdrive ground.

Tetrode positions

Following the surgery, the tetrodes were gradually moved to CA3 pyramidal layer. In addition, reference electrodes located in corpus callosum and stratum lacunosum-moleculare (EEG reference) were used during recordings.

Recording procedures

The recordings were performed during experimental procedures described by Jezek et al. (2011, bellow). The recordings were performed differentially with respect to a reference tetrode. The unity gain headstage was attached to the hyperdrive and the signal was transmitted by 82-channel commutator and registered by Neuralynx digital 64 channel data acquisition system.

The acquired signal was band-pass filtered at 600Hz -6 kHz. The spike detection was performed using customized threshold (45-70 μV). The registered events were sampled at 32 kHz. The light emitting diodes mounted on the headstage were tracked (50 Hz sampling) to determine the animal's trajectory. Broadband EEG signal was acquired continuously at 2000 Hz.

Spike sorting and cell classification

Spike sorting was performed manually using 3D graphical cluster-cutting program (SpikeSort, Neuralynx). The spike datapoints were visualized within three-dimensional feature space, consisting of selected combination of waveform amplitudes and energies. Autocorrelation and cross-correlation functions were used as additional separation tools. To distinguish between putative pyramidal cells and putative interneurons, average firing rate, spike width and presence of occasional complex spikes were considered. The isolated units with average firing frequency >10 Hz and with the peak to through duration < 0.3 milliseconds were classified as interneurons.

Behavioral apparatus and training

We trained the rats to run in two environments that were of identical shape (square enclosures with 60x60 cm surface and 50 cm high walls), but each contained specific configuration of visual cues. Black curtains around the apparatus were used to eliminate task-unrelated visual cues (Fig. 8). In environment A, circularly arranged LEDs were placed bellow the translucent floor and an additional polarizing light cue was located on one wall of the arena. In the environment B, the LEDs were arranged into 60 cm-long bar located near the upper edge of the wall, with the position opposite to the polarizing cue in the box A. Additional 20 cm LED array was mounted on one of the adjacent walls. The equivalent number of LED units was used for each of the environments. The training consisted of four stages (Fig. 8) to support development of distinct neural representations of each environment. In the first stage, the enclosures were positioned next to each other, connected by a corridor (20x20cm, width x length) that allowed the rat to freely move between the boxes. The rat completed three 20 min long sessions per day, which aimed to associate distinct path integrator coordinates with each environment. There were 20 min breaks between the sessions while the rat rested on a towel in a pedestal outside of the curtains (phase 1). In phase 2, the corridor was removed and the rat foraged in each environment separately, with alternating environment identity at respective original position (three 10 min sessions per environment, 10 min breaks). In the next stage (phase 3), the rat explored a single box containing both sets of LEDs, with its location alternating between the original positions. The light cues were lit specifically so that environment identity was congruent with its original location. In the test phase, the rat first completed two reference session (10 min in each environment). In the next session, the configuration of light cues corresponding to a given environment was instantaneously switched to the alternative configuration, thereby inducing abrupt change in environment identity ('teleportation'). The 'teleportations' were repeated every 40-60 s during the 10 min long session. The teleportation session was followed by other reference sessions, 10 min in each environment.

In the beginning of each sessions, the rat was placed into the enclosure with eyes covered by a palm of the experimenter. The boxes were carefully cleaned between subsequent sessions.

Animal movement was motivated by cookie crumbles delivered randomly throughout the environment. The distinct cookie flavor (vanilla/chocolate) was used for each environment, together with environment-nonspecific unflavored food. During teleportation procedure, only unflavored food was provided.

Histology

After the recordings were completed, the rat was administered lethal dose of Equithesin and subsequently was perfused intracardially with saline followed by 4 % formaldehyde. Brain coronal sections (30 µm) were stained with cresyl violet. Traces of all 14 tetrode locations were identified. The tetrode tip location was determined as the place in the section before the tissue damage became negligible. The analysis was restricted to the data recorded from tetrodes with confirmed CA3 location.

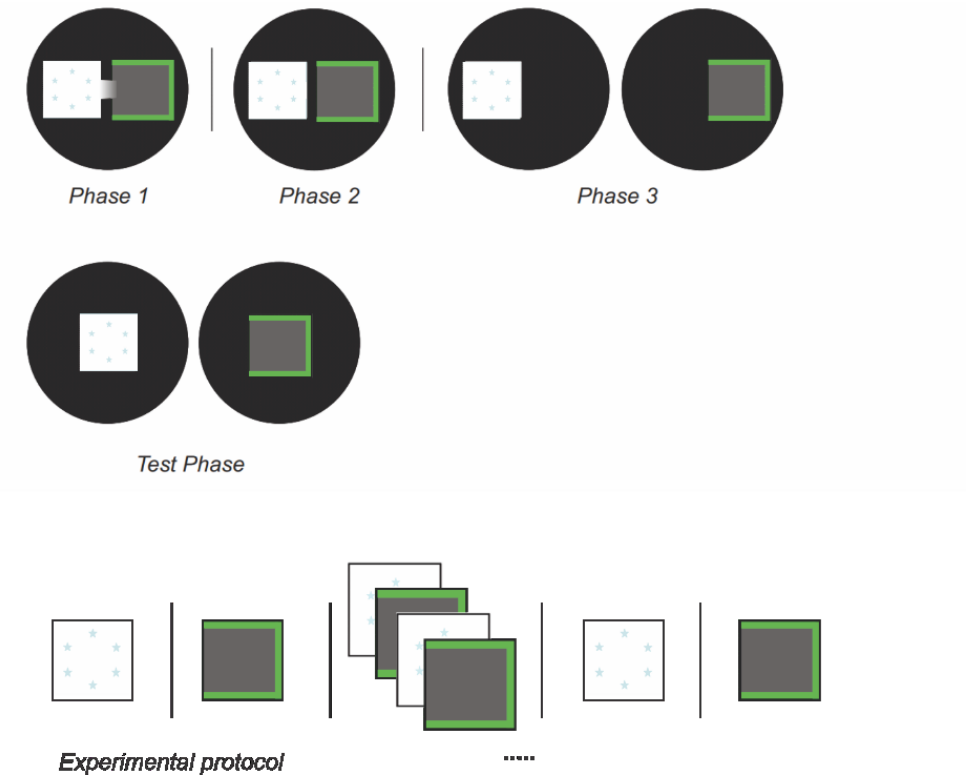

Figure 8 A scheme of pre-training and the experimental protocol. The pre-training was designed to induce development of uncorrelated neural maps for each environment (see Methods for detailed description). On a test day, the rats first completed 10 min reference session in each environment, which was followed by the teleportation session. Additional reference recordings in both environments were performed after the teleportation trial.

3.1.2 Methods – data analysis

Place cell classification

Putative pyramidal neurons (see above) were further tested for spatially selective activity. For each cell's spiking activity during the reference sessions we calculated corresponding spatial information, as described previously (Skaggs et al., 1996). The resulting value was compared to shuffled data, obtained by 200 times randomly shifting spike time-stamps along the trajectory. A cell was included into analysis if the respective spatial information was higher than 99th percentile of shuffle distribution in at least one of the environments.

Template rate map construction

For construction of template firing rate maps, the surface of arena was divided into 30 × 30 position bins (2 cm × 2 cm). Then for each unit, the mean firing rate was calculated for each position bin by dividing the number of spikes by occupancy at the respective position bin. The resulting rate maps were further smoothed with Gaussian average over surrounding 2 × 2 bins.
The template rate maps for all cells were than stacked together to construct template rate patterns (population vectors) for each environment, consisting of mean firing rate values for each place cell at given position.

Theta cycle population vectors

The population activity was segmented into theta cycle bins, with a border corresponding to theta phase with minimal population activity within the session. The corresponding theta oscillations phase for each spike was derived from LFP signal bandpassed for theta frequency (6–11 Hz), by interpolating between detected peaks and troughs.
Each population vector was associated with an instantaneous position of the rat. Division of arena surface into 10x10 bins was used to define position-matched population vectors.

In analyses comparing individual post-teleportation theta bins with position-matched control data, only databins with mean ratio of amplitude in theta (6-12 Hz) to delta (2-4 Hz) > 2 were included. Moreover, for epochs with speed < 10 cm/s putative sharp wave-ripples were detected: the signal was bandpass-filtered for 150-250 Hz and Hilbert-transformed to derive envelope of the filtered signal. A ripple was detected if the envelope exceeded threshold of 3 s.d., with the event extended until the envelope returned to the session average level. The databins that overlapped with the detected ripple event were excluded from analysis.
In analyses comparing whole pre-teleportation and post-teleportation periods, theta activity was evaluated as in Jezek et al (2011). The power in theta and wide-band spectrum (0-125 Hz) was calculated for epochs preceding and following cue switch and only events with theta/broadband power ratio >5 were included in the analysis.

Environment specificity index

To classify population vectors according to the expressed place cell ensemble, we constructed an Environment Specificity Index (*ESI*), defined as: $ESI = (f_A - f_B)/(f_A + f_B)$, where f is the average firing rate (Hz) of given neuron during refence sessions in environment A or B. *ESI* values therefore ranged between −1 and 1 and indicated how each cell activity was specific for each of the two environments.
The population vector was classified as expressing a respective map if it contained activity of at least one highly specific cell for the respective environment context ($ESI >= 0.8$) and no spikes of cell with $ESI < -0.2$. Only theta bins with at least 2 active units were considered. The population vectors expressing map congruent with currently present environment were classified as 'correct', while the population vectors expressing the alternative map were classified as 'incorrect'.
The 'mixed' bins corresponded to the population vectors containing activity of cells specific for each of the environments ($ESI >= 0.8$ & $ESI <= -0.8$ or $ESI >= 0.95$ & $ESI <= -0.95$ when stricter specificity was desired).

Poisson rate decoder

The complementary approach to spatial map decoding was based on calculating probability of the given activity pattern with respect to the individual contextual representations. The decoder was based on considering contextual, rather than positional specificity of cellular firing and thus the activity in given environment was modelled as a Poisson process with rate defined as mean firing for given context.

The probability of detecting activity pattern n given map M was then calculated as

$$P(n, M) = \prod_{i=1}^{N} \frac{(t\, f_i(M))^{n_i}}{n_i!} \exp(-t f_i(M))$$

Where n_i is number of spikes emitted by i-th neuron, f_i represents mean firing rate during reference session in given environment and t is duration of decoding window (theta bin).

For each activity pattern we then calculated log-ratio of probabilities (Posani et al., 2017):

$$\Delta L = \log \frac{P(n, A)}{P(n, B)}$$

and the resulting quantity was used to infer identity of activated map, with sufficiently high positive values indicative of map A and sufficiently low negative values indicative of map B. The specificity of decoder was regulated by setting a threshold for map detection. The map A was decoded when the ratio of probabilities P(n,A)/P(n,B) was higher than 100 and ΔL value was higher than 99th percentile of values for activity patterns in context B during baseline constant cue epoch. The map B was decoded in an analogous manner. To avoid zero probabilities, the zero rate values were set to single spike per session.

Post-teleportation and baseline period

The post-teleportation period corresponded to first 20 theta bins following the cue switch. The position-matched control data were sampled from baseline period, spanning stable cue epochs between subsequent teleportations, excluding first 80 theta bins after each cue switch. For some analyses, the activity directly preceding the teleportation was used as a control.

Hyperactivity analysis

The number of detected spikes of all recorded place cells was counted for intervals corresponding to 2 seconds before and 2 seconds following switch of light cues and averaged across events for each session. Temporal evolution of spiking activity around teleportation event was obtained by binning population spiking activity into 200 ms bins for 10 seconds before and after teleportation and averaging across the teleportations. The normalization was done by setting the average of 10 s pre-teleportation activity as 100 % baseline.

The activity level during theta bins expressing 'correct' and 'incorrect' map was evaluated by counting active cells within a theta bin classified as expressing the respective map. The activity during classified theta cycles within first 20 bins following teleportation was compared to average activity from theta bins expressing the same map at corresponding spatial location (6cm x 6cm binning) during baseline epochs with congruent environment identity. The post-teleportation data points from same location were averaged within a session.

Analysis of the mixed cycles

The number of mixed theta cycles were calculated for 20 theta bins before and after teleportation. The emergence of mixing at short timescale was evaluated by binning the activity into fixed-length 10 ms intervals and calculating number of mixed bins for 240 bins (approximately 20 theta bins) before and after cue switch for each teleportation.

To evaluate significance of ensemble separation within post-teleportation period, we randomly shuffled activity across post-teleportation population vectors and quantified number of mixed states for each of the 10 000 randomizations. The analysis was restricted to theta cycles with at least 2 active cells, occurring after first post-teleportation correct or mixed bin. Only the post-teleportation epochs containing at least 3 such cycles, and which included at least 4 spiking events (i. e. firing within a theta cycle) of cells with strong specificity (abs(*ESI*) > 0.8) for each context, were considered.

Spatial coding

The spatial coding accuracy was determined by calculating spatial coding error. The population vector from the respective theta cycle was correlated with reference firing rate vectors for each of the 30x30 bins across the surface of the arena, defined by template rate maps. The error, reported in units of spatial bin lengths, was defined as distance between the decoded bin that displayed the highest correlation value and the real position of the rat. The error values for theta cycles from post-teleportation epoch were compared with position matched control data from baseline stable cue condition as in activity level analysis.
The correlation of population vector was calculated as Pearson correlation of the respective population vector with reference firing rate vector for given position within decoded spatial map.

Statistical analysis

In analysis comparing pre-teleportation and post-teleportation epochs (total spikes, spikes per theta bin, active cells per theta bin, speed, mixed states and oscillations amplitude), pre-teleportation and post-teleportation data were averaged across the respective recording session and compared with paired sample Wilcoxon signed-rank test. Similarly, in theta bin level analysis comparing post-teleportation databins with location-matched controls (active cells, decoded position error, population vector correlation), the data were averaged within recordings and compared using Wilcoxon signed-rank test. Significance of the pattern separation was evaluated using randomization procedure, where number of mixed states was compared to distribution generated by randomly permuted data. The mean values are reported with standard error of mean (± SEM). The results of a statistical test were considered significant if $p < 0.05$.

3.2 Results

Teleportation induced hyperactivity of hippocampal place cell population

We analyzed activity of 355 CA3 pyramidal units recorded from dorsal hippocampus of rats during teleportation experiment (6 rats on 11 different recording days).
We first quantitatively analyzed spiking activity during times of putative network state transitions. We observed increase of place cells' spiking activity following switch of spatial context identity (Fig. 9a). The population hyperactivity peaked shortly after the cue switch and activity level returned to the baseline within few seconds on average. We thus assessed total spike count for short epochs (2 seconds) before and after cue switch, which confirmed increased activity triggered by teleportation (52,79 ± 4,53 spikes pre-tele, 69,52 ± 5,99 spikes post-tele, Wilcoxon signed-rank test: p = 0,002; n = 11 recordings, Fig. 9b). The increased population activity was still present when restricting the analysis to events occurring during epochs dominated by theta oscillations (53,81 ± 4,85 spikes pre-tele, 69,97 ± 6,33 spikes post-tele, Wilcoxon signed-rank test: p = 0,001, n = 11 recordings,).

The activity of place cells increases with speed of locomotion (McNaughton et al, 1983). However, there was an average decrease in speed of the rat during the respective post-teleportation epochs (10,62 ± 0,57 cm/s pre-tele; 8,70 ± 0,70 cm/s post-tele, n = 11 recordings, Wilcoxon signed-rank test: p = 0,0049, 2 seconds pre/post; Fig. 9d).

The hippocampal network state expression is robustly organized by theta oscillations. For further analysis we thus considered binning data according the individual cycles of local theta oscillations. The phase corresponding to minimum of population activity was set as a border between individual theta bins. Within theta-based framework, population hyperactivity was reflected in increased number of spikes (3,26 ± 0,30 spikes per TC pre, 4,16 ± 0,37 spikes per theta cycle (TC) post, n = 11 recordings, Wilcoxon signed-rank test: p = 0,0029) and increased number of active place cells per theta cycle during post-teleportation period (1,62 ± 0,15 cells per TC pre, 2,10 ± 0,20 cells per TC post, n = 11 recordings, Wilcoxon signed-rank test: p = 0,000977; Fig 9b).

Network activity with respect to decoded spatial map

Since theta oscillations organize expression of alternative place cell maps, we aimed at decoding cognitive map from population activity within individual theta cycles (TC). Taking advantage of a high degree of sparsity and orthogonality of CA3 spatial coding, we employed a decoder that was based on the mean firing rate of the individual cells during template reference sessions (Fig. 14). For each cell we defined an environment specificity index

$$ESI = (f_A - f_B)/(f_A + f_B)$$

where f represents the average activity in Hz for a given cell recorded in environment A or B, respectively. During the baseline epochs of the teleportation session, 63,33 ± 0,03 % of temporal bins with at least 2 active cells were classified as 'correct'-expressing place cell pattern congruent with present context, and

2,14 ± 0,00 % were classified as ‘incorrect’ -expressing the alternative map. The frequency of incorrect activity increased during brief post-teleportation period to 14,42 ± 0,03 % (p = 0,002 Wilcoxon signed-rank test, n = 11 sessions), reflecting the competitive network dynamics following context switch.

Next, we aimed to relate observed place cell hyperactivity triggered by teleportation to expression of respective contextual representations. We compared activity levels within a theta bin expressing a particular map and compared to matched data corresponding to expression of the same map occurring at the same position (6 cm x 6 cm tiling) during baseline stable cue period with corresponding context identity. We detected increased number of active cells during theta bins expressing ‘correct’ map (2,67 ± 0,12 cells per TC baseline, 2,89 ± 0,15 cells per TC post, Wilcoxon signed-rank test: p = 0,0098, n = 11 recordings,), but not ‘incorrect’ map (2,60 ± 0,16 cells per TC baseline, 2,70 ± 0,20 cells per TC post, , Wilcoxon signed-rank test: p = 0,2402, n = 11 recordings), using *ESI*-based contextual decoder (Fig. 9c).

For complementary analysis, we constructed an alternative decoder based on Poisson rate model of place cell activity. As in the case of the *ESI* decoder, we considered overall probability of place cell activation within a given context, which was modelled as a homogenous Poisson process.

This analysis detected increased activity levels both during theta cycles with decoded ‘correct’ (3,05 ± 0,19 cells per TC baseline, 3,40 ± 0,23 cells per TC post, Wilcoxon signed-rank test: p = 0,001, n = 11 recordings), and ‘incorrect’ spatial maps (2,87 ± 0,15 cells per TC baseline, 3,18 ± 0,21 cells per TC post, Wilcoxon signed-rank test: p = 0,0322, n=11 recordings) (Fig. 15b). However, the decoder can classify individual theta bins as expressing particular map despite some activity of cells specific for alternative environment. Accordingly, distribution of *ESI* values for active cells during theta bins classified with Poisson decoder revealed intrusion by activity within alternative map (Fig. 15c). We suggest that this might be related to different activity levels detected when applying different decoders and such co-activation of different ensembles might contribute to observed increase in network activity following switch of spatial context.

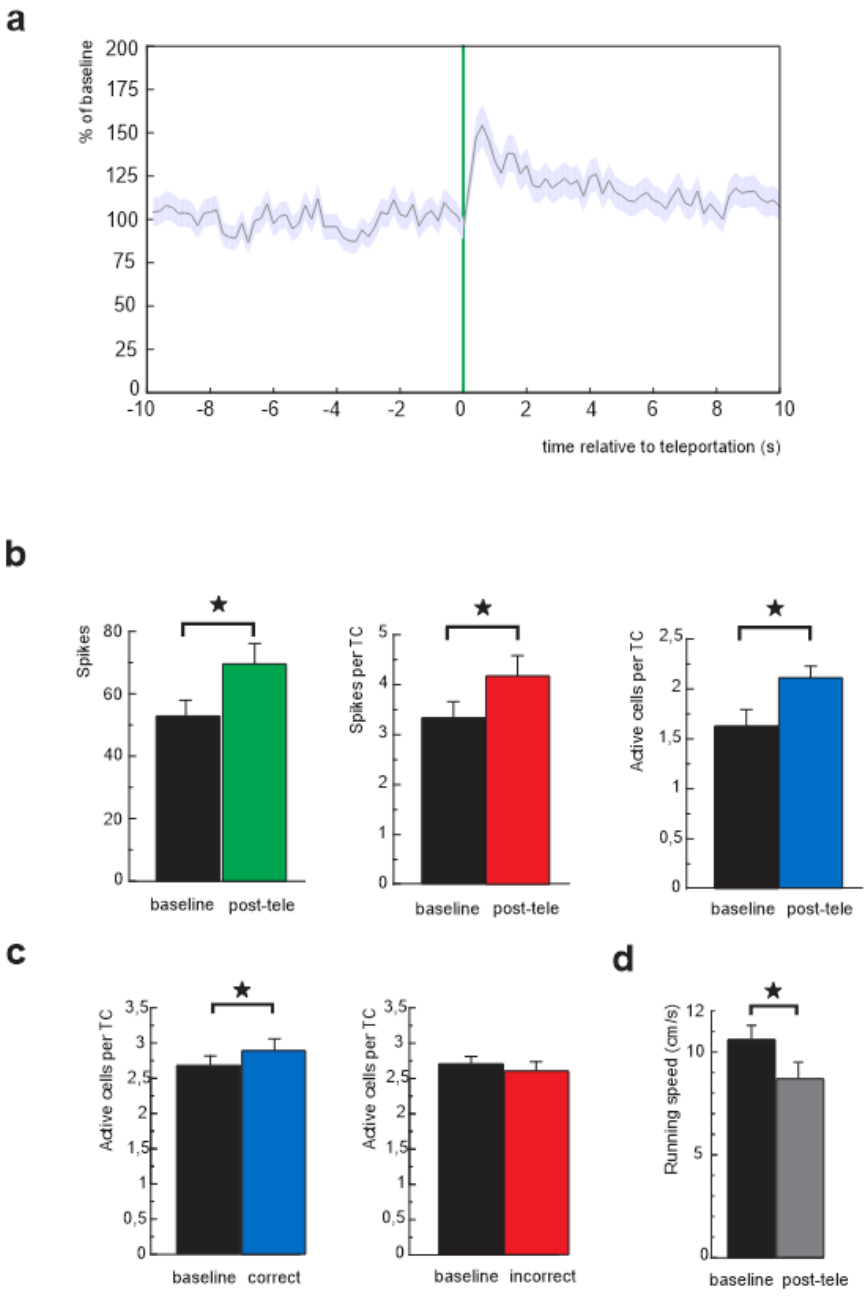

Figure 9 Hippocampal CA3 population activity during network state transitions.
(a) Evolution of population activity before and after teleportation (averaged across events). The values were normalized with respect to baseline, defined as average pre-teleportation activity level.
(b) Average numbers of spikes during 2 seconds before and after teleportation (left). Average number of spikes (middle) and active place cells (right) and per theta bin within 20 theta cycles before and after the teleportation.
(c) Average number of active cells during post-teleportation theta bins with decoded correct and incorrect representation and during location-matched control bins.
(d) Average speed of locomotion during 2 seconds before and after cue switch.

Mixed states

Jezek et al (2011) showed that theta oscillations orchestrate attractor-like pattern activation during transient flickering period, with activity pattern tending to be similar to one but not to the other of the alternative representations during single theta cycle. However, considerable coactivation of competing ensembles within a theta cycle window could be still possible. We thus decided to analyze eventual confluence of normally orthogonal network states during highly competitive post-teleportation network dynamics in further detail.
To this end, we defined mixed theta states as theta bins containing activity of at least one pair of cells with highly specific firing preference for mutually different environments ($ESI > 0.8$ & $ESI < -0.8$).

The inspection of network state evolution after individual teleportation events (Fig. 10a & Fig. 14c, d) revealed rather extensive incidence of detected mixed states. This was quantitatively confirmed by evaluating post-teleportation increase of mixed states across all the events (mixed bins per telep. event: 0,85 ± 0,16 pre, 2,78 ± 0,57 post, Wilcoxon signed-rank test: p = 0,002, n=11 recordings, Fig. 10a). The robust mixing was still present when employing more stringent criteria for environment specificity ($ESI > 0.95$ & $ESI < -0.95$; mixed bins per telep. event: 0,19 ± 0,10 pre, 1,28 ± 0,42 post, Wilcoxon signed-rank test: p = 0,0078, Fig 10a).
This suggests, that during spatial map transitions, the network state can undergo period of considerable activity pattern mixture before reaching stable state congruent with cues-defined context. However, the incidence of the mixed states shortly after light switch was significantly lower than in shuffled data, consistent with previous finding of attractor dynamics organized by theta rhythmicity (Fig. 10b).

We next investigated pattern segregation at shorter timescales. The analysis of time lags between spikes across different cells active within a mixed theta bin revealed that the place cells with activity specific for the same environment tended to be coactive at short timescale <20 ms. The distribution of time lags between spikes of cells specific for alternative environments showed shift towards longer intervals, which could reflect some level of ensemble segregation within a theta cycle (Fig. 10c).
However, the coactivation of the cells specific for alternative contexts was still considerable during short time windows. To support the assumption that the post-teleportation period was associated with the increased incidence of such coactivity at short timescales, we recut the data into 10 ms temporal bins and found an increased incidence of mixed bins in post-teleportation interval (mixed bins per telep. event: 0,03 ± 0,02 pre, 0,45 ± 0,23 post, Wilcoxon signed-rank test: p = 0,0313, Fig. 10d).
The coactivation of the orthogonal patterns thus occurred even at short timescales relevant for cell assembly dynamics and synaptic plasticity.

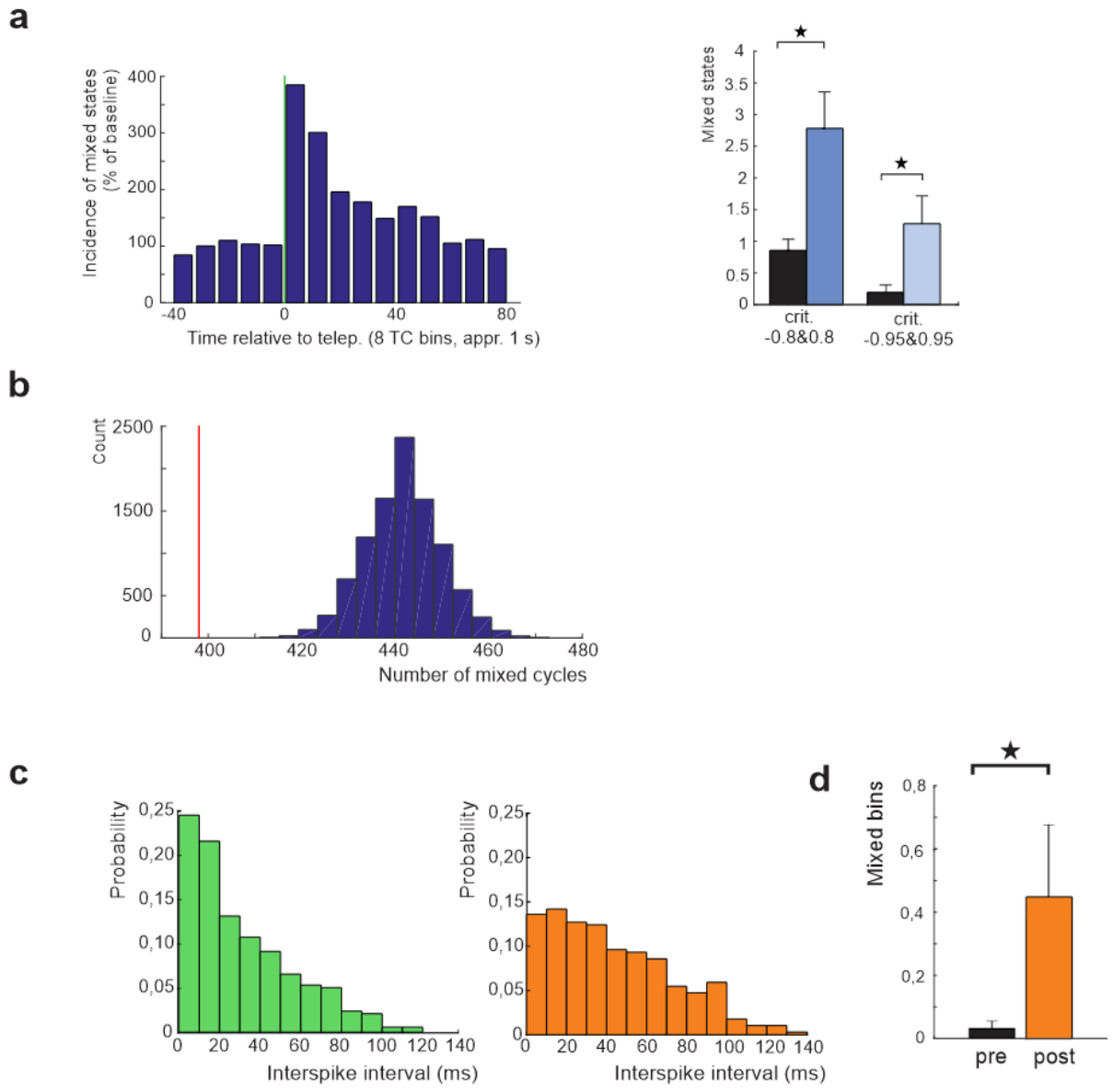

Figure 10 (a) Left: Evolution of mixed state incidence in response to context identity change. The values were averaged for eight subsequent theta bins (approximately 1 second). The baseline corresponds to average within pre-teleportation epoch. Right: Increase in mixed states occurrence after cue switch was detected with different inclusion criteria (black bars: pre-teleportation, black bars: post teleportation). (b)Incidence of mixed states (red mark) compared to the random distribution. We detected lower number of mixed bins than in 10 000 cases of random permutations across the post-teleportation population vectors (see Methods).
(c) Distribution of the time lags between the spikes from cells within (top) the same representation and across (bottom) both representations (cutoff $|ESI > 0.95|$). The place cells from the same representation are more likely to fire together at short timescales.
(d) The teleportation induced increase in distinct pattern coactivation at short timescale (10 ms bins).

Spatial coding during state transition period

In the next step, we analyzed how specifics of network dynamics after abrupt change of environment influence representation of spatial position by place cell ensemble.
To examine spatial code properties, we first decoded expression of respective contextual map within a single theta bin and then evaluated context-specific representation of position by place cell activity.
The respective spatial map expression within a theta bin was decoded using position-independent *ESI* decoder and Poisson rate model-based decoder. The employment of position-independent context decoders limits a priori assumption regarding of sufficient quality of positional representation within the respective map.

We assessed quality of positional representation by quantifying the decoded position error. The population vector activity within a theta cycle with decoded expression of one of the maps was correlated with template spatial bin population vectors across whole respective environment. The spatial coding error then corresponded to the deviation of a real animal's position from the coordinate with the highest correlation.
The evolution of decoded position error measured from theta bins expressing 'correct' map revealed its highest values shortly after cue switch, followed by a decline to the baseline state within few seconds (Fig. 11a).
Further analysis across 'correct' theta bins indicated higher positional error for post-teleportation theta cycles compared to position-matched controls from control conditions (6.36 ± 0,31 bins baseline, 7,35 ± 0.37 bins post, Wilcoxon signed-rank test: p=0,0137, n = 11 recordings, Fig. 11b). The correlation of 'correct' population vectors with template pattern for respective position was non-significantly lower than in control data (r=0,65 ± 0,02 baseline, r=0,61 ± 0,02 post, Wilcoxon signed-rank test: p=0,0830, n = 11 recordings, Fig. 11c)

The analysis of spatial code quality associated with 'incorrect' states did not detect significant difference in decoded position error (6,42 ± 0,30 bins baseline, 6,66 ± 0,77 bins post, Wilcoxon signed-rank test: p=0,9658, n = 11 recordings, Fig. 11b) or correlation with template pattern (r=0,70 ± 0,02 baseline, r=0,68 ± 0,04 post, Wilcoxon signed-rank test: p=0,7002, n = 11 recordings, Fig. 11c) . This suggests that place cells specific for the previous context continue to provide positional information without ongoing support from respective visual cues.

The complementary analysis with Poisson-rate decoder detected non-significant increase in decoded position error (6,08 ± 0,30 bins baseline, 7,36 ± 0,42 bins post, Wilcoxon signed-rank test: p=0,0537, n = 11 recordings, Fig. 15d) and significantly decreased correlation with the template pattern for population vectors classified as 'correct' (r=0,67 ± 0,02 baseline, r=0,61 ± 0,01 post, Wilcoxon signed-rank test: p=0,001, n = 11 recordings, Fig. 15d). The analysis of 'incorrect' states did not indicate significant change in spatial code quality by any of the metrics (Fig. 15d, pos. error: 6,40 ± 0,56 bins baseline, 6,70 ± 0,82 bins post, Wilcoxon signed-rank test: p=0,7646; correlation with template: r=0,67 ± 0,03 baseline, r=0,69 ± 0,03 post, Wilcoxon signed-rank test: p=0,3203).

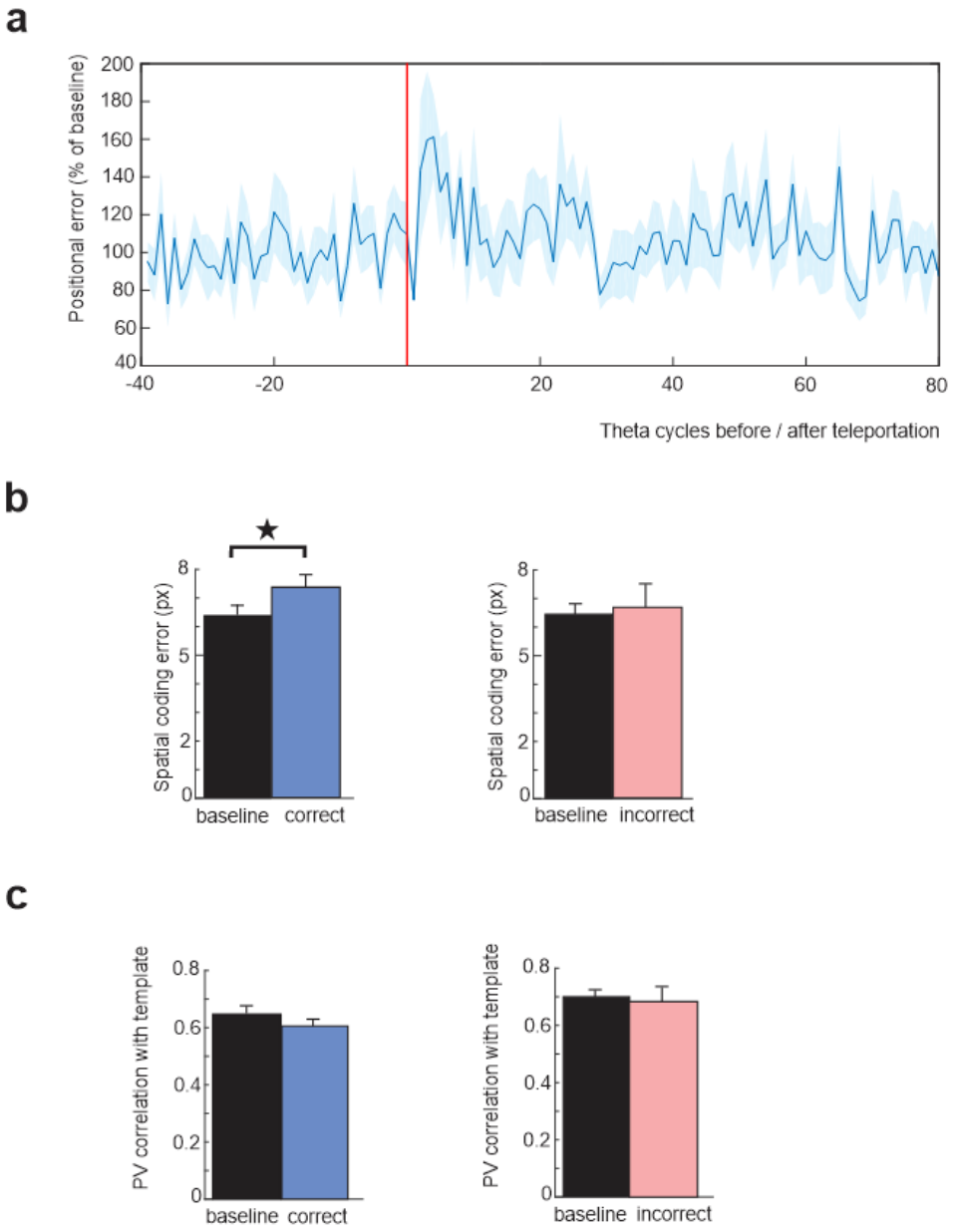

Figure 11 Spatial coding during place cell map transitions.
(a) Development of decoded position error for 'correct' theta bins before and after teleportation. The values were normalized with respect to baseline (pre-teleportation average).
(b) Decoded position error for 'correct' and 'incorrect' post-teleportation theta bins and location matched control theta bins.
(c) Correlation of post-teleportation 'correct' and 'incorrect' population vectors with template patterns.

Interneuronal activity after cue switch

We additionally analyzed behavior of simultaneously recorded interneurons during peri-teleportation period (n=16 units).
The examination of their spiking activity suggested dual response to the teleportation event, with majority of interneurons increasing their firing rate on average, while smaller subset of interneurons tended to decrease their spiking activity (Fig. 12a, b, f). To evaluate responsivity across all the analyzed interneurons we considered absolute value of z-scored activity, which allowed to capture firing rate change irrespective of its polarity. This analysis confirmed that interneurons changed their pre-teleportation baseline firing rate upon step-wise cue switch (Wilcoxon signed-rank test, $p< 0,01$ Fig 12d, e).

The results indicate expected engagement of interneurons in shaping network response to change of the spatial context. The non-uniform response profile is consistent with extensive functional heterogeneity in hippocampal interneuronal population with variable microcircuitry connectivity across different interneuron subtypes.

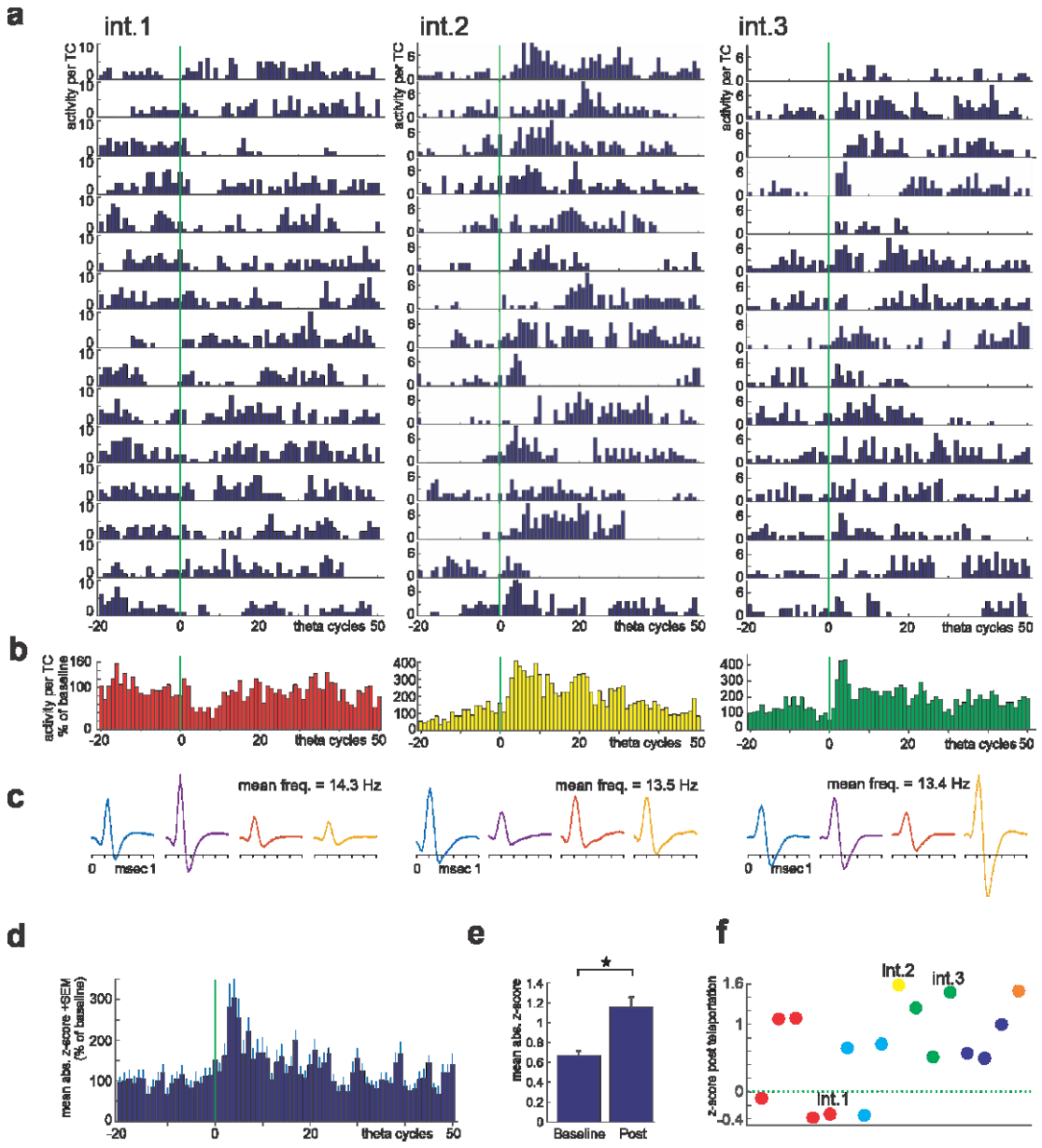

Figure 12 Activity of interneurons during teleportation events.

Spiking activity of three interneurons during teleportation epochs. (a) theta-binned activity during individual teleportation events, (b) averaged activity of the same neurons across all teleportation events, normalized with respect to baseline, (c) respective spike waveform registered on each channel and associated mean firing rate.

(d) Evolution of activity during teleportation events across all interneurons. The absolute values of z-scored activity were used to detect both increase and decrease in firing in response to teleportation.

(e) Average activity of interneurons before and after teleportation (n=16 interneurons, 20 theta bins pre/post).

(f) Average z-scored activity of individual interneurons during post-teleportation interval (20 TC). The values for cells recorded on same tetrode are plotted in same color; denoted values for three example interneurons (a-c).

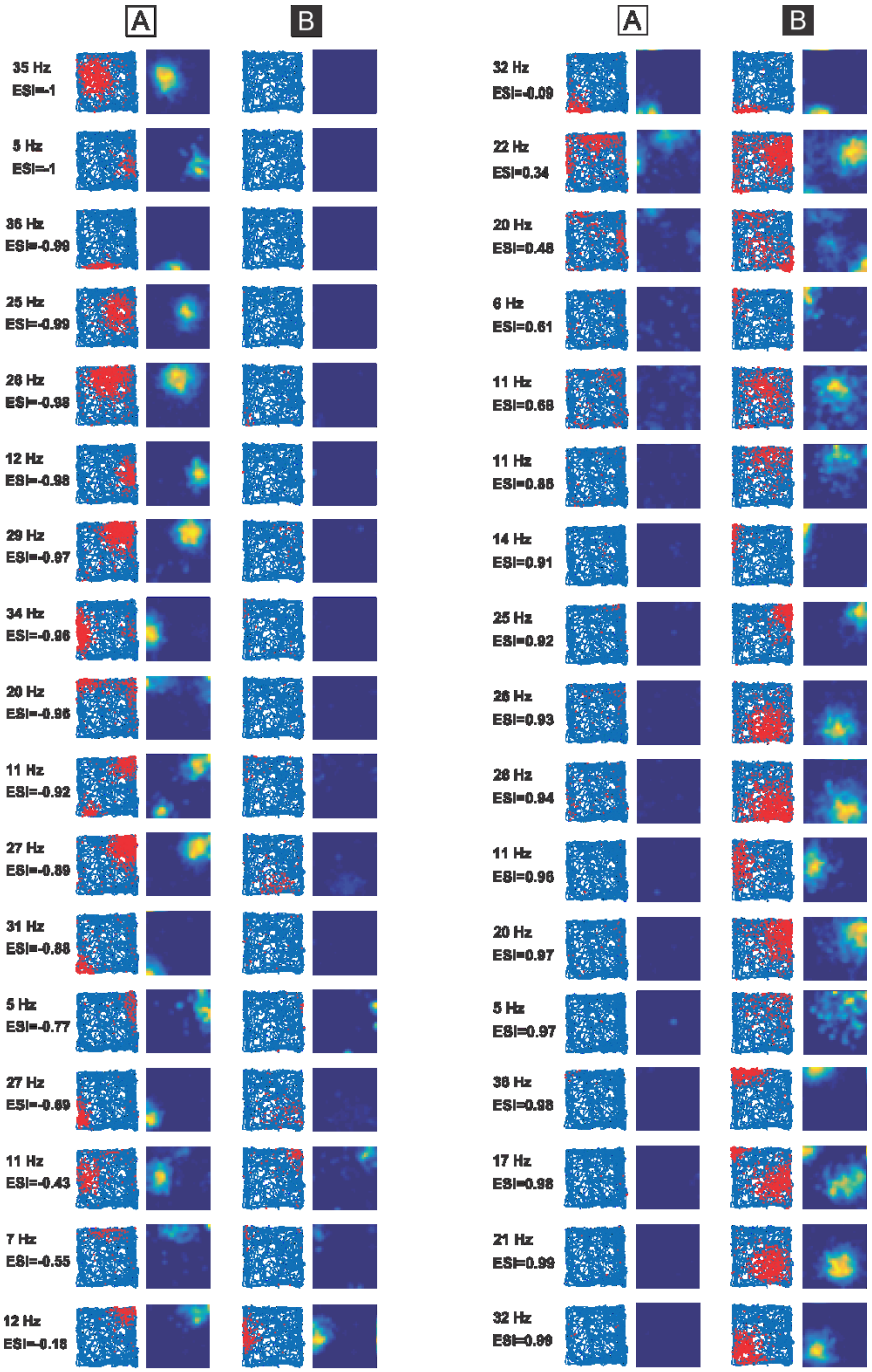

Figure 13 An example of place cell population recorded on single experimental day. For each cell, the rate maps and spikes depicted on trajectories are shown for reference sessions in environment A and B, respectively. The respective ESI values and peak rate value across both rate maps are reported for each place cell.

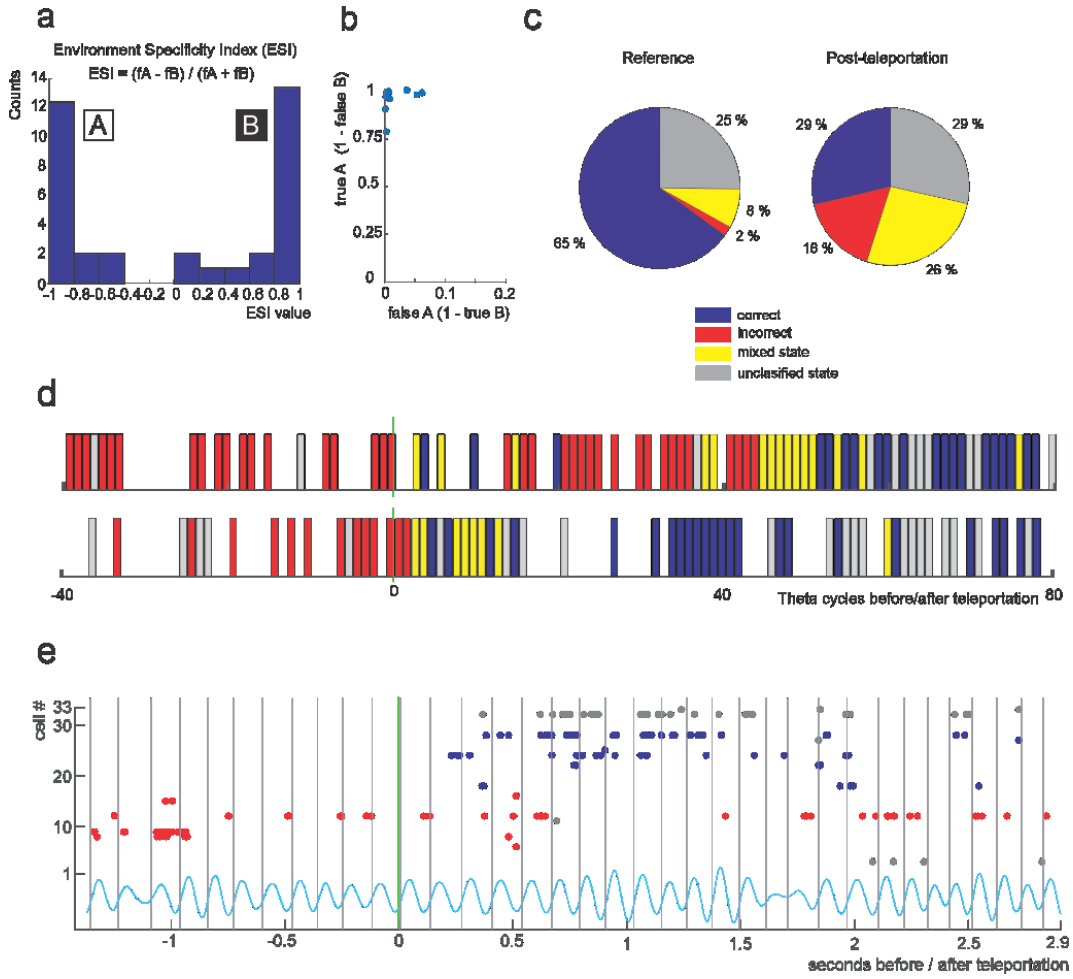

Figure 14 Classification of network activity with Environment-Specificity Index
(a) Distribution of *ESI* values for place cells recorded on a single day.
(b) Performance of *ESI* classifier applied on theta-binned population vectors from reference sessions on each recording day. The vertical axis represents instances when the map decoded from activity pattern in environment A was classified as map A (true A = 1 – false B). The horizontal axis represents instances when map A was decoded from population vectors in environment B (false A = 1 –true B).
(c) Proportion of decoded network states during teleportation sessions: stable cue epoch and post-teleportation period (20 theta bins following teleportation). Theta bins with 2 or more active cells were considered. The post-teleportation period is associated with marked increase in 'incorrect' and 'mixed' states.
(d) Examples of decoded states for period preceding and following teleportation event (red - theta bins with decoded map congruent with context after cue switch, blue - theta bins expressing map for the original context, yellow - mixed states, gray - unclassified bins with 2 or more active cells).
(e) Spike raster plots of recorded place cell population during example teleportation event (green bar). The spikes of cells classified as highly specific (abs(*ESI*)>0.8) for individual environments are depicted in red and blue color, respectively. The EEG trace filtered for theta frequency and borders between individual theta bins are shown.

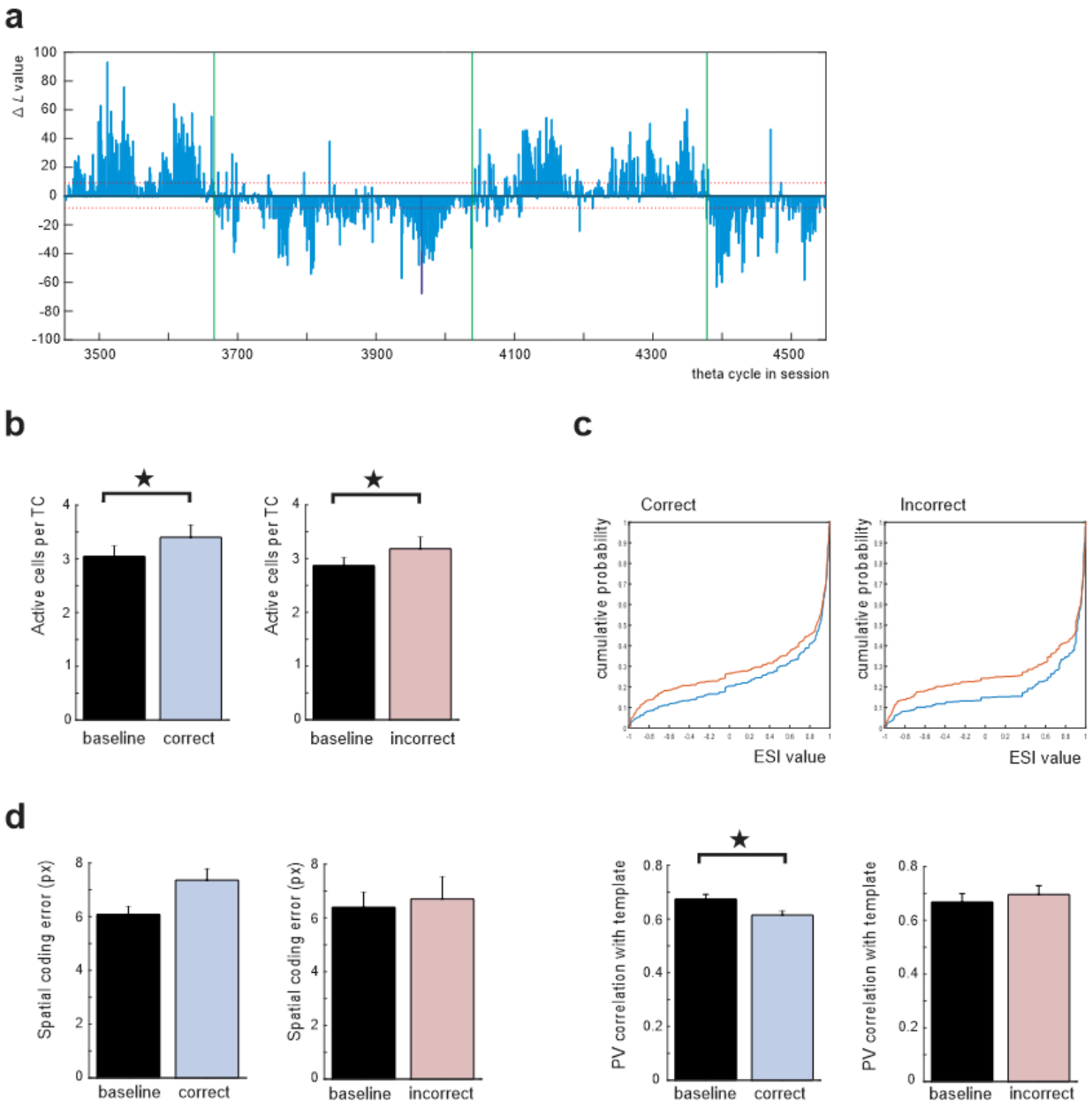

Figure 15 Analysis of network states decoded with Poisson rate decoder
(a) Evolution of Δ*L* values (see Methods) in response to switches of context identity (green bars - teleportations). The red dashed lines correspond to threshold for respective map detection.
(b) Number of active place cells during 'correct' and 'incorrect' post-teleportation bins and location-matched control bins.
(c) Cumulative distribution functions for ESI values associated with active cells across all 'correct' and 'incorrect' post-teleportation bins and location-matched control states (positive values indicate specificity for present context; red: post-telep., blue: baseline control).
(d) Decoded position error and correlation with template pattern for 'correct' and 'incorrect' post-teleportation states and associated control bins.

3.3 Discussion

Network hyperactivity during state transitions

We observed that change of spatial context is followed by increase in firing of CA3 place cell population that peaks shortly after cue switch. This was associated with increased number of place cells active within individual theta cycle. We then evaluated activity levels during theta states with respect to decoded spatial map. When classifying population vectors with *ESI*-based decoder, we detected increased activity levels associated with expression of map congruent with new context, but not during reactivation of map for previous environment. Such enhanced activity within newly recalled map might support successful network state shift and stabilization of correct spatial map. The alternative approach with Poisson decoder detected increased activity for both types of activity patterns but decoded states were associated with marked intrusion by activity within the concurrent map. This indicates that simultaneous entrainment of concurrent ensembles might contribute to the observed network hyperactivity.

What mechanism drives the network hyperactivity during state transition period? The changes in place cell excitability might reflect influence of neuromodulatory systems, possibly related to salient nature of contextual change (Prince et al., 2021). Alternatively, presumed presence of conflicting inputs (Posani et al., 2018) could lead to more widespread place cell entrainment and increase in overall population firing.

However, these mechanisms do not account for observation that hyperactivity predominantly involved place cell code for new environment.
The firing rates above baseline level within recalled representation could be potentially related to mechanisms of spike frequency adaptation (Madison and Nicoll, 1984). One of the putative underlying biophysical mechanisms are the dynamic changes in synaptic resources, as also considered by the computation model (Mark et al., 2017). The model implies that initially high synaptic resources enhance activity within just retrieved spatial map, which together with short-time plasticity contributes to ensemble competition during state interchange.

The activity of place cells is also dynamically modulated by sensory-motor factors such as speed of locomotion, where firing rate of a place cell positively correlates with velocity (McNaughton et al., 1983). In contrast, we observed average decrease in animal's speed shortly after teleportation. However, nature of our task did not enable us to exert full control of related sensory-motor and attentional variables and thus to fully assess their influence on network dynamics.

Increase in population activity during hippocampal network state transitions has been also observed in another recent study. Bulkin et al. (2020) analyzed CA1 activity of rats solving memory-guided odor discrimination task. The abrupt transitions between network states representing individual trials and inter-trial intervals were associated with large increase in population firing rate. The authors suggest that the increase in multiunit activity aids shift of contextual representations by pushing the activity through critical point for attractor state transitions. Notably, the study shows that the sharp attractor-like transitions in contextual representations with network hyperactivity occur also in the settings with predictable task structure. However, it is not clear to what extent the hyperactivity observations reported

by Bulkin et al. (2020) and in our work reflect the same phenomena, a potential task-invariant signature of state transitions.

Spatial map confluence during state transitions

We further focused our analysis on temporal separation of the competing activity patterns.
The previous work (Jezek et al., 2011) indicated that autoaossociative attractor dynamics within a theta cycle pushes network state towards one of the attractors, so that theta cycle population vectors tend to display high correlation with the reference pattern for one but not the other of the environments. This ensures substantial theta timescale segregation of the network patterns despite putative conflict of sensory inputs.
Here we built on previous findings and aimed to further investigate the extent of spatial representation mixture after change of environment identity at theta cycle and finer timescale levels.
We observed robust increase in theta bins categorized as 'mixed' occurring after the cue switch. The relatively high abundance of the mixed theta states suggests considerable confluence of the normally segregated representations. The spatial code mixing was also indicated by substantial intrusion of activity within alternative map during theta states classified with Poisson rate decoder.
The number of mixed states was still lower than in shuffled data, confirming the Jezek et al.'s results with our more categorical criteria for mixed state detection. This indicates that rather extensive pattern mixing revealed in our analysis is not inconsistent with higher order attractor-like organization of network state expression. Thus, individual theta states might be classified as significant expression of a particular map despite considerable intrusion of activity within the other representation.

The coactivation of concurrent activity patterns within a theta cycle does not preclude possible pattern segregation at finer timescale.
We observed that place cells specific for the same environment tended to be coactive at short time window <20 ms. A similar peak was not apparent in distribution of time lags between place cell activity across the ensembles.
A co-activation of cells specific for the concurrent environments within short temporal windows was however still present and displayed increase in response to cue switch.
The neuronal activity at such short time-scale is linked to emergence of functional cell assemblies (Buzsaki, 2010). Moreover, such co-firing corresponds to window of spike-timing-dependent plasticity (Buzsaki and Wang, 2012).
It is thus possible that synaptic plasticity mechanisms occurring during mixed states create associations between the originally segregated attractor states and influence their long-term dynamics. In line with this hypothesis, our recent work revealed that repeated teleportation experience leads to increased intrusion of incongruent alternative map during subsequent stable cue sessions and increase in place field map similarity across the environments (Kapl et al., 2022)

The existence of short-timescale coactivity of cells from different ensembles still doesn't rule out possibility of higher-order segregation of activity within a theta cycle. For example, it has been demonstrated that activity reflecting current stimuli occurs at different phase of theta cycle than activity associated with prediction or mental simulation (Wang et al. 2020, Kay et al., 2019, Kapl et al., 2022) On

the other hand, our finding of coincident activity across the maps is consistent with a model where conflicting visual cue and path integration inputs entrain simultaneous activity in the concurrent representations (Posani et al., 2018).

Representation of spatial position after teleportation

The network state shift is oftentimes accompanied by transient epoch of significant instability in contextual representation, where place cell ensemble within a map might receive incomplete or conflicting input compared to stable condition. Furthermore, we observed that population activity tends to be higher in response to change in spatial context. We thus analyzed quality of positional representation during highly dynamic retrieval period at a single theta cycle level.
We found compromised spatial code during theta states expressing map for new environment as corresponding spatial coding error values tended to be higher than during control stable-cue condition.
The same analysis performed on theta cycles reactivating map for the previous context did not return significant differences between post-teleportation and control data bins.
The detected magnitude in decoded position error increase during 'correct' states is consistent with a notion of partially degraded coding for spatial location within environment shortly after reinstatement of place cell map of new spatial context. In addition, the network can coherently represent current position during re-expression of the previously active representations.

The place cells' spatial activity is normally supported by two main streams of information flow (Knierim et al., 2014). The lateral entorhinal cortex feeds hippocampus with information about external sensory cues, which is combined with path integration signal, generated by the grid cells in the medial entorhinal cortex (Hargreaves et al., 2005). The inputs dynamically modulate place cell activity, with extrasensory cues providing ongoing correcting influence over path integration, which is prone to cumulation of errors (Jayakumar et al., 2019). Moreover, lesions of the medial entorhinal cortex are associated with partially decreased place cell code precision (Hales et al., 2014), suggesting that both inputs are required for optimal positional code.
The model postulating miss-match between visual cue and path integrator inputs after teleportation suggests that newly reactivated contextual code is initially guided solely by visual cue input, without support from grid cells' input (Posani et al., 2018). This might potentially decrease quality of positional coding.
Another possibility is potentially more dispersed entrainment of ensemble activity within newly retrieved map in relation to mechanisms of spike frequency adaptation, which would involve activity of place cells whose level of excitation would otherwise not cross firing threshold at given position.
The observed frequent mixing of ensembles at theta cycle level might also significantly impair performance of positional decoders (Posani et al., 2018). However, its influence was limited by using decoder that categorically rejects place cell activity specific for alternative map.

Interestingly, quality of spatial code during 'incorrect' states was comparable to control condition, despite lack of supporting specific light cues. This persisting position-specific activity could be possibly linked to path integrator input utilizing self-motion cues. The assumed source is the grid cell network in the medial entorhinal cortex, which might reset in delay with respect to the change in the context identity.

We observe that even during highly instable period of fast flickering between place maps shortly after cue switch, the hippocampus can provide relatively robust representation of subject's actual position. Despite increased coding error, the represented position tended to be biased to current location during most of the theta cycles representing current environment. We show this by using decoders that do not preselect data based on their position-specific activity patterns (in contrast to Jezek et al., 2011) as our contextual decoders were based on overall environment-specific firing rates. Similar observations were made by concurrent study (Posani et al., 2018).

Flexible coordination of activity in hippocampal network

Our analysis of competitive network state transitions adds to existing studies showing that hippocampus can display coordinated switching between different activity patterns (Kelemen and Fenton, 2016). Such fast alternations between different place cell ensembles have been observed in situations such as switching between navigational reference frames (Kelemen and Fenton, 2010) or modelling multiple future path alternatives (Johnson and Redish, 2007, Kay et al., 2020). The flexible transitions between ensemble activity are supported by theta oscillations, which mediate periodic update of the network state (Jezek et al., 2011). While we observed considerable coactivation of distinct patterns within individual theta cycle, the ensemble activity remained organized into distinct attractor states.

Moreover, finer temporal organization of activity exists within individual theta cycle window, where spiking reflecting current sensory stimuli occurs early in theta cycle, while the later phases are associated with non-local mental travel (Kay et al., 2020; Wang et al, 2020). This suggests that coordinated transitions between ensemble activity exists both within and across individual theta cycles.

In our recent work (Kapl et al., 2022) we show that theta oscillations can organize occasional switching between spatial map long after cessation of putative conflict in sensory cues associated with teleportation. Notably, activity representing non-current context was observed to appear later in theta cycle, in accord with the previous work.

From a point of normative theories of brain function, the switching between different activity patterns might be related to modelling probability distribution associated with alternative scenarios (Sanders et al., 2020; Savin et al., 2014). Within this framework, place cell map flickering following teleportation might reflect transient uncertainty about current context identity. Moreover, teleportation experience leads to increased flickering to the alternative representation during subsequent stable cue sessions, with gradual network stabilization in course of the session (Kapl et al., 2022). This might reflect gradual increase of rat's confidence in context identity. Theta oscillations thus might be instrumental in mediating changes in network state expression underlying adaptive probabilistic inference (Savin et al., 2014; Ujfalussy et al., 2021).

The fine-scale coordination of network activity is necessary for complex cognitive functions and its disruption might underlie symptoms of the brain disease. Accordingly, we have recently shown deficit in allothetic place-avoidance task in rat model of Alzheimer disease (Proskauer-Pena et al., 2021). The task requires a rat to flexibly distinguish between competing navigational reference frames and it revealed cognitive deficit in earlier stages of pathology development than more conventional spatial memory tests. This suggests that the associated demands placed on neural network make such cognitive control particularly vulnerable to influence by neural pathology.

Beyond the standard model: network response to gradual morphing of spatial context

The experiments with instant change of environment identity revealed ability of hippocampus to promptly reactivate appropriate contextual representation, with discrete attractor-like transitions between the alternative states, organized by theta oscillations.
Here we discuss further factors influencing network state transitions by considering preliminary results of complementary experiments, with gradual rather than instant change of corresponding light cues, thereby inducing gradual change of environment identity.
The variable intensity of both cue constellations during the morph epochs imposes an active conflict in present extrasensory cues, each of them supposedly entraining alternative representation.
Moreover, the gradual nature of contextual change suggests that network dynamics might be to a greater extent influenced by network state history. A strong influence of system history over current network state is referred to as hysteresis and is hallmark of autoassociative attractor systems (Solstad et al., 2014). The examination of network activity under such conditions thus might provide further important information about the nature of state dynamics in response to dynamically changing external inputs.

We thus trained rats in a training procedure similar to Jezek et. (2011). The main difference was that during the test morph sessions, the intensity of light cues was continuously modulated during 2 minutes long morph epochs, so that light cue configuration gradually changed from fully corresponding to one context to the configuration fully representing the alternative context. Several morph epochs were repeated during the morph session, with interposed stable cue periods.
The training led to emergence of distinct place cell representations for each of the environments (Fig. 16b).
We next assessed place cell ensemble dynamics during the session with gradual morphing of spatial context.
In analysis of preliminary data (Fig. 16), we studied evolution of activity of place cells with strong firing preference for one of the environments. We observed a sharp change between place cell activity from representation of the original context towards the representation of the gradually introduced new context, occurring approximately in the middle of the first morph epoch of the test session. Interestingly, the subsequent morph epochs were not associated with such a categorical change in spatial representation, as the network activity maintained established representation, despite the ongoing changes in the context identity (Fig. 16a).
In contrast, during subsequent test with abrupt teleportations (Fig. 16c), the network tended to display categorical changes in spatial map expression, hand-in-hand with changes of the contextual cues.
The observations indicate that change in contextual cues is not always associated with corresponding change in place cell firing, in particular when the change of the cues is introduced gradually. This is consistent with the idea of hysteresis, where the behavior of the system strongly depends on its previous states.
What might be the mechanisms behind the observed network state persistence?
In the view of dual input model (Posani et al., 2018), the changes in contextual sensory cues involve interplay between the extrasensory and the path integrator inputs, respectively, with the path integrator dwelling in the original state for some period of time after the change of the visual cues.
In the model, the path integrator realigns in a response to feedback input from hippocampus, signaling an update of the place cell activity pattern. However, in the situation with gradual change of the visual

cue input, the gradually diminishing cues defining the original context keep entraining the corresponding place cell ensemble, which significantly delays reset of the path integrator, which in turn keeps supporting the original representation. However, the corresponding state transition should eventually take place.
Thus, some extension of the existent model might be necessary to fully account for the observations reported here. An important factor to be considered is the ubiquitous phenomenon of synaptic plasticity. The gradual changes in sensory cues might lead to new associations between the stimuli and place cell activity pattern, which in turn would influence network state kinetics. However, such associations between neural representation and incongruent visual cues might be of limited nature, as further analysis shows that rats tend to activate mostly distinct maps in subsequent stable cue sessions in context-specific manner (Leemburg et al., unpublished).

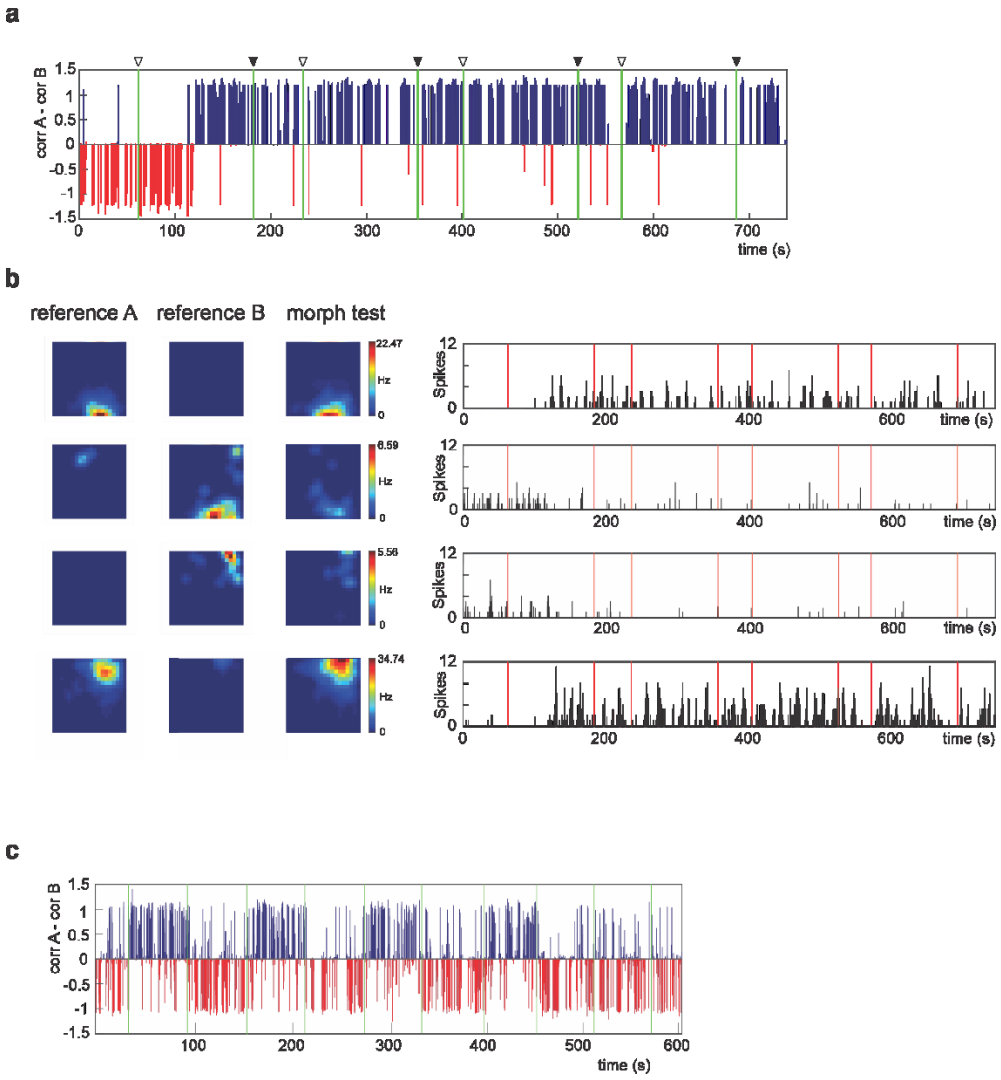

Figure 16 Network state dynamics during gradual change of context identity

(a) Theta-binned population vectors were correlated with position-specific templates (as in Jezek et al. (2011)). Difference in correlation with template for A and B are shown for each theta cycle. The green bars depict time of start (white mark) and end (black mark) of individual 2 min morph epochs.

(b) Four example place cells recorded during the morph experiment, with respective place fields for reference sessions in each environment and subsequent morph session (left). For each cell, the colormap is normalized to peak firing rate value across the sessions. Right: Theta-binned spiking activity of the same cells during the morph session (red bars demark morph epochs). The cells highly specific for context A continue to fire despite changes in context identity.

(c) Network state activity during experiment with instant changes of context identity, recorded in the same rat on a subsequent recording day.

4 Rhythmic network activity during state transitions

The information processing in cortical networks, including the hippocampal formation, is crucially influenced by ongoing oscillatory activity.
The most salient hippocampal rhythmic pattern during alert wakefulness are the theta oscillations, corresponding to the 6-12 Hz frequency band. Theta oscillations are essential for hippocampus-dependent memory and coordinate network activity via multiple mechanisms such as by supporting internally coordinated activity and interregional communication.
The results of teleportation experiments put forward another function of theta oscillations: theta-mediated network inhibition provides regular network reset to promptly update activity pattern. In particular, following abrupt change of spatial maps, theta oscillations pace transitions between expression of competing cognitive maps, reflecting conjectured conflict between idiothetic and extrasensory input, respectively.
In addition to theta, hippocampal activity is co-orchestrated by faster gamma oscillations. The gamma oscillations include multiple components, which differ in frequency and co-occur with theta in phase-specific manner. What is the possible role of hippocampal gamma in network state transitions? The gamma oscillations are implied in organization of cell assemblies and coordination of information flow within hippocampal formation. The mid-frequency gamma oscillations route flow of the information from the entorhinal cortex to the hippocampus. In contrast, the slow gamma oscillations underlie CA3-CA1 communication associated with internally coordinated memory recall.
To analyze involvement of hippocampal rhythmic activity during change of spatial context, we assessed rhythmicity in theta and gamma frequency bands after teleportation and compared to pre-teleportation baseline. We argued that capturing oscillatory signature of state shift period can reveal more about the mode of network processing and information flow during teleportation-triggered retrieval of spatial representation.

4.1 Methods

We analyzed recordings from teleportation experiments (Jezek et al., 2011). For each experimental session, representative tetrode with histologically verified position in vicinity to CA3 pyramidal layer was employed as a source of LFP signal.

Cross-frequency coherence

Cross-frequency coherence calculation was employed to determine phase-amplitude correlations between different frequencies (Fig. 17d). The magnitude-squared coherence was calculated between time-varying power for respective frequencies (estimated by Morlet's wavelet method) and original signal (Colgin et al., 2009).

Time-frequency representation of power spectra

Time-frequency representations of power spectra were calculated by Morlet's wavelet method, using a sliding window. To display spectra across gamma frequency range, the power values were z-scored in time for each frequency within examined time epoch. This accounts for the fact that brain oscillations power scales with 1/f and served for better visualization of power changes within higher frequency range.
To illustrate gamma power relationship to theta oscillations, time-frequency representations of gamma power were calculated for 600 ms window centered on theta bin border (defined as the phase reflecting minimum population activity). The resulting plot was generated by averaging across 1500 consecutive theta bins within a single example session. The similar approach was used for periods (20 theta cycles pre/post) surrounding teleportation events and the difference was calculated between the resulting power representations for post- and pre-teleportation epochs.

Amplitude

To evaluate change in amplitude of the oscillations in respective frequency bands, the LFP signal was bandpass filtered for given frequency range. The amplitude of the filtered signal was extracted using Hilbert transform and z-scored across the session. The average of z-scored amplitude was then computed for the intervals 2 seconds preceding and following the teleportation.
For the complementary analysis accounting for potential speed-dependence of detected amplitude, the amplitude values were divided into bins according the instantaneous speed of the animal with 2 cm/s increments and z-scored separately for each speed bin. The obtained z-score values were then used for calculation of teleportation-triggered change in amplitude.

4.2 Results

The examination of peri-teleportation spectrograms centered on theta band indicated increase in theta power following switch of spatial context (Fig. 17a). To quantitatively evaluate the effect, we considered amplitude of Hilbert-transformed LFP signal filtered for theta frequency during epochs preceding and following teleportation event. We confirmed increase in theta amplitude triggered by switch of the light cues (z-scored amplitude: 0,06 ± 0,04 pre-teleport, 0,28 ± 0,06 post-teleport; p= 0,0098 Wilcoxon signed-rank test, n=11 recordings).
We further focused on the analysis of gamma rhythmicity. We detected oscillations within gamma frequency range, with amplitude modulated by phase of theta (Fig.17d).
We asked, if teleportation procedure is associated with change in gamma rhythmicity. The perite-teleportation spectrograms suggested increase in power within faster gamma frequencies (60-90 Hz) during approximately 2 seconds after teleportation (Fig. 17b). This was confirmed quantitatively, as we detected increase in amplitude in respective frequency range (z-scored amplitude: 0,00 ± 0,01 pre-teleport, 0,29 ± 0,02 post-teleport, p= 0,0009 Wilcoxon signed-rank test; n=11 recordings; Fig. 17 c).
We further performed complementary analysis with amplitude within examined frequency bands normalized for instantaneous speed, taking into account that both theta and gamma oscillations are modulated by speed of locomotion (Whishaw and Vanderwolf, 1973; Zheng et al., 2015). The results of

analysis with speed-normalized data further supported finding of increase in theta (z-scored amplitude: 0,02 ± 0,03 pre-teleport, 0,32 ± 0,05 post-teleport; p< 0,001 Wilcoxon signed-rank test) and gamma band (z-scored amplitude: -0,01 ± 0,01 pre-teleport, 0,29 ± 0,02 post-teleport; p< 0,001 Wilcoxon signed-rank test).

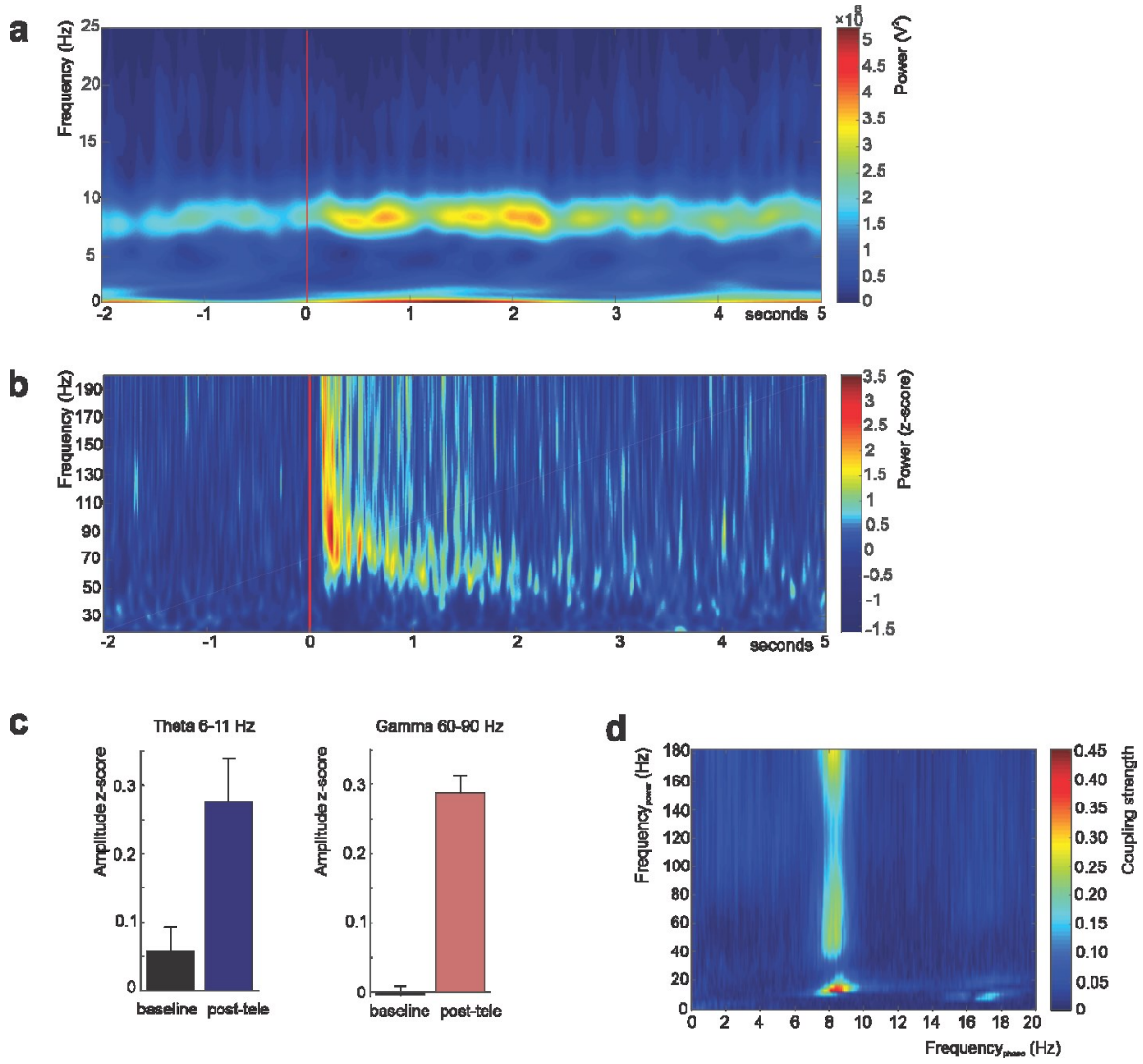

Figure 17 Local field potential dynamics during teleportation
(a)Time-frequency spectrogram centered on theta frequency band showing increases in theta power following teleportation (averaged across teleportation events in example recording).
(b) Time-frequency spectrogram indicating increase in gamma frequency band after teleportation (averaged across sessions). Z-scored power values for better visualization of changes across broad spectrum of frequencies.
(c)The increase in amplitude in 6-11 Hz theta and 60-90 Hz gamma band after teleportation (2 second pre/post).
(d) Cross-frequency commodulagram depicting rhythmic activity in gamma band modulated by phase of theta oscillations (averaged across sessions).

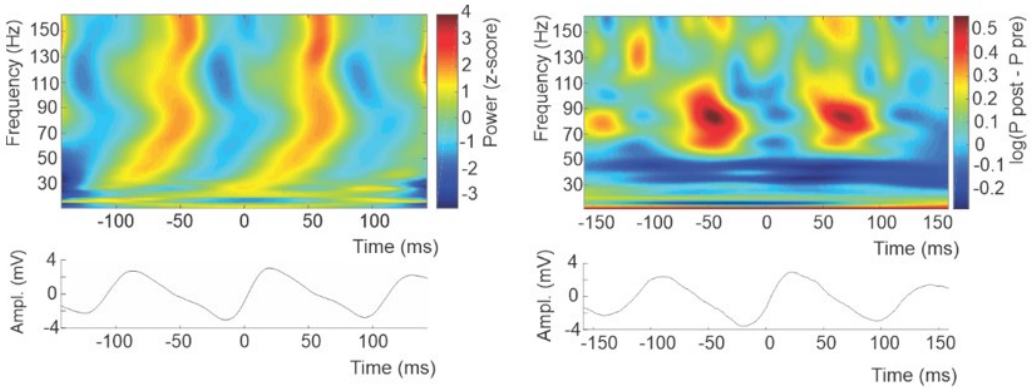

Figure 18 Left: Averaged time-frequency spectra during example baseline epoch. The spectra were calculated for consecutive short periods centered on border between subsequent theta cycles. The respective averaged theta trace is depicted. The plot indicates presence of rhythmic activity in gamma frequency range modulated by phase of theta. Right: Visualized difference in average time-frequency power spectrograms between epochs following and preceding teleportation, across teleportation events during example session.

4.3 Discussion

The analysis of local field potential during teleportation procedure revealed enhanced theta rhythmicity following the switch in context identity. The potential advantages of enhanced, robust theta oscillations upon the change of spatial context could be numerous.
Jezek et al. (2011) showed that theta oscillations enable fast transitions between hippocampal network states, which can occur across two subsequent theta cycles. The strong theta-mediated network inhibition after teleportation thus ensures that the entorhinal input can trigger a prompt retrieval of correct spatial representation.
The activity dynamics in CA3 region of the hippocampus is strongly affected by abundance of recurrent collaterals. In fact, the recurrent collaterals represent the vast majority of afferent synaptic connections on individual CA3 pyramidal cell (Rolls, 2007). The autoassociative connectivity tends to stabilize the network activity pattern within the respective attractor state. The network state can be then effectively updated only if this self-sustained firing is interrupted by sufficient inhibition. Such a robust network reset is provided by theta oscillations.
The situation has been quantitatively assessed by a computational model (Stella and Treves, 2011). It has been shown that only the CA3 network with strong inhibition can undergo fast transition between the attractor states. Moreover, the inhibition should occur in phase with the external input conveying sensory information (Stella and Treves, 2010). Thus, in the beginning of theta cycle, when population activity is low, the entorhinal input entrains the respective network pattern. The further amplification of expressed activity by recurrent collaterals takes place in later phases of theta cycles, until the attractor dynamics is disrupted by inhibition.

The computational modelling also suggested that theta oscillations might be essential for emergence of flickering in the context of short-term plasticity (Mark et al., 2017). It has been suggested that spatially uniform input modulating theta amplitude can give rise to expression of the previous ensemble, which has facilitated synaptic efficacy due to short-term plasticity. Accordingly, flickering frequency correlates with theta amplitude. Within the framework of the model, it could be speculated that strong theta during periods of high ambiguity promotes bistable 'explorative' mode of the hippocampal network. This could be of adaptive advantage as it would enable the network to settle down in respective state only after sufficient evidence has been provided by the sensory input.

Theta oscillations are also proposed to mediate effective communication within hippocampal formation (Mizuseki, 2009) and between hippocampus and connected structures, such as prefrontal cortex. The prefrontal cortex extracts contextual information from hippocampus and performs top-down control of context-specific memory retrieval (Rajasethupathy et al., 2015; Eichenbaum, 2017). Accordingly, the retrieval of contextual memory was observed to be associated with theta synchrony-based bidirectional hippocampal-prefrontal interactions (Place et al., 2016). In particular, hippocampal theta oscillations led prefrontal theta upon entry to the environment and reversed relationship was observed during subsequent retrieval of context-dependent memory.
It is not clear if teleportation-induced retrieval of appropriate spatial representation involves any possible top-down influence from the prefrontal network. Given the conflicting nature of the post-teleportation period and the role of prefrontal cortex in supporting appropriate network state by discarding similar, but

context-inappropriate activity patterns (Eichenbaum, 2017), involvement of prefrontal cortex should be considered. The strong theta following hippocampal state transition would also support bottom-up hippocampo-prefrontal interaction, updating contextual information in the prefrontal cortex. This would in general promote the prefrontal cortex's role in recalling context-specific memories.

Furthermore, we observed increase in amplitude of 60-90 Hz gamma oscillations following switch of spatial environment.
The gamma oscillations are linked to emergence of functional cell assemblies and coordination of communication between subregions of hippocampal formation. The observed increase in gamma after cue switch might thus reflect enhanced information flow within hippocampal formation. The gamma synchronization of activity in the upstream population facilitates effective input integration in the downstream target. Consequently, gamma oscillations are expected to support computations underling network state transitions, for example by facilitating the new ensemble entrainment by coordinated flow of input conveying change of contextual cues.

The previous work focusing mostly on CA1 region has established existence of three robust components of hippocampal gamma rhythmicity. In particular, the slow gamma with maximal power at CA1 stratum radiatum underlies CA3-CA1 coupling, while mid-frequency gamma routes flow of information from the medial entorhinal cortex to CA1.
In contrast, the gamma rhythms in CA3 network have been much less studied so far. In our data, the spectral profiles of LFP traces superimposed on theta wave suggested existence of slower and faster forms of gamma oscillations in CA3, differentially modulated by phase of theta (Fig. 18). This is in accord with previous observations (Jiang et al., 2019).
The slow gamma oscillations have been linked to retrieval mode with non-local CA1 ensemble activity (Zheng et al., 2016; Dvorak et. al, 2016) during CA3-CA1 synchrony. In addition, slow gamma has been reported to underlie synchrony between LEC and CA1, LEC and dentate gyrus (Igarashi et al., 2014; Fernandez-Ruiz et al., 2021), as well as to organize flow of activity across whole LEC-DG-CA3-CA1 trisynaptic loop (Dvorak et al., 2021).
The faster mid-frequency gamma in CA1 associated with input from layer III of medial entorhinal cortex has been linked to place cell coding adherent to current position and might reflect attendance to sensory stimuli (Takahashi et al., 2014; Colgin. 2015).
Accordingly, it can be hypothesized that observed increase in 60-90 Hz range shortly after teleportation reflects enhanced sensory information flow upon change of visual cues. However, it is yet to be elucidated how frequency of gamma routes information flow between layer II of entorhinal cortex and CA3 neuronal population. A recent report suggested gamma rhythmicity in layer II of the MEC to be dominated by faster band oscillations (>100 Hz; Fernandez-Ruiz et al., 2021).
Moreover, separate involvement of LEC and MEC inputs in teleportation-triggered activity pattern interchange needs to be considered. LEC activity reflects egocentrically perceived aspects of experience related to local sensory cues. Thus, it is possible that initial information about contextual change is provided to CA3 by input from LEC, with only subsequent realignment of MEC allocentric representation.

Altogether, we observed that introduction of new spatial context, which induced recall of respective memory state, was associated with increased rhythmicity in theta and gamma frequency bands in CA3 network. Our research opens the door for further study of mechanisms by which neural oscillations

orchestrate flow of information associated with memory retrieval. Moreover, disturbances in oscillatory coordination underlie aberrant network dynamics associated with brain disease (Buzsaki and Watson, 2012). The study of neural oscillation thus provides insight into mechanisms of coordinated network activity during memory processing and its disruption in neuropsychiatric disorders, such as Alzheimer's disease and schizophrenia (Uhlhaas and Singer, 2015).

5 Conclusions

1. We detected increased place cell activity following change of the spatial environment identity. The averaged activity levels peaked shortly after cue change and returned to the baseline within a few seconds. The analysis of data with respect to theta oscillations revealed increase in total spikes and number of active cells within a theta bin. When decoding contextual representation with stringent criteria for place cell environment specificity, we detected increased place cell activity during network states expressing 'correct map' (reflecting present environment) but not during states expressing 'incorrect' map (corresponding to the previous environment).

2. We detected compromised representation of current position during network states expressing map for present environment shortly after switch of context-defining cues. This was revealed by increased decoded position error associated with these states. We did not find any significant change in spatial code quality during network states with decoded map for the previous context, suggesting ongoing representation of current position. We show this by using map decoders that do not preselect data based on activity patterns specific for given position. Our analysis provides insight into nature of spatial code during first moments of place cell map reinstatement and associated transient network state competition.

3. We observed that hippocampal network state shift induced by change in spatial context identity is accompanied by considerable coactivation of distinct place cell representations. The abundant activity pattern mixing occurred at level of individual theta bins, as well as at shorter timescale. Such coactivation might facilitate associations between originally distinct ensembles and influence long-term network state dynamics.

4. We show that change in spatial context is followed by transient increase in amplitude of hippocampal theta and faster gamma (60-90 Hz) oscillations. The robust theta oscillations might provide sufficient inhibition supporting prompt update of the network state. The activity in gamma band might be related to coordinated information processing across hippocampal formation during spatial map recollection.

6 References

1. Allegra M, Posani L, Gómez-Ocádiz R, Schmidt-Hieber C. Differential Relation between Neuronal and Behavioral Discrimination during Hippocampal Memory Encoding. *Neuron*. 2020;108(6):1103-1112.e6. doi:https://doi.org/10.1016/j.neuron.2020.09.032

2. Alme CB, Miao C, Jezek K, Treves A, Moser EI, Moser M-B. Place cells in the hippocampus: eleven maps for eleven rooms. *Proc Natl Acad Sci U S A*. 2014;111(52):18428-18435. doi:10.1073/pnas.1421056111

3. Amaral DG, Dent JA. Development of the mossy fibers of the dentate gyrus: I. A light and electron microscopic study of the mossy fibers and their expansions. *J Comp Neurol*. 1981;195(1):51-86. doi:10.1002/cne.901950106

4. Amaral DG. Introduction: What is where in the medial temporal lobe? *Hippocampus*. 1999;9(1):1-6. doi:https://doi.org/10.1002/(SICI)1098-1063(1999)9:1<1::AID-HIPO1>3.0.CO;2-T

5. Amaral DG. Emerging principles of intrinsic hippocampal organization. *Curr Opin Neurobiol*. 1993;3(2):225-229. doi:https://doi.org/10.1016/0959-4388(93)90214-J

6. Ambrose RE, Pfeiffer BE, Foster DJ. Reverse Replay of Hippocampal Place Cells Is Uniquely Modulated by Changing Reward. *Neuron*. 2016;91(5):1124-1136. doi:10.1016/j.neuron.2016.07.047

7. Amit DJ, del Giudice P, Denby B, Rolls ET, Treves A. NEURAL NETWORKS. In: *Neural Networks*. Hargreaves, E. L., Rao, G., Lee, I., & Knierim, J. J. (2005). Major dissociation between medial and lateral entorhinal input to dorsal hippocampus. Science (New York, N.Y.), 308(5729), 1792–1794. https://doi.org/10.1126/science.1110449 Knierim, J. J., Neu; 1995:1-308. doi:doi:10.1142/9789814531962

8. Andersen P, Bliss TVP, Skrede KK. Lamellar organization of hippocampal excitatory pathways. *Exp Brain Res*. 1971;13(2):222-238. doi:10.1007/BF00234087

9. Aronov D, Nevers R, Tank DW. Mapping of a non-spatial dimension by the hippocampal-entorhinal circuit. *Nature*. 2017;543(7647):719-722. doi:10.1038/nature21692

10. Battaglia FP, Treves A. Attractor neural networks storing multiple space representations: A model for hippocampal place fields. *Phys Rev E*. 1998;58(6):7738-7753. doi:10.1103/PhysRevE.58.7738

11. Behrens TEJ, Muller TH, Whittington JCR, et al. What Is a Cognitive Map? Organizing Knowledge for Flexible Behavior. *Neuron*. 2018;100(2):490-509. doi:10.1016/j.neuron.2018.10.002

12. Bellmund JLS, Gärdenfors P, Moser EI, Doeller CF. Navigating cognition: Spatial codes for human thinking. *Science (80-)*. 2018;362(6415):eaat6766. doi:10.1126/science.aat6766

13. Benchenane K, Peyrache A, Khamassi M, et al. Coherent theta oscillations and reorganization of spike timing in the hippocampal- prefrontal network upon learning. *Neuron*. 2010;66(6):921-936. doi:10.1016/j.neuron.2010.05.013

14. Bezaire MJ, Raikov I, Burk K, Vyas D, Soltesz I. Interneuronal mechanisms of hippocampal theta oscillations in a full-scale model of the rodent CA1 circuit. *Elife*. 2016;5. doi:10.7554/eLife.18566

15. Bieri KW, Bobbitt KN, Colgin LL. Slow and fast γ rhythms coordinate different spatial coding modes in hippocampal place cells. *Neuron*. 2014;82(3):670-681. doi:10.1016/j.neuron.2014.03.013

16. Bliss T V, Gardner-Medwin AR. Long-lasting potentiation of synaptic transmission in the dentate area of the unanaestetized rabbit following stimulation of the perforant path. *J Physiol*. 1973;232(2):357-374. doi:10.1113/jphysiol.1973.sp010274

17. Bliss T V, Lomo T. Long-lasting potentiation of synaptic transmission in the dentate area of the anaesthetized rabbit following stimulation of the perforant path. *J Physiol*. 1973;232(2):331-356. doi:10.1113/jphysiol.1973.sp010273

18. Boccara C. Spatial Coding in the Hippocampal Region. Published online 2014.

19. Boccara CN, Nardin M, Stella F, O'Neill J, Csicsvari J. The entorhinal cognitive map is attracted to goals. *Science (80-)*. 2019;363(6434):1443 LP - 1447. doi:10.1126/science.aav4837

20. Bonnevie T, Dunn B, Fyhn M, et al. Grid cells require excitatory drive from the hippocampus. *Nat Neurosci*. 2013;16(3):309-317. doi:10.1038/nn.3311

21. Brun VH, Otnass MK, Molden S, et al. Place cells and place recognition maintained by direct entorhinal-hippocampal circuitry. *Science*. 2002;296(5576):2243-2246. doi:10.1126/science.1071089

22. Bulkin DA, Sinclair DG, Law LM, Smith DM. Hippocampal state transitions at the boundaries between trial epochs. *Hippocampus*. 2020;30(6):582-595. doi:10.1002/hipo.23180

23. Bunsey M, Eichenbaum H. Conservation of hippocampal memory function in rats and humans. *Nature*. 1996;379(6562):255-257. doi:10.1038/379255a0

24. Burak Y, Fiete IR. Accurate path integration in continuous attractor network models of grid cells. *PLoS Comput Biol*. 2009;5(2):e1000291.

25. Butler WN, Hardcastle K, Giocomo LM. Remembered reward locations restructure entorhinal spatial maps. *Science (80-)*. 2019;363(6434):1447 LP - 1452. doi:10.1126/science.aav5297

26. Butler WN, Smith KS, van der Meer MAA, Taube JS. The Head-Direction Signal Plays a Functional Role as a Neural Compass during Navigation. *Curr Biol*. 2017;27(9):1259-1267. doi:https://doi.org/10.1016/j.cub.2017.03.033

27. Buzsáki G. Two-stage model of memory trace formation: a role for "noisy" brain states. *Neuroscience*. 1989;31(3):551-570. doi:10.1016/0306-4522(89)90423-5

28. Buzsáki G. Neural syntax: cell assemblies, synapsembles, and readers. *Neuron*. 2010;68(3):362-385. doi:10.1016/j.neuron.2010.09.023

29. Buzsáki G. Theta oscillations in the hippocampus. *Neuron*. 2002;33(3):325-340. doi:10.1016/s0896-6273(02)00586-x

30. Buzsáki G. Hippocampal sharp wave-ripple: A cognitive biomarker for episodic memory and planning. *Hippocampus*. 2015;25(10):1073-1188. doi:10.1002/hipo.22488

31. Buzsáki G, Draguhn A. Neuronal oscillations in cortical networks. *Science*. 2004;304(5679):1926-1929. doi:10.1126/science.1099745

32. Buzsáki G, Moser EI. Memory, navigation and theta rhythm in the hippocampal-entorhinal system. *Nat Neurosci*. 2013;16(2):130-138. doi:10.1038/nn.3304

33. Buzsáki G, Vanderwolf CH. Cellular bases of hippocampal EEG in the behaving rat. *Brain Res Rev*. 1983;6(2):139-171.

34. Buzsáki G, Wang X-J. Mechanisms of gamma oscillations. *Annu Rev Neurosci*. 2012;35:203-225. doi:10.1146/annurev-neuro-062111-150444

35. Buzsáki G, Watson BO. Brain rhythms and neural syntax: implications for efficient coding of cognitive content and neuropsychiatric disease. *Dialogues Clin Neurosci*. 2012;14(4):345-367. doi:10.31887/DCNS.2012.14.4/gbuzsaki

36. Carr MF, Karlsson MP, Frank LM. Transient Slow Gamma Synchrony Underlies Hippocampal Memory Replay. *Neuron*. 2012;75(4):700-713. doi:https://doi.org/10.1016/j.neuron.2012.06.014

37. Cermak LS, O'Connor M. The anterograde and retrograde retrieval ability of a patient with amnesia due to encephalitis. *Neuropsychologia*. 1983;21(3):213-234. doi:10.1016/0028-3932(83)90039-8

38. Churchland PS, Sejnowski TJ. *The Computational Brain*. 1992

39. Citri A, Malenka RC. Synaptic Plasticity: Multiple Forms, Functions, and Mechanisms. *Neuropsychopharmacology*. 2008;33(1):18-41. doi:10.1038/sj.npp.1301559

40. Clelland CD, Choi M, Romberg C, et al. A functional role for adult hippocampal neurogenesis in spatial pattern separation. *Science*. 2009;325(5937):210-213. doi:10.1126/science.1173215

41. Colgin LL, Leutgeb S, Jezek K, et al. Attractor-map versus autoassociation based attractor dynamics in the hippocampal network. *J Neurophysiol*. 2010;104(1):35-50. doi:10.1152/jn.00202.2010

42. Colgin LL. Rhythms of the hippocampal network. *Nat Rev Neurosci*. 2016;17(4):239-249. doi:10.1038/nrn.2016.21

43. Colgin LL, Denninger T, Fyhn M, et al. Frequency of gamma oscillations routes flow of information in the hippocampus. *Nature*. 2009;462(7271):353-357. doi:10.1038/nature08573

44. Colgin LL, Moser EI, Moser M-B. Understanding memory through hippocampal remapping. *Trends Neurosci*. 2008;31(9):469-477. doi:10.1016/j.tins.2008.06.008

45. Constantinescu AO, O'Reilly JX, Behrens TEJ. Organizing conceptual knowledge in humans with a gridlike code. *Science (80-)*. 2016;352(6292):1464 LP - 1468. doi:10.1126/science.aaf0941

46. Damasio AR. Time-locked multiregional retroactivation: A systems-level proposal for the neural substrates of recall and recognition. *Cognition*. 1989;33(1):25-62. doi:https://doi.org/10.1016/0010-0277(89)90005-X

47. de Lavilléon G, Lacroix MM, Rondi-Reig L, Benchenane K. Explicit memory creation during sleep demonstrates a causal role of place cells in navigation. *Nat Neurosci*. 2015;18(4):493-495. doi:10.1038/nn.3970

48. Diba K, Buzsáki G. Forward and reverse hippocampal place-cell sequences during ripples. *Nat Neurosci*. 2007;10(10):1241-1242. doi:10.1038/nn1961

49. Dragoi G, Buzsáki G. Temporal encoding of place sequences by hippocampal cell assemblies. *Neuron*. 2006;50(1):145-157. doi:10.1016/j.neuron.2006.02.023

50. Dupret D, O'Neill J, Csicsvari J. Dynamic reconfiguration of hippocampal interneuron circuits during spatial learning. *Neuron*. 2013;78(1):166-180. doi:10.1016/j.neuron.2013.01.033

51. Dvorak D, Chung A, Park EH, Fenton AA. Dentate spikes and external control of hippocampal function. *Cell Rep*. 2021;36(5):109497. doi:10.1016/j.celrep.2021.109497

52. Dvorak D, Fenton AA. Toward a proper estimation of phase-amplitude coupling in neural oscillations. *J Neurosci Methods*. 2014;225:42-56. doi:10.1016/j.jneumeth.2014.01.002

53. Dvorak D, Radwan B, Sparks FT, Talbot ZN, Fenton AA. Control of recollection by slow gamma dominating mid-frequency gamma in hippocampus CA1. *PLoS Biol*. 2018;16(1):e2003354. doi:10.1371/journal.pbio.2003354

54. Eichenbaum H, Stewart C, Morris RG. Hippocampal representation in place learning. *J Neurosci*. 1990;10(11):3531 LP - 3542. doi:10.1523/JNEUROSCI.10-11-03531.1990

55. Eichenbaum H. Prefrontal-hippocampal interactions in episodic memory. *Nat Rev Neurosci*. 2017;18(9):547-558. doi:10.1038/nrn.2017.74

56. Ekstrom AD, Kahana MJ, Caplan JB, et al. Cellular networks underlying human spatial navigation. *Nature*. 2003;425(6954):184-188.

57. Eschenko O, Ramadan W, Mölle M, Born J, Sara SJ. Sustained increase in hippocampal sharp-wave ripple activity during slow-wave sleep after learning. *Learn Mem*. 2008;15(4):222-228. doi:10.1101/lm.726008

58. Feng T, Silva D, Foster DJ. Dissociation between the experience-dependent development of hippocampal theta sequences and single-trial phase precession. *J Neurosci*. 2015;35(12):4890-4902. doi:10.1523/JNEUROSCI.2614-14.2015

59. Fernández-Ruiz A, Oliva A, Soula M, et al. Gamma rhythm communication between entorhinal cortex and dentate gyrus neuronal assemblies. *Science*. 2021;372(6537). doi:10.1126/science.abf3119

60. Fink GR, Markowitsch HJ, Reinkemeier M, Bruckbauer T, Kessler J, Heiss WD. Cerebral representation of one's own past: neural networks involved in autobiographical memory. *J Neurosci*. 1996;16(13):4275-4282. doi:10.1523/JNEUROSCI.16-13-04275.1996

61. Foster DJ, Wilson MA. Reverse replay of behavioural sequences in hippocampal place cells during the awake state. *Nature*. 2006;440(7084):680-683. doi:10.1038/nature04587

62. Foster DJ, Wilson MA. Hippocampal theta sequences. *Hippocampus*. 2007;17(11):1093-1099. doi:10.1002/hipo.20345

63. Fries P. Rhythms for Cognition: Communication through Coherence. *Neuron*. 2015;88(1):220-235. doi:10.1016/j.neuron.2015.09.034

64. Fuhs MC, Touretzky DS. A spin glass model of path integration in rat medial entorhinal cortex. *J Neurosci*. 2006;26(16):4266-4276.

65. Fyhn M, Molden S, Witter MP, Moser EI, Moser M-B. Spatial representation in the entorhinal cortex. *Science*. 2004;305(5688):1258-1264. doi:10.1126/science.1099901

66. Gardner RJ, Lu L, Wernle T, Moser M-B, Moser EI. Correlation structure of grid cells is preserved during sleep. *Nat Neurosci*. 2019;22(4):598-608.

67. Gauthier JL, Tank DW. A Dedicated Population for Reward Coding in the Hippocampus. *Neuron*. 2018;99(1):179-193.e7. doi:10.1016/j.neuron.2018.06.008

68. Gil M, Ancau M, Schlesiger MI, et al. Impaired path integration in mice with disrupted grid cell firing. *Nat Neurosci*. 2018;21(1):81-91. doi:10.1038/s41593-017-0039-3

69. Gilmore AW, Quach A, Kalinowski SE, et al. Evidence supporting a time-limited hippocampal role in retrieving autobiographical memories. *Proc Natl Acad Sci*. 2021;118(12):e2023069118. doi:10.1073/pnas.2023069118

70. Girardeau G, Benchenane K, Wiener SI, Buzsáki G, Zugaro MB. Selective suppression of hippocampal ripples impairs spatial memory. *Nat Neurosci*. 2009;12(10):1222-1223. doi:10.1038/nn.2384

71. GoodSmith D, Chen X, Wang C, et al. Spatial Representations of Granule Cells and Mossy Cells of the Dentate Gyrus. *Neuron*. 2017;93(3):677-690.e5. doi:10.1016/j.neuron.2016.12.026

72. Goutagny R, Jackson J, Williams S. Self-generated theta oscillations in the hippocampus. *Nat Neurosci*. 2009;12(12):1491-1493. doi:10.1038/nn.2440

73. Goyal A, Miller J, Qasim SE, et al. Functionally distinct high and low theta oscillations in the human hippocampus. *Nat Commun*. 2020;11(1):2469. doi:10.1038/s41467-020-15670-6

74. Gray CM, König P, Engel AK, Singer W. Oscillatory responses in cat visual cortex exhibit inter-columnar synchronization which reflects global stimulus properties. *Nature*. 1989;338(6213):334-337. doi:10.1038/338334a0

75. Gridchyn I, Schoenenberger P, O'Neill J, Csicsvari J. Assembly-Specific Disruption of Hippocampal Replay Leads to Selective Memory Deficit. *Neuron*. 2020;106(2):291-300.e6. doi:https://doi.org/10.1016/j.neuron.2020.01.021

76. Griffiths BJ, Parish G, Roux F, et al. Directional coupling of slow and fast hippocampal gamma with neocortical alpha/beta oscillations in human episodic memory. *Proc Natl Acad Sci*. 2019;116(43):21834 LP - 21842. doi:10.1073/pnas.1914180116

77. Grion N, Akrami A, Zuo Y, Stella F, Diamond ME. Coherence between Rat Sensorimotor System and Hippocampus Is Enhanced during Tactile Discrimination. *PLOS Biol*. 2016;14(2):e1002384. https://doi.org/10.1371/journal.pbio.1002384

78. Gulyás AI, Hájos N, Freund TF. Interneurons containing calretinin are specialized to control other interneurons in the rat hippocampus. *J Neurosci*. 1996;16(10):3397-3411. doi:10.1523/JNEUROSCI.16-10-03397.1996

79. Hafting T, Fyhn M, Bonnevie T, Moser M-B, Moser EI. Hippocampus-independent phase precession in entorhinal grid cells. *Nature*. 2008;453(7199):1248-1252. doi:10.1038/nature06957

80. Hafting T, Fyhn M, Molden S, Moser M-B, Moser EI. Microstructure of a spatial map in the entorhinal cortex. *Nature*. 2005;436(7052):801-806. doi:10.1038/nature03721

81. Hainmueller T, Bartos M. Dentate gyrus circuits for encoding, retrieval and discrimination of episodic memories. *Nat Rev Neurosci*. 2020;21(3):153-168. doi:10.1038/s41583-019-0260-z

82. Hales JB, Schlesiger MI, Leutgeb JK, Squire LR, Leutgeb S, Clark RE. Medial entorhinal cortex lesions only partially disrupt hippocampal place cells and hippocampus-dependent place memory. *Cell Rep*. 2014;9(3):893-901. doi:10.1016/j.celrep.2014.10.009

83. Hargreaves EL, Rao G, Lee I, Knierim JJ. Major dissociation between medial and lateral entorhinal input to dorsal hippocampus. *Science*. 2005;308(5729):1792-1794. doi:10.1126/science.1110449

84. Hartley T, Burgess N, Lever C, Cacucci F, O'Keefe J. Modeling place fields in terms of the cortical inputs to the hippocampus. *Hippocampus*. 2000;10(4):369-379. doi:10.1002/1098-1063(2000)10:4<369::AID-HIPO3>3.0.CO;2-0

85. Hassabis D, Kumaran D, Vann SD, Maguire EA. Patients with hippocampal amnesia cannot imagine new experiences. *Proc Natl Acad Sci U S A*. 2007;104(5):1726-1731. doi:10.1073/pnas.0610561104

86. Hassabis D, Maguire EA. Deconstructing episodic memory with construction. *Trends Cogn Sci*. 2007;11(7):299-306. doi:10.1016/j.tics.2007.05.001

87. Hasselmo ME, Bodelón C, Wyble BP. A proposed function for hippocampal theta rhythm: separate phases of encoding and retrieval enhance reversal of prior learning. *Neural Comput*. 2002;14(4):793-817.

88. He H, Boehringer R, Huang AJY, et al. CA2 inhibition reduces the precision of hippocampal assembly reactivation. *Neuron*. 2021;109(22):3674-3687.e7. doi:10.1016/j.neuron.2021.08.034

89. Hebb DO. The organization of behavior; a neuropsycholocigal theory. *A Wiley B Clin Psychol*. 1949;62:78.

90. Henze DA, Wittner L, Buzsáki G. Single granule cells reliably discharge targets in the hippocampal CA3 network in vivo. *Nat Neurosci*. 2002;5(8):790-795. doi:10.1038/nn887

91. Herweg NA, Solomon EA, Kahana MJ. Theta Oscillations in Human Memory. *Trends Cogn Sci*. 2020;24(3):208-227. doi:10.1016/j.tics.2019.12.006

92. Hitti FL, Siegelbaum SA. The hippocampal CA2 region is essential for social memory. *Nature*. 2014;508(7494):88-92. doi:10.1038/nature13028

93. Hopfield JJ. Neural networks and physical systems with emergent collective computational abilities. *Proc Natl Acad Sci*. 1982;79(8):2554 LP - 2558. doi:10.1073/pnas.79.8.2554

94. Høydal ØA, Skytøen ER, Andersson SO, Moser M-B, Moser EI. Object-vector coding in the medial entorhinal cortex. *Nature*. 2019;568(7752):400-404. doi:10.1038/s41586-019-1077-7

95. Huxter JR, Senior TJ, Allen K, Csicsvari J. Theta phase-specific codes for two-dimensional position, trajectory and heading in the hippocampus. *Nat Neurosci*. 2008;11(5):587-594. doi:10.1038/nn.2106

96. Igarashi KM, Lu L, Colgin LL, Moser M-B, Moser EI. Coordination of entorhinal-hippocampal ensemble activity during associative learning. *Nature*. 2014;510(7503):143-147. doi:10.1038/nature13162

97. Jacobs J, Weidemann CT, Miller JF, et al. Direct recordings of grid-like neuronal activity in human spatial navigation. *Nat Neurosci*. 2013;16(9):1188-1190. doi:10.1038/nn.3466

98. Jayakumar RP, Madhav MS, Savelli F, Blair HT, Cowan NJ, Knierim JJ. Recalibration of path integration in hippocampal place cells. *Nature*. 2019;566(7745):533-537. doi:10.1038/s41586-019-0939-3

99. Jezek K, Henriksen EJ, Treves A, Moser EI, Moser M-B. Theta-paced flickering between place-cell maps in the hippocampus. *Nature*. 2011;478(7368):246-249. doi:10.1038/nature10439

100. Ji D, Wilson MA. Coordinated memory replay in the visual cortex and hippocampus during sleep. *Nat Neurosci*. 2007;10(1):100-107. doi:10.1038/nn1825

101. Jiang H, Bahramisharif A, van Gerven MAJ, Jensen O. Distinct directional couplings between slow and fast gamma power to the phase of theta oscillations in the rat hippocampus. *Eur J Neurosci*. 2020;51(10):2070-2081. doi:https://doi.org/10.1111/ejn.14644

102. Johnson A, Redish AD. Neural Ensembles in CA3 Transiently Encode Paths Forward of the Animal at a Decision Point. *J Neurosci*. 2007;27(45):12176 LP - 12189. doi:10.1523/JNEUROSCI.3761-07.2007

103. Jones MW, Wilson MA. Theta Rhythms Coordinate Hippocampal–Prefrontal Interactions in a Spatial Memory Task. *PLOS Biol*. 2005;3(12):e402. https://doi.org/10.1371/journal.pbio.0030402

104. Joo HR, Frank LM. The hippocampal sharp wave-ripple in memory retrieval for immediate use and consolidation. *Nat Rev Neurosci*. 2018;19(12):744-757. doi:10.1038/s41583-018-0077-1

105. Kamondi A, Acsády L, Wang X-J, Buzsáki G. Theta oscillations in somata and dendrites of hippocampal pyramidal cells in vivo: Activity-dependent phase-precession of action potentials. *Hippocampus*. 1998;8(3):244-261. doi:https://doi.org/10.1002/(SICI)1098-1063(1998)8:3<244::AID-HIPO7>3.0.CO;2-J

106. Kant I. *Critique of Pure Reason.*1899

107. Kapl S, Tichanek F, Zitricky F, Jezek K. Context-independent expression of spatial code in hippocampus. *bioRxiv*. Published online January 1, 2022:2022.03.28.486068. doi:10.1101/2022.03.28.486068

108. Karlsson MP, Frank LM. Awake replay of remote experiences in the hippocampus. *Nat Neurosci*. 2009;12(7):913-918. doi:10.1038/nn.2344

109. Kay K, Sosa M, Chung JE, Karlsson MP, Larkin MC, Frank LM. A hippocampal network for spatial coding during immobility and sleep. *Nature*. 2016;531(7593):185-190. doi:10.1038/nature17144

110. Kayser C, Montemurro MA, Logothetis NK, Panzeri S. Spike-phase coding boosts and stabilizes information carried by spatial and temporal spike patterns. *Neuron*. 2009;61(4):597-608. doi:10.1016/j.neuron.2009.01.008

111. Kelemen E, Fenton AA. Coordinating different representations in the hippocampus. *Neurobiol Learn Mem*. 2016;129:50-59. doi:10.1016/j.nlm.2015.12.011

112. Kelemen E, Fenton AA. Dynamic Grouping of Hippocampal Neural Activity During Cognitive Control of Two Spatial Frames. *PLOS Biol*. 2010;8(6):e1000403. https://doi.org/10.1371/journal.pbio.1000403

113. Kesner RP, Rolls ET. A computational theory of hippocampal function, and tests of the theory: new developments. *Neurosci Biobehav Rev*. 2015;48:92-147. doi:10.1016/j.neubiorev.2014.11.009

114. Khona M, Fiete IR. Attractor and integrator networks in the brain. *arXiv Prepr arXiv211203978*. Published online 2021.

115. Killian NJ, Jutras MJ, Buffalo EA. A map of visual space in the primate entorhinal cortex. *Nature*. 2012;491(7426):761-764. doi:10.1038/nature11587

116. Kim S, Jung D, Royer S. Place cell maps slowly develop via competitive learning and conjunctive coding in the dentate gyrus. *Nat Commun*. 2020;11(1):4550. doi:10.1038/s41467-020-18351-6

117. Kim SS, Rouault H, Druckmann S, Jayaraman V. Ring attractor dynamics in the Drosophila central brain. *Science (80-)*. 2017;356(6340):849 LP - 853. doi:10.1126/science.aal4835

118. Kitamura T, Ogawa SK, Roy DS, et al. Engrams and circuits crucial for systems consolidation of a memory. *Science (80-)*. 2017;356(6333):73 LP - 78. doi:10.1126/science.aam6808

119. Kitamura T, Sun C, Martin J, Kitch LJ, Schnitzer MJ, Tonegawa S. Entorhinal Cortical Ocean Cells Encode Specific Contexts and Drive Context-Specific Fear Memory. *Neuron*. 2015;87(6):1317-1331. doi:10.1016/j.neuron.2015.08.036

120. Kjelstrup KB, Solstad T, Brun VH, et al. Finite Scale of Spatial Representation in the Hippocampus. *Science (80-)*. 2008;321(5885):140 LP - 143. doi:10.1126/science.1157086

121. Knierim JJ, Neunuebel JP, Deshmukh SS. Functional correlates of the lateral and medial entorhinal cortex: objects, path integration and local-global reference frames. *Philos Trans R Soc London Ser B, Biol Sci*. 2014;369(1635):20130369. doi:10.1098/rstb.2013.0369

122. Kropff E, Carmichael JE, Moser EI, Moser M-B. Frequency of theta rhythm is controlled by acceleration, but not speed, in running rats. *Neuron*. 2021;109(6):1029-1039.e8. doi:https://doi.org/10.1016/j.neuron.2021.01.017

123. Kropff E, Carmichael JE, Moser M-B, Moser EI. Speed cells in the medial entorhinal cortex. *Nature*. 2015;523(7561):419-424. doi:10.1038/nature14622

124. Krupic J, Bauza M, Burton S, Barry C, O'Keefe J. Grid cell symmetry is shaped by environmental geometry. *Nature*. 2015;518(7538):232-235. doi:10.1038/nature14153

125. Lavenex P, Amaral DG. Hippocampal-neocortical interaction: A hierarchy of associativity. *Hippocampus*. 2000;10(4):420-430. doi:https://doi.org/10.1002/1098-1063(2000)10:4<420::AID-HIPO8>3.0.CO;2-5

126. Lee AK, Wilson MA. Memory of sequential experience in the hippocampus during slow wave sleep. *Neuron*. 2002;36(6):1183-1194. doi:10.1016/s0896-6273(02)01096-6

127. Lee I, Yoganarasimha D, Rao G, Knierim JJ. Comparison of population coherence of place cells in hippocampal subfields CA1 and CA3. *Nature*. 2004;430(6998):456-459. doi:10.1038/nature02739

128. Lee MG, Chrobak JJ, Sik A, Wiley RG, Buzsáki G. Hippocampal theta activity following selective lesion of the septal cholinergic system. *Neuroscience*. 1994;62(4):1033-1047. doi:10.1016/0306-4522(94)90341-7

129. Leutgeb JK, Leutgeb S, Moser M-B, Moser EI. Pattern separation in the dentate gyrus and CA3 of the hippocampus. *Science*. 2007;315(5814):961-966. doi:10.1126/science.1135801

130. Leutgeb S, Mizumori SJ. Excitotoxic septal lesions result in spatial memory deficits and altered flexibility of hippocampal single-unit representations. *J Neurosci*. 1999;19(15):6661-6672. doi:10.1523/JNEUROSCI.19-15-06661.1999

131. Leutgeb S, Leutgeb JK, Treves A, Moser M-B, Moser EI. Distinct ensemble codes in hippocampal areas CA3 and CA1. *Science*. 2004;305(5688):1295-1298. doi:10.1126/science.1100265

132. Lever C, Burton S, Jeewajee A, O'Keefe J, Burgess N. Boundary Vector Cells in the Subiculum of the Hippocampal Formation. *J Neurosci*. 2009;29(31):9771 LP - 9777. doi:10.1523/JNEUROSCI.1319-09.2009

133. Liu X, Ramirez S, Pang PT, et al. Optogenetic stimulation of a hippocampal engram activates fear memory recall. *Nature*. 2012;484(7394):381-385. doi:10.1038/nature11028

134. Lopes-Dos-Santos V, van de Ven GM, Morley A, Trouche S, Campo-Urriza N, Dupret D. Parsing Hippocampal Theta Oscillations by Nested Spectral Components during Spatial Exploration and Memory-Guided Behavior. *Neuron*. 2018;100(4):940-952.e7. doi:10.1016/j.neuron.2018.09.031

135. Lubenov E V, Siapas AG. Hippocampal theta oscillations are travelling waves. *Nature*. 2009;459(7246):534-539. doi:10.1038/nature08010

136. MacDonald CJ, Lepage KQ, Eden UT, Eichenbaum H. Hippocampal “time cells” bridge the gap in memory for discontiguous events. *Neuron*. 2011;71(4):737-749. doi:10.1016/j.neuron.2011.07.012

137. MacKay DJC, Mac Kay DJC. *Information Theory, Inference and Learning Algorithms*. Cambridge university press; 2003.

138. Madison D V, Nicoll RA. Control of the repetitive discharge of rat CA 1 pyramidal neurones in vitro. *J Physiol*. 1984;354:319-331. doi:10.1113/jphysiol.1984.sp015378

139. Maier N, Nimmrich V, Draguhn A. Cellular and network mechanisms underlying spontaneous sharp wave-ripple complexes in mouse hippocampal slices. *J Physiol*. 2003;550(Pt 3):873-887. doi:10.1113/jphysiol.2003.044602

140. Mark S, Romani S, Jezek K, Tsodyks M. Theta-paced flickering between place-cell maps in the hippocampus: A model based on short-term synaptic plasticity. *Hippocampus*. 2017;27(9):959-970. doi:10.1002/hipo.22743

141. Marr D. Simple memory: a theory for archicortex. *Philos Trans R Soc London Ser B, Biol Sci*. 1971;262(841):23-81. doi:10.1098/rstb.1971.0078

142. McClelland JL, McNaughton BL, O’Reilly RC. Why there are complementary learning systems in the hippocampus and neocortex: insights from the successes and failures of connectionist models of learning and memory. *Psychol Rev*. 1995;102(3):419-457. doi:10.1037/0033-295X.102.3.419

143. McMahon DBT, Barrionuevo G. Short- and long-term plasticity of the perforant path synapse in hippocampal area CA3. *J Neurophysiol*. 2002;88(1):528-533. doi:10.1152/jn.2002.88.1.528

144. McNaughton BL, Barnes CA, O’Keefe J. The contributions of position, direction, and velocity to single unit activity in the hippocampus of freely-moving rats. *Exp Brain Res*. 1983;52(1):41-49. doi:10.1007/BF00237147

145. McNaughton BL, Morris RGM. Hippocampal synaptic enhancement and information storage within a distributed memory system. *Trends Neurosci*. 1987;10(10):408-415. doi:https://doi.org/10.1016/0166-2236(87)90011-7

146. Meira T, Leroy F, Buss EW, Oliva A, Park J, Siegelbaum SA. A hippocampal circuit linking dorsal CA2 to ventral CA1 critical for social memory dynamics. *Nat Commun*. 2018;9(1):4163. doi:10.1038/s41467-018-06501-w

147. Middleton SJ, McHugh TJ. Silencing CA3 disrupts temporal coding in the CA1 ensemble. *Nat Neurosci*. 2016;19(7):945-951. doi:10.1038/nn.4311

148. Middleton SJ, McHugh TJ. CA2: A Highly Connected Intrahippocampal Relay. *Annu Rev Neurosci*. 2020;43(1):55-72. doi:10.1146/annurev-neuro-080719-100343

149. Milner B, Passquant P. Physiologie de l’hippocampe. Published online 1962.

150. Mizumori SJ, Perez GM, Alvarado MC, Barnes CA, McNaughton BL. Reversible inactivation of the medial septum differentially affects two forms of learning in rats. *Brain Res*. 1990;528(1):12-20. doi:10.1016/0006-8993(90)90188-h

151. Mizuseki K, Sirota A, Pastalkova E, Buzsáki G. Theta oscillations provide temporal windows for local circuit computation in the entorhinal-hippocampal loop. *Neuron*. 2009;64(2):267-280. doi:10.1016/j.neuron.2009.08.037

152. Moita MAP, Rosis S, Zhou Y, LeDoux JE, Blair HT. Putting Fear in Its Place: Remapping of Hippocampal Place Cells during Fear Conditioning. *J Neurosci*. 2004;24(31):7015 LP - 7023. doi:10.1523/JNEUROSCI.5492-03.2004

153. Montgomery SM, Buzsáki G. Gamma oscillations dynamically couple hippocampal CA3 and CA1 regions during memory task performance. *Proc Natl Acad Sci*. 2007;104(36):14495 LP - 14500. doi:10.1073/pnas.0701826104

154. Morris RGM, Schenk F, Tweedie F, Jarrard LE. Ibotenate Lesions of Hippocampus and/or Subiculum: Dissociating Components of Allocentric Spatial Learning. *Eur J Neurosci*. 1990;2(12):1016-1028. doi:10.1111/j.1460-9568.1990.tb00014.x

155. Morris RG, Davis S, Butcher SP. Hippocampal synaptic plasticity and NMDA receptors: a role in information storage? *Philos Trans R Soc London Ser B, Biol Sci*. 1990;329(1253):187-204. doi:10.1098/rstb.1990.0164

156. Moser EI, Kropff E, Moser M-B. Place cells, grid cells, and the brain's spatial representation system. *Annu Rev Neurosci*. 2008;31:69-89. doi:10.1146/annurev.neuro.31.061307.090723

157. Muessig L, Hauser J, Wills TJ, Cacucci F. Place Cell Networks in Pre-weanling Rats Show Associative Memory Properties from the Onset of Exploratory Behavior. *Cereb Cortex*. 2016;26(8):3627-3636. doi:10.1093/cercor/bhw174

158. Muller RU, Kubie JL. The effects of changes in the environment on the spatial firing of hippocampal complex-spike cells. *J Neurosci*. 1987;7(7):1951-1968. doi:10.1523/JNEUROSCI.07-07-01951.1987

159. Muller RU, Kubie JL, Ranck JBJ. Spatial firing patterns of hippocampal complex-spike cells in a fixed environment. *J Neurosci*. 1987;7(7):1935-1950. doi:10.1523/JNEUROSCI.07-07-01935.1987

160. Nabavi S, Fox R, Proulx CD, Lin JY, Tsien RY, Malinow R. Engineering a memory with LTD and LTP. *Nature*. 2014;511(7509):348-352. doi:10.1038/nature13294

161. Nádasdy Z, Hirase H, Czurkó A, Csicsvari J, Buzsáki G. Replay and time compression of recurring spike sequences in the hippocampus. *J Neurosci*. 1999;19(21):9497-9507. doi:10.1523/JNEUROSCI.19-21-09497.1999

162. Nadel L, Moscovitch M. Memory consolidation, retrograde amnesia and the hippocampal complex. *Curr Opin Neurobiol*. 1997;7(2):217-227. doi:10.1016/s0959-4388(97)80010-4

163. Nakashiba T, Cushman JD, Pelkey KA, et al. Young dentate granule cells mediate pattern separation, whereas old granule cells facilitate pattern completion. *Cell*. 2012;149(1):188-201. doi:10.1016/j.cell.2012.01.046

164. Nakazawa K, Quirk MC, Chitwood RA, et al. Requirement for hippocampal CA3 NMDA receptors in associative memory recall. *Science*. 2002;297(5579):211-218. doi:10.1126/science.1071795

165. Neunuebel JP, Knierim JJ. CA3 retrieves coherent representations from degraded input: direct evidence for CA3 pattern completion and dentate gyrus pattern separation. *Neuron*. 2014;81(2):416-427. doi:10.1016/j.neuron.2013.11.017

166. Norman Y, Yeagle EM, Khuvis S, Harel M, Mehta AD, Malach R. Hippocampal sharp-wave ripples linked to visual episodic recollection in humans. *Science (80-)*. 2019;365(6454):eaax1030. doi:10.1126/science.aax1030

167. O'Keefe J, Dostrovsky J. The hippocampus as a spatial map. Preliminary evidence from unit activity in the freely-moving rat. *Brain Res*. 1971;34(1):171-175. doi:10.1016/0006-8993(71)90358-1

168. O'Keefe J, Nadel L *The Hippocampus as a Cognitive Map*. 1978 Oxford University Press

169. O'Keefe J, Recce ML. Phase relationship between hippocampal place units and the EEG theta rhythm. *Hippocampus*. 1993;3(3):317-330. doi:10.1002/hipo.450030307

170. Okuyama T, Kitamura T, Roy DS, Itohara S, Tonegawa S. Ventral CA1 neurons store social memory. *Science (80-)*. 2016;353(6307):1536 LP - 1541. doi:10.1126/science.aaf7003

171. Oliva A, Fernández-Ruiz A, Buzsáki G, Berényi A. Role of Hippocampal CA2 Region in Triggering Sharp-Wave Ripples. *Neuron*. 2016;91(6):1342-1355. doi:10.1016/j.neuron.2016.08.008

172. Oliva A, Fernández-Ruiz A, Fermino de Oliveira E, Buzsáki G. Origin of Gamma Frequency Power during Hippocampal Sharp-Wave Ripples. *Cell Rep*. 2018;25(7):1693-1700.e4. doi:10.1016/j.celrep.2018.10.066

173. Oliva A, Fernández-Ruiz A, Leroy F, Siegelbaum SA. Hippocampal CA2 sharp-wave ripples reactivate and promote social memory. *Nature*. 2020;587(7833):264-269. doi:10.1038/s41586-020-2758-y

174. Pastalkova E, Itskov V, Amarasingham A, Buzsáki G. Internally Generated Cell Assembly Sequences in the Rat Hippocampus. *Science (80-)*. 2008;321(5894):1322 LP - 1327. doi:10.1126/science.1159775

175. Pastalkova E, Serrano P, Pinkhasova D, Wallace E, Fenton AA, Sacktor TC. Storage of spatial information by the maintenance mechanism of LTP. *Science*. 2006;313(5790):1141-1144. doi:10.1126/science.1128657

176. Pavlides C, Winson J. Influences of hippocampal place cell firing in the awake state on the activity of these cells during subsequent sleep episodes. *J Neurosci*. 1989;9(8):2907 LP - 2918. doi:10.1523/JNEUROSCI.09-08-02907.1989

177. Peyrache A, Lacroix MM, Petersen PC, Buzsáki G. Internally organized mechanisms of the head direction sense. *Nat Neurosci*. 2015;18(4):569-575.

178. Place R, Farovik A, Brockmann M, Eichenbaum H. Bidirectional prefrontal-hippocampal interactions support context-guided memory. *Nat Neurosci*. 2016;19(8):992-994. doi:10.1038/nn.4327

179. Posani L, Cocco S, Ježek K, Monasson R. Functional connectivity models for decoding of spatial representations from hippocampal CA1 recordings. *J Comput Neurosci*. 2017;43(1):17-33. doi:10.1007/s10827-017-0645-9

180. Posani L, Cocco S, Monasson R. Integration and multiplexing of positional and contextual information by the hippocampal network. Bush D, ed. *PLOS Comput Biol*. 2018;14(8):e1006320. doi:10.1371/journal.pcbi.1006320

181. Prince LY, Bacon T, Humphries R, Tsaneva-Atanasova K, Clopath C, Mellor JR. Separable actions of acetylcholine and noradrenaline on neuronal ensemble formation in hippocampal CA3 circuits. *PLoS Comput Biol*. 2021;17(10):e1009435.

182. Proskauer Pena SL, Mallouppas K, Oliveira AMG, Zitricky F, Nataraj A, Jezek K. Early Spatial Memory Impairment in a Double Transgenic Model of Alzheimer's Disease TgF-344 AD. *Brain Sci*. 2021;11(10):1300. doi:10.3390/brainsci11101300

183. Rajasethupathy P, Sankaran S, Marshel JH, et al. Projections from neocortex mediate top-down control of memory retrieval. *Nature*. 2015;526(7575):653-659. doi:10.1038/nature15389

184. Ranck Jr JB. Head direction cells in the deep layer of dorsal presubiculum in freely moving rats. In: *Society of Neuroscience Abstract*. Vol 10. Hargreaves, E. L., Rao, G., Lee, I., & Knierim, J. J. (2005). Major dissociation between medial and lateral entorhinal input to dorsal hippocampus. Science (New York, N.Y.), 308(5729), 1792–1794. https://doi.org/10.1126/science.1110449 Knierim, J. J., Neu; 1984:599.

185. Rennó-Costa C, Tort ABL. Place and Grid Cells in a Loop: Implications for Memory Function and Spatial Coding. *J Neurosci*. 2017;37(34):8062-8076. doi:10.1523/JNEUROSCI.3490-16.2017

186. Robbe D, Buzsáki G. Alteration of Theta Timescale Dynamics of Hippocampal Place Cells by a Cannabinoid Is Associated with Memory Impairment. *J Neurosci*. 2009;29(40):12597 LP - 12605. doi:10.1523/JNEUROSCI.2407-09.2009

187. Robinson NTM, Descamps LAL, Russell LE, et al. Targeted Activation of Hippocampal Place Cells Drives Memory-Guided Spatial Behavior. *Cell*. 2020;183(6):1586-1599.e10. doi:https://doi.org/10.1016/j.cell.2020.09.061

188. Rolls ET. Theoretical and neurophysiological analysis of the functions of the primate hippocampus in memory. *Cold Spring Harb Symp Quant Biol*. 1990;55:995-1006. doi:10.1101/sqb.1990.055.01.095

189. Rolls ET. Information representation, processing and storage in the brain: analysis at the single neuron level. *neural Mol bases Learn*. Published online 1987:503-540.

190. Rolls ET. Memory, Attention, and Decision-Making: A Unifying Computational Neuroscience. Published online 2007.

191. Rolls ET. Attractor cortical neurodynamics, schizophrenia, and depression. *Transl Psychiatry*. 2021;11(1):215. doi:10.1038/s41398-021-01333-7

192. Rolls ET. A theory of hippocampal function in memory. *Hippocampus*. 1996;6(6):601-620. doi:https://doi.org/10.1002/(SICI)1098-1063(1996)6:6<601::AID-HIPO5>3.0.CO;2-J

193. Rolls ET, Loh M, Deco G, Winterer G. Computational models of schizophrenia and dopamine modulation in the prefrontal cortex. *Nat Rev Neurosci*. 2008;9(9):696-709.

194. Rothschild G, Eban E, Frank LM. A cortical-hippocampal-cortical loop of information processing during memory consolidation. *Nat Neurosci*. 2017;20(2):251-259. doi:10.1038/nn.4457

195. Ryan TJ, Roy DS, Pignatelli M, Arons A, Tonegawa S. Memory. Engram cells retain memory under retrograde amnesia. *Science*. 2015;348(6238):1007-1013. doi:10.1126/science.aaa5542

196. Samsonovich A, McNaughton BL. Path Integration and Cognitive Mapping in a Continuous Attractor Neural Network Model. *J Neurosci*. 1997;17(15):5900 LP - 5920. doi:10.1523/JNEUROSCI.17-15-05900.1997

197. Sanders H, Wilson MA, Gershman SJ. Hippocampal remapping as hidden state inference. *Elife*. 2020;9. doi:10.7554/eLife.51140

198. Savin C, Dayan P, Lengyel M. Optimal recall from bounded metaplastic synapses: predicting functional adaptations in hippocampal area CA3. *PLoS Comput Biol*. 2014;10(2):e1003489.

199. Schlesiger MI, Cannova CC, Boublil BL, et al. The medial entorhinal cortex is necessary for temporal organization of hippocampal neuronal activity. *Nat Neurosci*. 2015;18(8):1123-1132. doi:10.1038/nn.4056

200. Schlingloff D, Káli S, Freund TF, Hájos N, Gulyás AI. Mechanisms of sharp wave initiation and ripple generation. *J Neurosci*. 2014;34(34):11385-11398. doi:10.1523/JNEUROSCI.0867-14.2014

201. Schmidt B, Marrone DF, Markus EJ. Disambiguating the similar: the dentate gyrus and pattern separation. *Behav Brain Res*. 2012;226(1):56-65. doi:10.1016/j.bbr.2011.08.039

202. Schomburg EW, Fernández-Ruiz A, Mizuseki K, et al. Theta phase segregation of input-specific gamma patterns in entorhinal-hippocampal networks. *Neuron*. 2014;84(2):470-485. doi:10.1016/j.neuron.2014.08.051

203. Schultz S, Panzeri S, Treves A, Rolls ET. Analogue resolution in a model of the Schaffer collaterals. In: *International Conference on Artificial Neural Networks*. Springer; 1997:61-66.

204. Scoville WB, Milner B. Loss of recent memory after bilateral hippocampal lesions. *J Neurol Neurosurg Psychiatry*. 1957;20:11-21. doi:10.1136/jnnp.20.1.11

205. Seidenbecher T, Laxmi TR, Stork O, Pape H-C. Amygdalar and hippocampal theta rhythm synchronization during fear memory retrieval. *Science*. 2003;301(5634):846-850. doi:10.1126/science.1085818

206. Senzai Y, Buzsáki G. Physiological Properties and Behavioral Correlates of Hippocampal Granule Cells and Mossy Cells. *Neuron*. 2017;93(3):691-704.e5. doi:10.1016/j.neuron.2016.12.011

207. Sigurdsson T, Stark KL, Karayiorgou M, Gogos JA, Gordon JA. Impaired hippocampal-prefrontal synchrony in a genetic mouse model of schizophrenia. *Nature*. 2010;464(7289):763-767. doi:10.1038/nature08855

208. Skaggs WE, Knierim JJ, Kudrimoti HS, McNaughton BL. A model of the neural basis of the rat's sense of direction. *Adv Neural Inf Process Syst*. 1995;7:173-180.

209. Skaggs WE, McNaughton BL, Wilson MA, Barnes CA. Theta phase precession in hippocampal neuronal populations and the compression of temporal sequences. *Hippocampus*. 1996;6(2):149-172. doi:10.1002/(SICI)1098-1063(1996)6:2<149::AID-HIPO6>3.0.CO;2-K

210. Solstad T, Boccara CN, Kropff E, Moser M-B, Moser EI. Representation of geometric borders in the entorhinal cortex. *Science*. 2008;322(5909):1865-1868. doi:10.1126/science.1166466

211. Solstad T, Yousif HN, Sejnowski TJ. Place Cell Rate Remapping by CA3 Recurrent Collaterals. *PLOS Comput Biol*. 2014;10(6):e1003648. https://doi.org/10.1371/journal.pcbi.1003648

212. Spalding KN, Jones SH, Duff MC, Tranel D, Warren DE. Investigating the Neural Correlates of Schemas: Ventromedial Prefrontal Cortex Is Necessary for Normal Schematic Influence on Memory. *J Neurosci*. 2015;35(47):15746-15751. doi:10.1523/JNEUROSCI.2767-15.2015

213. Squire LR. Mechanisms of memory. *Science*. 1986;232(4758):1612-1619. doi:10.1126/science.3086978

214. Squire LR, Zola-Morgan S. Memory: brain systems and behavior. *Trends Neurosci*. 1988;11(4):170-175. doi:10.1016/0166-2236(88)90144-0

215. Stackman RW, Taube JS. Firing properties of head direction cells in the rat anterior thalamic nucleus: dependence on vestibular input. *J Neurosci*. 1997;17(11):4349-4358. doi:10.1523/JNEUROSCI.17-11-04349.1997

216. Stackman RW, Zugaro MB. Self-motion cues and resolving intermodality conflicts: Head direction cells, place cells, and behavior. *Head Dir cells neural Mech Spat Orientat*. Published online 2005:137-162.

217. Stella F. Spatial Representations in the Entorhino-Hippocampal Circuit. Published online 2014.

218. Stella F, Treves A. Associative memory storage and retrieval: involvement of theta oscillations in hippocampal information processing. *Neural Plast*. 2011;2011:683961. doi:10.1155/2011/683961

219. Stensola H, Stensola T, Solstad T, Frøland K, Moser M-B, Moser EI. The entorhinal grid map is discretized. *Nature*. 2012;492(7427):72-78. doi:10.1038/nature11649

220. Steward O, Scoville SA. Cells of origin of entorhinal cortical afferents to the hippocampus and fascia dentata of the rat. *J Comp Neurol*. 1976;169(3):347-370. doi:https://doi.org/10.1002/cne.901690306

221. Sutherland RJ, Lee JQ, McDonald RJ, Lehmann H. Has multiple trace theory been refuted? *Hippocampus*. 2020;30(8):842-850. doi:https://doi.org/10.1002/hipo.23162

222. Takahashi M, Nishida H, David Redish A, Lauwereyns J. Theta phase shift in spike timing and modulation of gamma oscillation: a dynamic code for spatial alternation during fixation in rat hippocampal area CA1. *J Neurophysiol*. 2014;111(8):1601-1614.

223. Taube JS, Muller RU, Ranck JBJ. Head-direction cells recorded from the postsubiculum in freely moving rats. II. Effects of environmental manipulations. *J Neurosci*. 1990;10(2):436-447. doi:10.1523/JNEUROSCI.10-02-00436.1990

224. Taube JS. The Head Direction Signal: Origins and Sensory-Motor Integration. *Annu Rev Neurosci*. 2007;30(1):181-207. doi:10.1146/annurev.neuro.29.051605.112854

225. Teles-Grilo Ruivo LM, Mellor JR. Cholinergic modulation of hippocampal network function. *Front Synaptic Neurosci*. 2013;5:2. doi:10.3389/fnsyn.2013.00002

226. Tolman EC, Ritchie BF, Kalish D. Studies in spatial learning. I. Orientation and the short-cut. *J Exp Psychol*. 1946;36(1):13-24. doi:10.1037/h0053944

227. Tonegawa S, Morrissey MD, Kitamura T. The role of engram cells in the systems consolidation of memory. *Nat Rev Neurosci*. 2018;19(8):485-498. doi:10.1038/s41583-018-0031-2

228. Tort ABL, Kramer MA, Thorn C, et al. Dynamic cross-frequency couplings of local field potential oscillations in rat striatum and hippocampus during performance of a T-maze task. *Proc Natl Acad Sci*. 2008;105(51):20517 LP - 20522. doi:10.1073/pnas.0810524105

229. Tóth K, Freund TF, Miles R. Disinhibition of rat hippocampal pyramidal cells by GABAergic afferents from the septum. *J Physiol*. 1997;500 (Pt 2(Pt 2):463-474. doi:10.1113/jphysiol.1997.sp022033

230. Trettel SG, Trimper JB, Hwaun E, Fiete IR, Colgin LL. Grid cell co-activity patterns during sleep reflect spatial overlap of grid fields during active behaviors. *Nat Neurosci*. 2019;22(4):609-617.

231. Treves A, Rolls ET. Computational constraints suggest the need for two distinct input systems to the hippocampal CA3 network. *Hippocampus*. 1992;2(2):189-199. doi:10.1002/hipo.450020209

232. Treves A, Rolls ET. What determines the capacity of autoassociative memories in the brain? *Netw Comput Neural Syst*. 1991;2(4):371-397.

233. Tsao A, Moser M-B, Moser EI. Traces of experience in the lateral entorhinal cortex. *Curr Biol*. 2013;23(5):399-405. doi:10.1016/j.cub.2013.01.036

234. Tsao A, Sugar J, Lu L, et al. Integrating time from experience in the lateral entorhinal cortex. *Nature*. 2018;561(7721):57-62. doi:10.1038/s41586-018-0459-6

235. Tsodyks M, Sejnowski T. Associative memory and hippocampal place cells. *Int J Neural Syst*. 1995;6:81-86.

236. Uhlhaas PJ, Singer W. Abnormal neural oscillations and synchrony in schizophrenia. *Nat Rev Neurosci*. 2010;11(2):100-113. doi:10.1038/nrn2774

237. Ujfalussy BB, Orbán G. Sampling motion trajectories during hippocampal theta sequences. *bioRxiv*. Published online January 1, 2021:2021.12.14.472575. doi:10.1101/2021.12.14.472575

238. van Dijk MT, Fenton AA. On How the Dentate Gyrus Contributes to Memory Discrimination. *Neuron*. 2018;98(4):832-845.e5. doi:10.1016/j.neuron.2018.04.018

239. van Groen T, Wyss JM. The postsubicular cortex in the rat: characterization of the fourth region of the subicular cortex and its connections. *Brain Res*. 1990;529(1):165-177. doi:https://doi.org/10.1016/0006-8993(90)90824-U

240. van Vugt MK, Schulze-Bonhage A, Litt B, Brandt A, Kahana MJ. Hippocampal Gamma Oscillations Increase with Memory Load. *J Neurosci*. 2010;30(7):2694 LP - 2699. doi:10.1523/JNEUROSCI.0567-09.2010

241. Vaz AP, Wittig JH, Inati SK, Zaghloul KA. Replay of cortical spiking sequences during human memory retrieval. *Science (80-)*. 2020;367(6482):1131 LP - 1134. doi:10.1126/science.aba0672

242. Wang C, Chen X, Lee H, et al. Egocentric coding of external items in the lateral entorhinal cortex. *Science (80-)*. 2018;362(6417):945 LP - 949. doi:10.1126/science.aau4940

243. Wang M, Foster DJ, Pfeiffer BE. Alternating sequences of future and past behavior encoded within hippocampal theta oscillations. *Science (80-)*. 2020;370(6513):247 LP - 250. doi:10.1126/science.abb4151

244. Wang Y, Romani S, Lustig B, Leonardo A, Pastalkova E. Theta sequences are essential for internally generated hippocampal firing fields. *Nat Neurosci*. 2015;18(2):282-288. doi:10.1038/nn.3904

245. Watrous AJ, Lee DJ, Izadi A, Gurkoff GG, Shahlaie K, Ekstrom AD. A comparative study of human and rat hippocampal low-frequency oscillations during spatial navigation. *Hippocampus*. 2013;23(8):656-661. doi:10.1002/hipo.22124

246. Wei X-X, Prentice J, Balasubramanian V. A principle of economy predicts the functional architecture of grid cells. *Elife*. 2015;4:e08362.

247. Whishaw IQ, Vanderwolf CH. Hippocampal EEG and behavior: changes in amplitude and frequency of RSA (theta rhythm) associated with spontaneous and learned movement patterns in rats and cats. *Behav Biol*. 1973;8(4):461-484. doi:10.1016/s0091-6773(73)80041-0

248. Wikenheiser AM, Redish AD. Hippocampal theta sequences reflect current goals. *Nat Neurosci*. 2015;18(2):289-294. doi:10.1038/nn.3909

249. Wills TJ, Lever C, Cacucci F, Burgess N, O'Keefe J. Attractor dynamics in the hippocampal representation of the local environment. *Science*. 2005;308(5723):873-876. doi:10.1126/science.1108905

250. Wilson MA, McNaughton BL. Reactivation of hippocampal ensemble memories during sleep. *Science (80-)*. 1994;265(5172):676 LP - 679. doi:10.1126/science.8036517

251. Winson J. Loss of hippocampal theta rhythm results in spatial memory deficit in the rat. *Science*. 1978;201(4351):160-163. doi:10.1126/science.663646

252. Witter MP, Amaral DG. Entorhinal cortex of the monkey: V. Projections to the dentate gyrus, hippocampus, and subicular complex. *J Comp Neurol*. 1991;307(3):437-459. doi:10.1002/cne.903070308

253. Wittner L, Henze DA, Záborszky L, Buzsáki G. Three-dimensional reconstruction of the axon arbor of a CA3 pyramidal cell recorded and filled in vivo. *Brain Struct Funct*. 2007;212(1):75-83. doi:10.1007/s00429-007-0148-y

254. Yamamoto J, Suh J, Takeuchi D, Tonegawa S. Successful execution of working memory linked to synchronized high-frequency gamma oscillations. *Cell*. 2014;157(4):845-857. doi:10.1016/j.cell.2014.04.009

255. Yamamoto J, Tonegawa S. Direct Medial Entorhinal Cortex Input to Hippocampal CA1 Is Crucial for Extended Quiet Awake Replay. *Neuron*. 2017;96(1):217-227.e4. doi:10.1016/j.neuron.2017.09.017

256. Zhang K. Representation of spatial orientation by the intrinsic dynamics of the head-direction cell ensemble: a theory. *J Neurosci*. 1996;16(6):2112 LP - 2126. doi:10.1523/JNEUROSCI.16-06-02112.1996

257. Zhang L, Lee J, Rozell C, Singer AC. Sub-second dynamics of theta-gamma coupling in hippocampal CA1. *Elife*. 2019;8. doi:10.7554/eLife.44320

258. Zheng C, Bieri KW, Hsiao Y-T, Colgin LL. Spatial Sequence Coding Differs during Slow and Fast Gamma Rhythms in the Hippocampus. *Neuron*. 2016;89(2):398-408. doi:10.1016/j.neuron.2015.12.005

259. Zheng C, Bieri KW, Trettel SG, Colgin LL. The relationship between gamma frequency and running speed differs for slow and fast gamma rhythms in freely behaving rats. *Hippocampus*. 2015;25(8):924-938. doi:10.1002/hipo.22415

260. Zitrický F, Ježek K. Neuronal oscillations and memory retrieval. *Plzeňský lékařský sborník*. 2017;2017(83).

261. Zitricky F, Jezek K. Retrieval of spatial representation on network level in hippocampal CA3 accompanied by overexpression and mixture of stored network patterns. *Sci Rep*. 2019;9(1):11512. doi:10.1038/s41598-019-47842-w

262. Zola-Morgan S, Squire LR, Amaral DG. Human amnesia and the medial temporal region: enduring memory impairment following a bilateral lesion limited to field CA1 of the hippocampus. *J Neurosci*. 1986;6(10):2950 LP - 2967. doi:10.1523/JNEUROSCI.06-10-02950.1986

263. Zola-Morgan S, Squire LR, Rempel NL, Clower RP, Amaral DG. Enduring memory impairment in monkeys after ischemic damage to the hippocampus. *J Neurosci*. 1992;12(7):2582 LP - 2596. doi:10.1523/JNEUROSCI.12-07-02582.1992

264. Zutshi I, Fu ML, Lilascharoen V, Leutgeb JK, Lim BK, Leutgeb S. Recurrent circuits within medial entorhinal cortex superficial layers support grid cell firing. *Nat Commun*. 2018;9(1):3701. doi:10.1038/s41467-018-06104-5